

UNIVERSIDADE FEDERAL DE MINAS GERAIS



INSTITUTO DE CIÊNCIAS EXATAS

LOCAL QUENCHES ON QUANTUM MANY BODY SYSTEMS

Natália Salomé Móller

Belo Horizonte

2018

Natália Salomé Móller

Local Quenches on Quantum Many Body Systems

Tese apresentada ao Programa de Pós-Graduação em Física do Instituto de Ciências Exatas da Universidade Federal de Minas Gerais como requisito parcial para obtenção do título de Doutor em Ciências.

Orientador: Raphael Campos Drumond

Belo Horizonte

2018

Agradecimentos

Em um mundo tão normal surge a criatividade para alimentar a mente daqueles que sonham com a fantasia. Mal podia eu imaginar que o Universo seria muito mais incrível do que naquelas velhas histórias de magia. Obrigada às ideias, às teorias e aos teoremas vindos das mentes de tantas pessoas, que desde os tempos mais remotos, curiosas, buscaram uma forma de entender a natureza material e abstrata. Agradeço a cada pessoa que ajudou a construir a Ciência e a Matemática para a nossa sociedade.

Ainda assim, não são todos que possuem acesso à este conhecimento. Por isso agradeço minha mãe, Sônia Salomé, por se preocupar tanto com o meu futuro. Obrigada principalmente pelo seu amor infinito e por todo seu apoio. Obrigada ao meu pai, Leonardo Móller, que também esteve ao meu lado até onde pode. Vale lembrar daquele dia na estrada que você contou que o caminho mais curto entre dois pontos nem sempre era uma reta.

Muito obrigada ao meu orientador, Raphael Campos Drumond, sem seu apoio eu não teria conseguido. Trabalhar ao seu lado foi uma honra e uma grande alegria. Agradeço a todas as professoras e a todos os professores que tive, desde aquelas e aqueles da infância até as(os) mais recentes. Dentre estes, Socorro¹, Gilson², Júnior³, Marcos Montenegro⁴ e Elmo Salomão⁵ me inspiraram de uma forma especial. Agradeço ao meu grupo de pesquisa, EnLight, e às(aos) “EnLighters”, pelas reuniões, discussões e oportunidades. Agradeço também às alunas e aos alunos que já tive, pois o aprendizado é uma via de mão dupla.

Obrigada à minha irmã e ao meu irmão, Débora e Breno, sempre ao meu lado. Obrigada aos

¹Na 3a série: “talvez um de vocês aqui vai fazer uma descoberta...”.

²Meu professor de Química do 1o ano, foi nas suas aulas que eu descobri a carreira que iria seguir.

³Meu professor de Física do 1o ano e também quem falou para que eu lesse “O Universo numa Casca de Noz”.

⁴Meu orientador de mestrado que me incentivou a estudar matemática desde o início da minha graduação.

⁵Chefe do laboratório que mais enche meu coração de alegria.

cães, aos gatos, e a todo e qualquer bichinho que esteve por perto. Em especial, Sarah, Helena, Hanna, Monique, Lui, Xexeu, Glück, Pelé, Rouf, Caco, Cacau, e por aí vai. Obrigada à minha família que torce por mim. À Vó Many que nem entende mais o que está acontecendo, mas com certeza estaria orgulhosa.

Obrigada às minhas amigas e aos meus amigos presentes nessa trajetória. Ousarei citar alguns nomes, com muito medo de que minha memória não seja proporcional ao carinho que sinto. Gabriel Fagundes, que tem caminhado comigo nessa confusão que inventamos, aqui chegamos! Alice Cançado, mais tempo ainda por perto, confio e me apoio em ti. Giovanna Cotta, Dani Telles, Aninha Avelar e Juliana Pereira, não pensaria em encontrar por aí pessoas com as quais em me identificasse tanto. Alberto de Paula, coautor do meu principal artigo, obrigada pela parceria, você quer par ou ímpar? Sheilla Oliveira, minha irmãzinha científica que me mata de raiva, mas que me acompanha, apoia e deu alguns palpites certeiros.

Luca, que fez com que eu me sentisse sempre tão bem e tão inteligente, obrigada por seu enorme interesse em entender o que era o meu trabalho. Paulinho (literalmente todo dia ao meu lado), Anne e Egleidson, valeu pelas risadas das coisas mais absurdas que eu poderia ouvir. Itapecerica, Marcelo Dohanik, Mariana Barros, Ana Clara, Orlando, Renan e cia, físicas e físicos que coloriram os corredores do ICEx e os meus almoços às 11h. Gláucia Murta, fico feliz de ter sido sua primeira coautora. Willian Leal, que morre de saudade de mim, mas só aparece virtualmente me fazendo rir horrores até hoje. Pedro Daldegan, Sheila Maciel e toda a turma do forró, samba, zouk, só fizeram com que tudo isso fosse mais alegre. Andréia Castro, por causa das suas aulas posso cantar “home, home again...” sem passar (tanta) vergonha. Davi de Castro, Gilberto Borges e Juliana Freitas, fazem minha mente transceder e sonhar com um mundo melhor. De cada um que expliquei ou não, guardo com carinho cada conversa, cada dança, cada sorriso, cada abraço.

Obrigada a todas as trabalhadoras e a todos os trabalhadores que auxiliaram minha jornada através de seus serviços. Pouco valor se costuma dar ao seu trabalho, mas quero lembrar que ele é imprescindível para toda e qualquer tarefa que se pretenda realizar. Desses pessoas, ressalto meus agradecimentos à Cledir, que sempre fez com que minha sala estivesse limpinha.

Agradeço à da minha bicicleta, companheira sob sol e chuva, noite, dia e madrugada. Obrigada por me levar para cima e para baixo e ajudar a oxigenar meu cérebro, para que eu pudesse pensar melhor. Obrigada também à quem construiu o ICEx de forma tão aleatória, criando passagens

secretas e labirintos. Cada parede desses corredores e salas carrega uma história muito especial, fazendo com que o aprendizado aqui fosse tão prazeroso para mim.

Obrigada aos grupos e às pessoas que foram de extrema importância para minha saúde emocional, em especial agradeço ao meu psicólogo, ao Picadeirro e ao Centro Espírita Manoel Felipe Santiago (CEMFS). Agradeço às mulheres que lutaram em prol do feminismo e também ao coletivo feminista Lise Meitner. Obrigada às pessoas que pagam impostos, espero um dia poder retribuir para a sociedade o que investiram em mim. Agradeço às agências de fomento financeiro: CAPES, CNPq e FAPEMIG.

E por último, obrigada à Deusa, mais conhecida como Deus. Obrigada pela sua criação, meu objeto de estudo. Sem suas obras nada disso seria possível e nem impossível, não faria sentido existir e nem mesmo não existir.

Resumo

Nesta tese estudamos quenches locais sobre sistemas quânticos de muitos corpos. Investigamos, após um quench local, a variação da entropia de von Neumann do estado reduzido de um subsistema contido em um sistema geral de spin de muitos corpos. Encontramos desigualdades do tipo Lieb-Robinson que são independentes do volume do subsistema. Essas desigualdades crescem exponencialmente com o tempo, mas decrescem exponencialmente com a distância do subsistema à região onde o quench é realizado. O fato de que as desigualdades são independentes do volume do subsistema garante uma limitação na propagação de informação em sistemas de muitos corpos mais forte do que se é conhecido previamente. Em particular, mostramos que o emaranhamento em sistemas bipartites satisfaz um “cone de luz” efetivo, independente do tamanho do sistema.

Um modelo particular de sistema de muitos corpos é o modelo de Ising quântico em cadeias unidimensionais. Nós encontramos um novo fenômeno para ele, o qual denominamos de *propriedade de blindagem*. Suponha que o sistema se encontre no estado de Gibbs e que o campo magnético externo aplicado em um certo sítio dessa cadeia seja nulo, então não importa quais são as interações nem os campos magnéticos aplicados nessa cadeia, os estados reduzidos das subcadeias à esquerda e à direita desse sítio são exatamente o estado de Gibbs de cada subcadeia sozinha. Sendo assim, mesmo que a interação entre os sítios extremais das subcadeias seja arbitrariamente forte, o estado de Gibbs de cada subcadeia se comporta como se não houvesse interação entre as subcadeias. Em geral, considere uma rede que pode ser dividida em duas regiões desconexas e separadas por uma interface. Se essa interface possui apenas um sítio e o campo magnético externo nesse sítio se anula, então nós garantimos para essas redes o mesmo resultado válido para cadeias. Quando essa interface possui mais de um sítio, a propriedade de blindagem é satisfeita, sob certas hipóteses, para o estado fundamental. Uma situação particular em que essas hipóteses são satisfeitas ocorre quando o sistema é livre de frustração.

Abstract

In this thesis we have studied local quenches on quantum many body systems. We have investigated the variation of von Neumann entropy of subsystem reduced states of general many-body lattice spin systems due to local quantum quenches. We obtained Lieb-Robinson like bounds that are independent of the subsystem volume. More specifically, the bound exponentially increases with time but exponentially decreases with the distance between the subsystem and the region where the quench takes place. The fact that the bounds are independent of the subsystem volume leads to stronger constraints (than previously known) on the propagation of information throughout many-body systems. In particular, it shows that bipartite entanglement satisfies an effective "light cone", regardless of system size.

A particular model for a quantum many body system is the quantum Ising model. We have found a new phenomenon for it, which we have called *shielding property*. Namely, suppose that the state of the system is the Gibbs state and that the field in one particular site is null, then whatever the fields on each spin and exchange couplings between neighbouring spins are, the reduced states of the subchains to the right and to the left of this site are exactly the Gibbs states of each subchain alone. Therefore, even if there is a strong exchange coupling between the extremal sites of each subchain, the Gibbs states of the each subchain behave as if there is no interaction between them. In general, if a lattice can be divided into two disconnected regions separated by an interface of sites with zero applied field, we can guarantee the same result if the surface contains a single site. When there are more sites in the interface, the system satisfies the shielding property for the ground state under some conditions. We show that one particular situation where the system satisfies these required conditions is when it is frustration free.

Contents

Introduction	1
1 Preliminaries	3
1.1 Definitions and Experimental Motivation	3
1.2 Global and Local Quenches; Effective Light-Cone	8
2 Bounding Entanglement Spreading After a Local Quench	14
2.1 Norms of Operators	16
2.2 Lieb-Robinson Bounds	16
2.3 The von Neumann Entropy and Continuity Inequalities	18
2.4 A Bound for the Variation of Von Neumann Entropy under Local Quenches	19
2.5 Discussion	26
3 A Shielding Property for Thermal Equilibrium States on the Quantum Ising Model	29
3.1 The Ising Models	30
3.2 Further Definitions: Subsets and Gibbs State	32
3.2.1 Subsets of the Lattice	32
3.2.2 Gibbs State	33
3.3 Dynamics After a Local Quench on Systems with Locally Commuting Hamiltonians	33
3.4 The Equilibrium States of Locally Perturbed Systems	36
3.4.1 The Shielding Property for Thermal Equilibrium States on the Quantum Ising Model	37
3.4.2 The Shielding Property on General Lattices with One Site in the Interface	42

3.4.3	The Shielding Property for an Open Chain of Three Spins	44
3.5	Duality for the Tranverse Ising Model	45
3.6	Inconclusive Proofs for Lattices with More Sites in the Interface	47
3.7	Correlations and the Shielding Property	51
3.8	The Parity Operator and the Shielding Property	52
3.9	Implicit Dependence	58
3.10	Frustration Free Satisfy the Shielding Property	60
Conclusions		62
A	Detailing the Hypothesis for the Proof of Lieb-Robinson Bound	64
B	Thermal Equilibrium States	67
C	Calculations for the Ising Model in a Chain with Three Sites	69
D	Calculations for the Ising Model in a Lattice with Four Sites	73
E	Calculation for the Ising Lattice with Implicit Dependence	77

Introduction

In the field of quantum many body systems we study and understand a lot of curious quantum phenomena and properties of matter. It has a vast range of applications, which goes from the control of the matter states to the transmission of quantum information. It is important to the fundamental physics point of view and to the construction of new technologies.

The non-equilibrium dynamics of a many body system has a wide variety of techniques to deal with it and one important case is to follow a perturbation of an equilibrated system. It is common to assume an abrupt perturbation, usually called a quench. It is a *global* quench if the perturbation is made in the whole system and *local* if it is made only on a small portion of the system.

One daily experience which we have with local quenches, not necessarily quantum, is the keyboard of our computer. We press a button and it makes a fast change in the system near that key. This changing “flows” along the system providing the desired modifications to perform the computation tasks. To be able to predict how this quench in the keyboard button would provide changes in the system and make the right task, someone had to study this perturbation flows along this system. However, if we want to build a *quantum* computer, we have to know how quenches flow along quantum systems, since their components must be modelled by Quantum Mechanics.

One question raised is how long a local quench takes to “arrive” in a distant part of the system. That is, if we can measure just one distant part of the system, how long we have to wait until our measurement is able to give us certainty that a quench, and which quench, was done in that first part. In the example of the computer, if someone has access only to the screen of this computer, how much time she/he have to wait to know that another person had typed a letter in the keyboard and which letter was typed.

Schrödinger’s equation is non-relativistic, so, in principle, it does not forbid instantaneous

propagation of information across space. On the other hand, the seminal paper by Lieb and Robinson [1] suggests that a *de facto* causality should be valid when a perturbation propagates on a many-body system with short-range interactions. Further refinements [2] of their work led to a number of results, collectively known as Lieb-Robinson bounds. In reference [3] the authors show that if a many-body system satisfies a Lieb-Robinson bound, there is indeed a limit for the speed of propagation of (any significant amount of) information, giving rise to the notion of an *effective light-cone*. Applications of Lieb-Robinson bounds include clustering of correlations for the ground state of gapped systems⁶ [4]. It can also be used to show an *area law*, again for ground states of gapped systems, which means that the entropy of some region of this system grows proportionally with the area of this region, not its volume [6].

Lieb-Robinson bounds guarantee that information in systems with short-range interactions flows with a finite velocity. A particular family with this behaviour are systems with locally commuting Hamiltonians, that is, systems such that the terms of the Hamiltonian which are non-trivial in different subsets of the system commute with each other, even if these subsets have non-null intersection. In these cases a local perturbation in one subset, respecting commutation, does not change the state of subsets outside it. One example of system like this is the quantum Ising chain when we force the external magnetic field in one site to be null. Thus, changing parameters in one side of the chain, relative to that site where the external magnetic field is null, does not change the reduced state of the other side. Furthermore, we will see that the quantum Ising model has an equilibrium property related to this dynamical behaviour, which other models with locally commuting Hamiltonians do not exhibit, called *shielding property*.

In Chapter 1 we will give some important definitions with some experimental motivations. We also discuss and give examples of global and local quenches and effective light-cones. In Chapter 2 we explain in details the Lieb-Robinson bounds and the concept of effective light-cone. After it we are able to show our first result, published in [7]. In Chapter 3 we discuss the locally commuting Hamiltonians and show one second main result, the shielding property of the quantum Ising model. This result is published in [8]. In the rest of the chapter we discuss further refinements and consequences of it. In the end we present our conclusions.

⁶An equivalent relation between spectral gap and exponential decay of correlations is already presented in Quantum Field Theory [5].

Chapter 1

Preliminaries

In this chapter we discuss some important concepts for the development of this thesis. In the first section we define the family of systems we work with and experimental implementations. Since our definitions are quite general and abstract, we show some examples. After it, we discuss global and local quenches. We give examples of them and their implications on the spreading of correlations and entanglement, obeying a so called light-cone effect.

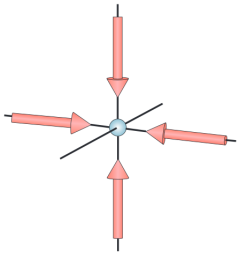
1.1 Definitions and Experimental Motivation

Ultracold quantum gases can be stored in artificial potentials of light [9] and are good experimental examples of lattice systems. In Figure 1.1 we can see two or three orthogonal standing waves superimposed, which create optical lattice potentials. Cold neutral atoms can then be trapped in these potentials. These lattices can be described by the mathematical sets \mathbb{Z}^2 and \mathbb{Z}^3 , respectively.

In these examples the lattice is given by the spatial position of the minimum of the optical potentials, that is, the probable position of the atoms. But we could prefer to define some lattice systems in a more abstract way. For example, a chain with long range interaction could be described by a lattice of higher dimension where the interactions are of first neighbours¹. However,

¹Actually, any many body system with N bodies can be described by a lattice of dimension N and interactions of first neighbours. Put site i in the position 1 of the i -th axis and connect the sites by an arrow when they have interactions between each other.

a)



b)

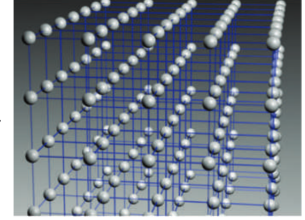
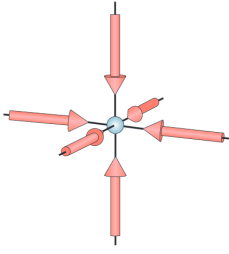
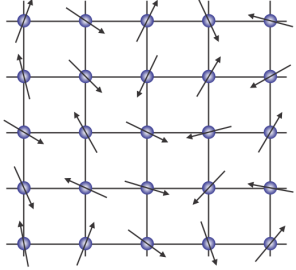


Figure 1.1: Optical lattices created superimposing two or three orthogonal standing waves. **a)** Two dimensional case; the potential minima are like tubes along the space and are well described by the lattice \mathbb{Z}^2 . **b)** Three dimensional case; here the potential minima are well described by \mathbb{Z}^3 and have the same illustration of this lattice. (Figure extracted from reference [9]).

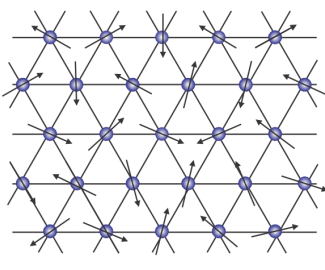
if the reader prefers keep in mind a lattice which describes spatial positions, there is no problem for the purposes of this thesis.

Some examples of two dimensional lattices can be viewed in Figure 1.2. The first is a square lattice, the same as Figure 1.1.a. The second is a triangular lattice and the third a Kagome lattice. The last one is a Bethe lattice, and it is contained in a family of lattices which we give as an example in Example 3 of the next chapter. For the biggest part of this thesis, however, we will not work with a particular lattice. Our results hold quite generally, for a wide class of lattices.

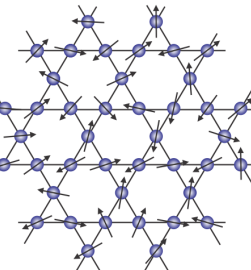
a)



b)



c)



d)

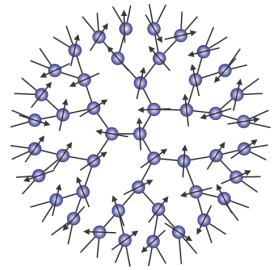


Figure 1.2: Examples of two dimensional lattices. The arrows illustrate the spin of each site, example to be considered latter. **a)** Square lattice, also called \mathbb{Z}^2 ; it is the lattice which describes Figure 1.1.a. **b)** Triangular lattice. **c)** Kagome lattice. **d)** Bethe lattice; this lattice is contained in a family of lattices which we give as an example in the end of next chapter, in Example 3.

The letter we will use to denote the lattice of the whole system is Γ and, at least theoretically, it can have an infinite size. On the other hand, to properly define the mathematical objects, we will work most part of the time on a finite part of this lattice, which we will denote by Λ .

The distance $d(i, j)$ between two sites $i, j \in \Gamma$ is defined by the number of edges of a shortest path connecting these two sites. In Figure 1.3 we illustrate this definition for the lattices of Figure 1.2. In the middle of each lattice we have site i in black. The sites in pink are in a distance 1 from i , the blue ones are in a distance 2 from i , and so on.

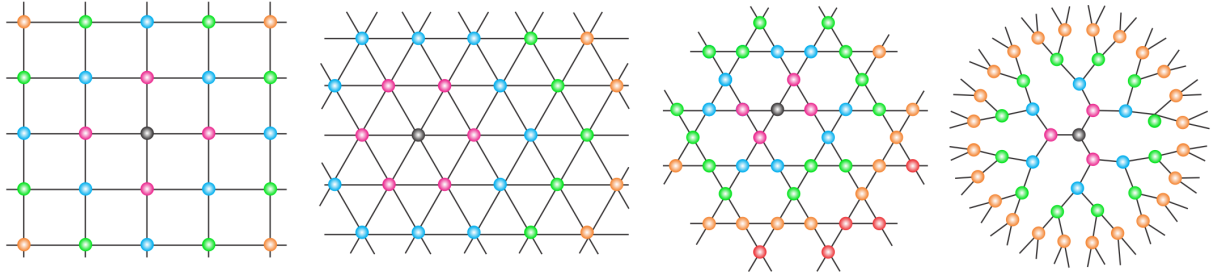


Figure 1.3: For each lattice of Figure 1.2 we consider a site i coloured of black and the sites of distance d from this site coloured of the same color. For $d = 1$ they are coloured pink, for $d = 2$ they are coloured blue, and so on.

To each site $i \in \Gamma$ we will associate a Hilbert space \mathcal{H}_i . In the example of a quantum gas we could have a sufficiently high potential such that each atom occupies one site of the lattice and each site contains only one atom (Figure 1.4.a) [9, 10]. It could be done in a way such that the relevant physical degree of freedom is only the spin of these atoms or of their valence electrons. In this case the Hilbert space of each site i is the space of the atomic spin. This situation is illustrated in Figure 1.2, where the arrow in each site represents the magnetization of that site.

Another example given is if the potential is not too high and the atoms are able to move from one site to another with some probability (Figure 1.4.b). The Hilbert space to be considered here would be the Fock space [11].

In any case, the Hilbert space of the system correspondent to the lattice Λ is given by the tensorial product of the Hilbert space of the sites contained on it

$$\mathcal{H} = \bigotimes_{i \in \Lambda} \mathcal{H}_i \quad (1.1)$$

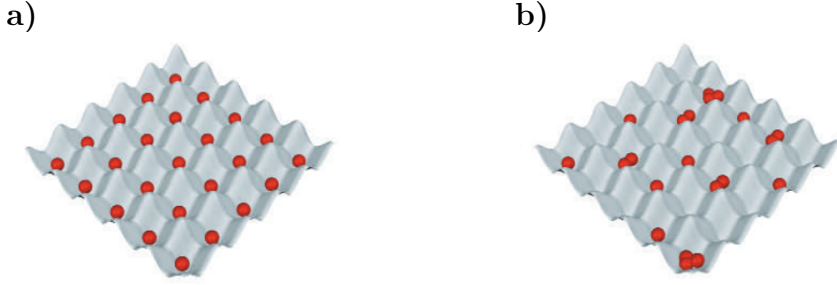


Figure 1.4: Two dimmensional optical lattice. **a)** If the lattice depth is high it is possible to arrange the atoms such that we have only one occupation per site. **b)** If the lattice depth is not too high, it is possible to the atoms to hop from one site to another, creating a non-trivial occupation of the sites. (Figure extracted from reference [9]).

This is a finite tensorial product and if each \mathcal{H}_i has finite dimension, then also \mathcal{H} has finite dimension. We do not define the Hilbert space of the whole system, since it is not always well defined if Γ has infinite size.

To each finite set $X \subset \Gamma$ we define an interaction by a self-adjoint operator $\Phi(X)$ on \mathcal{H}_X . For every finite $\Lambda \subset \Gamma$ the Hamiltonian of that portion of the system is defined by

$$H_\Lambda = \sum_{X \subset \Lambda} \Phi(X) \otimes \mathbb{1}_{\Lambda \setminus X}. \quad (1.2)$$

For every operator A which can be written as $A_X \otimes \mathbb{1}_{\Lambda \setminus X}$, where A_X is not the identity operator on \mathcal{H}_X , we say that it has support X and denote it by $\text{supp}(A) = X$.

Note that we have defined two finite sets, Λ and X , contained in Γ , and the purposes of these definitions must be clarified. We use Λ to denote a “big” subset, in the sense that it can be arbitrarily large. Moreover, once we deal with short-range interactions we would have that $\Phi(\Lambda) = 0$. The set X is any set contained in Λ . For short range interactions only the small sets X are relevant.

Now, an important example is the Bose-Hubbard model, which describes a gas of bosons where the particles can occupy positions in the sites of some lattice. Let the finite lattice Λ which we are considering this model be given as in figure Figure 1.4.b., that is, $\Lambda = \{1, 2, 3, 4, 5\}^2$, a subset of $\Gamma = \mathbb{Z}^2$. The Hilbert space of this model is given by the Fock space and its Hamiltonian is given

by

$$H = -J \sum_{\substack{\langle i,j \rangle \\ i,j \in \Lambda}} a_i^\dagger a_j \otimes \mathbb{1}_{\Lambda \setminus \{i,j\}} + \frac{1}{2} U \sum_{i \in \Lambda} n_i(n_i - 1) \otimes \mathbb{1}_{\Lambda \setminus \{i\}}. \quad (1.3)$$

The operator a_i^\dagger is the creation operator and it creates one particle in the site i . The operator a_j is the annihilation operator and it destroys one particle in the site j . These two operators together $a_i^\dagger a_j$ act moving one particle from site j to site i . The index $\langle i,j \rangle$ under the summation means that we are summing only over first neighbours. So, the first terms of Hamiltonian (1.3) mean that the particles can hop only to neighbouring sites of its current localization. The parameter J is the strength of this hopping amplitude.

The number operator is given by $n_i = a_i^\dagger a_i$, while the term $\frac{1}{2}U n_i(n_i - 1)$ represents the interaction among the particles occupying the same site i . Note that if the number of particles in a site is N then the number of interactions is $\frac{1}{2}N(N - 1)$, since one particle do not interact with itself and the factor $\frac{1}{2}$ appears to avoid counting twice the same interaction between two particles. The parameter U which appears in the Hamiltonian is the strength of these interactions.

It is usual to hide the identity operators when writing a Hamiltonian, then it is more common to find the Hamiltonian of the Bose-Hubbard model written as the following.

$$H = -J \sum_{\substack{\langle i,j \rangle \\ i,j \in \Lambda}} a_i^\dagger a_j + \frac{1}{2} U \sum_{i \in \Lambda} n_i(n_i - 1) \quad (1.4)$$

The interactions $\Phi(X)$ and sets X of this example have the following relation.

$$\Phi(X) = \begin{cases} \frac{1}{2}U \cdot n_i(n_i - 1) & \text{if } X = \{i\}; \\ -J \cdot a_i^\dagger a_j & \text{if } X = \{i, j\}, i, j \text{ neighbours;} \\ 0 & \text{on the other cases.} \end{cases} \quad (1.5)$$

Note that the interactions between the sites of the lattices do not necessarily correspond to the interactions between the atoms. However, for a spin lattice system, the interactions between the sites can be the interactions between the atoms or electrons. In the next section we shall discuss an example in more details.

Finally, we make a summary of all the definitions we have made in this section:

- Lattice Γ (it can have infinite size);

- Finite subset $\Lambda \subset \Gamma$;
- Finite subset $X \subset \Lambda \subset \Gamma$;
- Sites $i, j \in \Gamma$;
- Distance $d(i, j) =$ number of vertices of a shortest path connecting i and j ;
- $\mathcal{H}_i =$ Hilbert space of site i ;
- $\mathcal{H} = \bigotimes_{i \in \Lambda} \mathcal{H}_i =$ Hilbert space of Λ (it has finite dimension, if each \mathcal{H}_i also has finite dimension);
- Self-adjoint operator $\Phi(X) =$ interaction among sites of set X ;
- $H_\Lambda =$ Hamiltonian of set Λ .

1.2 Global and Local Quenches; Effective Light-Cone

In this section we discuss two works in the literature to show examples of global and local quenches on lattice systems. Furthermore, in these references they compute the velocity of correlations, magnetization and entanglement spreading, being also examples of effective light-cones.

One of them is an experimental realization of an effective light-cone [10] while the other one is a numerical computation via t -DMRG method [12]. Both of them deal, of course, with specific systems and models, in contrast with our work described in Chapter 2 where we consider a large class of lattice models. We compute a rigorous bound for the velocity of a class of effective light-cones, which is not tight, while in references [10, 12] they compute the velocity of the effective light-cones of their respective models.

In reference [10] it is experimentally implemented a global quench on a system which is well described by the Bose-Hubbard model (Equation (1.4)). As we mentioned in the beginning of the previous section, it is possible to trap ultracold atoms in optical lattices. The authors of [10] have made this with atoms of Rubidium ^{87}Rb and aligned them in a chain. In the various realizations which they have done, the number of atoms in each chain ranged between 10 to 18.

At the begining of the experiment, they put the system in equilibrium for a high value for the depth of barrier between the sites. Suddenly, they decrease the depth of this barrier to some lower value, which is the global quench which they have done, as we can see in Figure 1.5.a. This quench gives rise to the creation of entangled quasi-particles in the sites of the chain (Figure 1.5.b). These

quasi-particles are called hollons and doublons, which correspond to a null and a double on-site occupation, respectively.

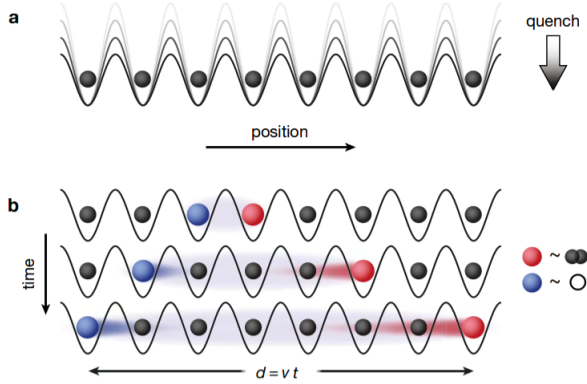


Figure 1.5: **a)** Global quench done in the system. Initially the barrier between the sites had a certain depth. Suddenly it gets smaller. **b)** The quench creates entangled quasiparticles which propagate in opposite directions. These quasiparticles are called hollons and doublons, which are states of null and double occupations in some site, respectively. (Figure extracted from reference [10]).

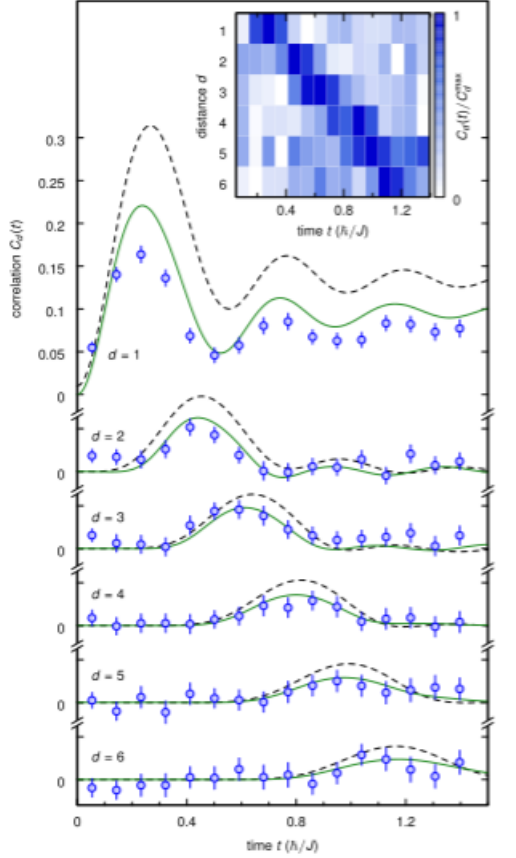


Figure 1.6: Correlations in the system after the quench of Figure 1.5, for sites of distances d from each other for many values of d . We can see that correlations propagate across the system. (Figure extracted from reference [10]).

After a variable evolution time, the authors rapidly raise the height of the barrier to “freeze” the density distribution. Finally they detect the atoms by fluorescence imaging. With the data of many realizations in hand they could compute the average of correlations between sites of distance d , for various values of d . Their results are shown in Figure 1.6. We can see that the peak of correlations behave as propagating along the system, from closer sites to more distant sites as a function of time. This is the first experimental observation of an effective light-cone for the spreading of correlations.

In reference [12] it is considered the spin-1/2 XXZ chain and open boundary conditions, which

is given by the Hamiltonian

$$H = \sum_{i=1}^{N-1} \sigma_i^x \sigma_{i+1}^x + \sigma_i^y \sigma_{i+1}^y + \Delta \sigma_i^z \sigma_{i+1}^z. \quad (1.6)$$

Each term of this equation represents a spin interaction between the labelled sites in the labelled directions. In this case these interactions are between first neighbours only, they have strength 1 in the x and y -directions and strength Δ in the z -direction. The value of Δ defines the phase of the system at zero temperature. For $\Delta \leq -1$, the system is in a ferromagnetic phase, where all spins tend to align in the z -direction; for $\Delta > 1$ the system is in a antiferromagnetic phase, where the spins tend to anti-align in the z -direction; and for $-1 < \Delta \leq 1$ the system is in a critical phase, where the spins do not have a clear alignment between each other (actually, the spins have null expected value in this phase). See Figure 1.7 for an illustration of these phases.

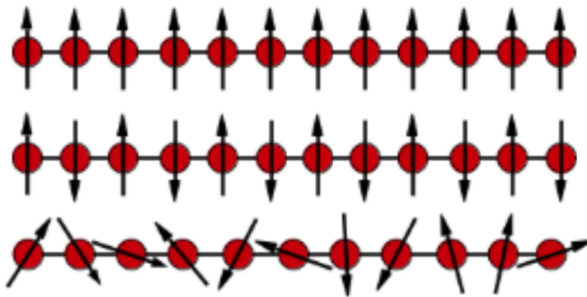


Figure 1.7: Illustration of the three phases of the Hamiltonian (1.6). The first chain, where all spins are aligned, represents the ferromagnetic phase; the second, where all spins are aligned but in opposite directions when they are first neighbours, represents the antiferromagnetic phase; the last one, where there are no well defined alignment for the spins, represents the critical phase (the spins have null expected value in this phase). It is also a good illustration for some phases of the Ising model: ferromagnetic, antiferromagnetic and paramagnetic, which we comment in Section 3.1. (Adapted figure from reference [12]).

The authors of [12] considered two finite chains, one in the ferromagnetic phase and the other in the critical phase, which was separated and in the ground state for $t < 0$. At $t = 0$ they join these two chains creating an interaction between the sites at the boundary of each chain, as illustrated in Figure 1.8. More precisely, the Hamiltonian of this chain is given by

$$H(t) = H_L + \Theta(t) (\sigma_i^x \sigma_{i+1}^x + \sigma_i^y \sigma_{i+1}^y + \delta \sigma_i^z \sigma_{i+1}^z) + H_R, \quad (1.7)$$

where H_L and H_R are Hamiltonians of the form (1.6) for the left and right chains, respectively, i is the index of the most right site of the left chain and δ is some constant. $\Theta(t)$ is the step function. It is zero for $t < 0$ and equal 1 for $t \geq 0$. Therefore, this is indeed a local quench. The left chain is chosen to be in the ferromagnetic phase, so the parameter $\Delta = \Delta_L$ of H_L is lower than -1 . The right chain is chosen to be in the critical phase, so the parameter $\Delta = \Delta_R$ of H_R is between -1 and 1 .

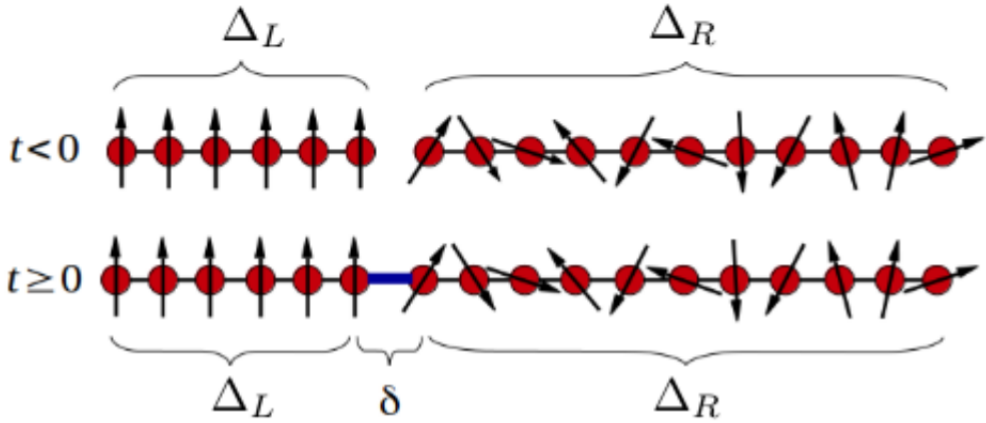


Figure 1.8: Illustration of the local quench considered by the authors of [12]. In the first moment ($t < 0$) the two chains are decoupled and in their respective ground states. For $t \geq 0$ there is a coupling between the two chains. In the equation of the Hamiltonian (1.7) it is described by the term $\Theta(t)$ which was null for $t < 0$ and equal 1 for $t \geq 0$. (Figure extracted from reference [12]).

For $t < 0$ the system is in equilibrium and the authors calculated via DMRG the ground state of this system. For $t \geq 0$, after the quench, they calculated the evolved state of the system via t -DMRG. We can see the effective light-cone of this system in Figure 1.9.

A color map of the expected value of the magnetization and of the variation of von Neumann entropy of each site of the right chain as a function of time is shown in Figure 1.9.a. and c., respectively. These maps were made for the values of $\Delta_L = -20$, $\Delta_R = 0.5$ and $\delta = \Delta_R$. This variation of entropy in each site is the entropy of this site for the evolved state subtracted by the entropy of this same site for the ground state. The solid line in these maps shows a linear fit of the “wave front”. The dotted lines indicate cuts in time and the spin profile of these cuts are shown in Figure 1.9.b. and d., respectively.

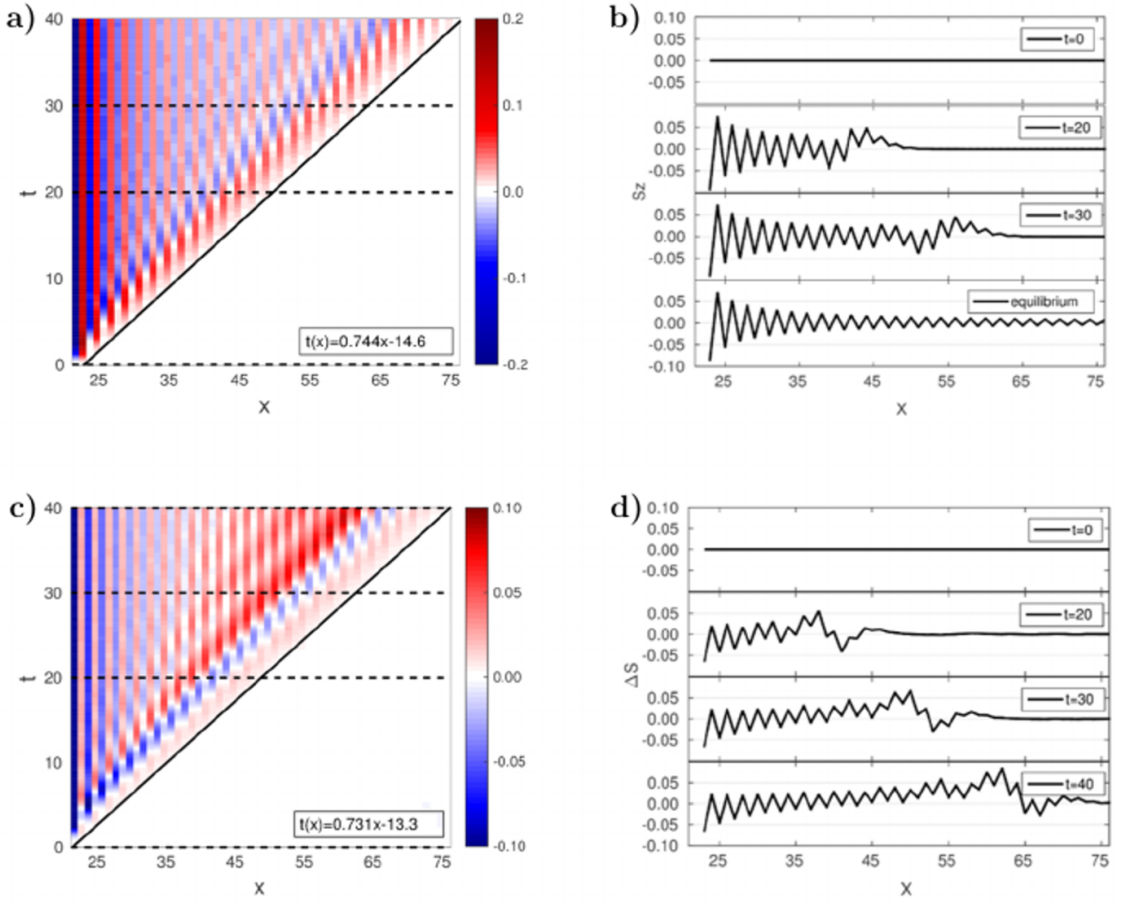


Figure 1.9: Color maps and profiles of spin and variation of von Neumann entropy in the right chain for the parameters $\Delta_L = -20$, $\Delta_R = 0.5$ and $\delta = \Delta_R$. **a)** Color map of the magnetization of each site as a function of time. Lines represent cuts in time and their profiles are given in item b. **b)** Profile of the magnetization of each site for certain values of time, indicated in item a. **c)** Color map of the variation of von Neumann entropy of each site as a function of time. The dotted lines represent cuts in time and their profiles are given in item d. **d)** Profile of the variation of von Neumann entropy of each site for certain values of time, indicated in item c. (Figure extracted from reference [12]).

We can see that when the system is in the ground state (Figure 1.9.b. and d., first panel) the magnetization and variation of entropy are null. For the evolved state after the quench (second panel) we can see that these quantities have considerable values for sites closer the quench and they are almost zero for the distant sites. In the third panel the situation is similar, but both

quantities are significantly non-zero in more sites than before. In the fourth panel the “wave” front has already reached all the sites.

Chapter 2

Bounding Entanglement Spreading After a Local Quench

Entanglement is a fundamental quantity of quantum information and computation, being essential to perform tasks such as teleportation or superdense coding [13]. In recent years it is becoming increasingly relevant also to quantum many-body physics. It can be a good order parameter for quantum phase transitions [14]. Algorithms for computing one-dimensional quantum many body ground states, such as the density matrix renormalization group (DMRG) [15] method or the variational calculus over matrix product states (MPS) [16], have their efficiency based essentially on the spatial scaling of entanglement within these states [17]. It is a key ingredient for the (subsystem) thermalization of many-body isolated quantum systems [18].

Entanglement may also be of interest for non-equilibrium phenomena [19, 20]. The spatial scaling of entanglement within the eigenstates of a many-body Hamiltonian, as well as its growth in time, is a signature of the many-body localized phase [21]. The dynamics of entanglement due to global or local quenches may be computed by conformal field theory techniques [22], or by the time variants of DMRG or MPS based algorithms [23], or at least have its growth bounded [3, 24].

The behavior of a many-body system after a quantum quench can raise fundamental questions, such as whether the system equilibrates or not (see, e.g., [25]). It can be investigated with increasing detail in modern experimental settings such as ultracold atoms in optical lattices [10] or trapped ions [26]. Moreover, novel numerical techniques, such as t -DMRG, allow one to simulate the evolution of significantly large systems, especially spin chains [23, 27]. In simulations of

quantum chains by t -DMRG the entanglement of every bipartition of the chain (in two contiguous regions) is naturally computed for every instant of time. After a local quantum quench, it can be seen that entanglement of these bipartitions satisfies an effective “light-cone” in the same way as any other local quantity of the system, such as magnetization, as we have explained in the last chapter.

In [3] this light-cone effect can be partially explained for a local quench on the initial state of the system. There, a unitary operation with support on a small region of the system can be applied, with the purpose of establishing a communication channel between distant regions of the system. The authors of [3] estimate the variation of quantum entropy—with respect to the evolutions with and without an applied unitary—for any region away from the quench. They found a bound for its growth in time assuming a Lieb-Robinson bound [1] for the model. However, their bound is proportional to the volume of the region, restricting its validity. For instance, it cannot be applied if one takes the thermodynamic limit of the subsystem. Moreover, the bound could not be used to guarantee an area law for entanglement [6] of the evolved states, since it is proportional to the subsystem volume.

Here we provide Lieb-Robinson-like bounds for the variation of quantum entropy of the reduced states of any region away from a quench. We consider two kinds of quenches: a local perturbation on the Hamiltonian and on the initial state. We assume only that the model satisfies a Lieb-Robinson bound and that the volume of lattice spheres grows at most exponentially with their radius.

We discuss three consequences of the bounds. First, we show the validity of an effective light-cone for entanglement, in a sense we shall explain in detail later. Second, we point out how the bounds guarantee, for every instant of time, an area law for entanglement of the evolved states, as long as the initial state also satisfies an area law and is an eigenstate of the Hamiltonian. And third, we discuss how the bound implies a strong restriction on the information capacity of quantum channels established between distant regions of a many-body system.

This chapter is organized as follows. In Section 2.1 we defined some norms of operators, in Section 2.2 we state a Lieb-Robinson bound and in Section 2.3 we state further necessary concepts and results. In Section 2.4 we prove bounds for the variation of entanglement after a local quench and point out some special cases. In Section 2.5 we discuss implications of the bounds obtained.

2.1 Norms of Operators

In this section we will give some definitions and necessary results. Denote by $L(\mathcal{X}, \mathcal{Y})$ the set of linear operator $A : \mathcal{X} \rightarrow \mathcal{Y}$, between two Hilbert spaces \mathcal{X} and \mathcal{Y} . When $\mathcal{X} = \mathcal{Y}$, denote $L(\mathcal{X}, \mathcal{X})$ by $L(\mathcal{X})$. Denote by A^* the adjoint operator of A . The set of *unitary operators* $U(\mathcal{X})$ is a subset of $L(\mathcal{X})$, which has the property that $UU^* = U^*U = \mathbb{1}_{\mathcal{X}}$, for all $U \in U(\mathcal{X})$.

The *trace norm* is defined by

$$\|A\|_1 = \text{Tr}(\sqrt{A^*A}). \quad (2.1)$$

When $A \in L(\mathcal{X})$, there is another useful and equivalent form for the trace norm given by

$$\|A\|_1 = \max\{|\text{Tr}(AU)| : U \in U(\mathcal{X})\}. \quad (2.2)$$

The *spectral norm* is defined by

$$\|A\|_{\infty} = \max\{\|Au\| : u \in \mathcal{X}, \|u\| = 1\}. \quad (2.3)$$

We will denote $\|A\|_{\infty}$ only by $\|A\|$ for simplicity¹.

To read more details about these norms and demonstrations of the above statements, see reference [28].

You will see that in Equations (2.4) and (2.6) we use the same notation “ $\|\cdot\|$ ” to another quantities, which are not norms in general. We will keep these double notations in order to maintain consistence with the literature.

2.2 Lieb-Robinson Bounds

In the following we shall state and explain the Lieb-Robinson bounds derived in references [2, 29]. The large class of quantum many-body systems considered here are those defined in Section 1.1, with some additional assumptions.

In order to get a Lieb-Robinson bound, the interaction must decay fast enough with the diameter of finite subsets of Γ . This is encoded by a non-increasing function $F := [0, \infty) \rightarrow (0, \infty)$ that must satisfy, for some $\mu \geq 0$:

¹There is one family of norms called *Schatten p-norms* usually denoted by $\|A\|_p$ and the trace norm is the Schatten 1-norm. The spectral norm is the limit of $\|A\|_p$ when $p \rightarrow \infty$, which justify its name.

$$\|F\| := \sup_{i \in \Gamma} \sum_{j \in \Gamma} F(d(i, j)) < \infty, \quad (2.4)$$

$$C_\mu := \sup_{i, j \in \Gamma} \sum_{k \in \Gamma} \frac{e^{-\mu[d(i, k) + d(k, j) - d(i, j)]} F(d(i, k)) F(d(k, j))}{F(d(i, j))} < \infty. \quad (2.5)$$

With such an F , the following condition guarantees a fast enough decay of Φ :

$$\|\Phi\|_\mu := \sup_{i, j \in \Gamma} \sum_{X \ni i, j} \frac{\|\Phi(X)\|}{e^{-\mu(d(i, j))} F(d(i, j))} < \infty. \quad (2.6)$$

To become more familiar with these hypothesis, consider a concrete example ². Take $\Gamma = \mathbb{Z}^d$ and $d(x, y) = |x - y|$. In this case we can chose the function $F(x) = (1 + x)^{-d-\epsilon}$ for any $\epsilon > 0$. We can see directly that this function satisfy Equation (2.4). Moreover, we have that

$$C_0 \leq 2^{d+\epsilon+1} \sum_{n \in \mathbb{Z}^d} \frac{1}{(1 + |n|)^{d+\epsilon}} < \infty \quad (2.7)$$

which guarantees that condition (2.5) is also satisfied for $\mu = 0$. But note that $C_\mu \leq C_0$ for every $\mu > 0$, and this guarantee that $F(x)$ satisfy (2.5) for every $\mu \geq 0$.

Two types of systems which satisfy equation (2.6) in the lattice $\Gamma = \mathbb{Z}^d$ are:

- those with first neighbour interactions;
- those with interactions that decay exponentially.

We give more details of these examples in Appendix A.

We define the Φ boundary of a subset X by

$$\partial_\Phi X = \{i \in X : \exists Y \subset \Gamma \text{ with } Y \cap X^c \neq \emptyset, i \in Y \text{ and } \Phi(Y) \neq 0\}. \quad (2.8)$$

This is the set of sites contained in X which have interactions with other sites outside set X . It is a boundary defined by the interactions between the sites, not only by the geometry of the lattice.

²These hypothesis are quite abstract and one question which could arise is how someone has thought about them. It usually happens in this way: the mathematician has an intuition that the theorem is true and thinks about how to make the proof. During the calculations she/he perceives that with these technical conditions she/he can get into the desired conclusions. Thus, the mathematician puts these conditions as hypothesis of the Theorem and then the proof is done. In the particular case of Equations (2.4), (2.5) and (2.6), we do not know if it really happened in this way, but many times it is like this that technical conditions appear.

For example, consider a chain, that is, the lattice $\Gamma = \mathbb{Z}$, with first neighbours interactions. The Φ boundary of the set $X = \{5, 6, 7, 8, 9\}$ is the set $\partial_\Phi X = \{5, 9\}$. If we take an interaction of first and second neighbours in this same chain the Φ boundary of the set $X = \{5, 6, 7, 8, 9\}$ is the set $\partial_\Phi X = \{5, 6, 8, 9\}$.

Denote by $|X|$ the number of elements of a set X . Then, the following bound can then be obtained [2, 29]:

Lieb-Robinson Bounds. *Let $X, Y \subset \Lambda$ with $d(X, Y) > 0$; let A and B be operators defined on H_Λ with support on X and Y , respectively; and let $A(t) = e^{iH_\Lambda t} A e^{-iH_\Lambda t}$. Then, the following inequality holds true for every $\mu > 0$ and $t \in \mathbb{R}$:*

$$\|[A(t), B]\| \leq \frac{2\|A\|\|B\|\|F\|}{C_\mu} \min \{|\partial_\Phi X|, |\partial_\Phi Y|\} e^{-\mu(d(X, Y) - v_\mu|t|)}, \quad (2.9)$$

where $v_\mu = \frac{2\|\Phi\|_\mu C_\mu}{\mu}$.

Note that, in the right hand of the above equation, the only term with temporal dependence is $e^{-\mu(d(X, Y) - v_\mu|t|)}$. Since $d(X, Y)$ has unit of length, v_μ has unit of velocity. When we have small times t and large distances $d(X, Y)$ between the sets, the exponential will be very small, making the quantity $\|[A(t), B]\|$ correspondingly small. So, for $d(X, Y) > v_\mu|t|$ we would have insignificantly values for $\|[A(t), B]\|$ and it is what we are calling by effective light-cone.

The physical meaning of $\|[A(t), B]\|$ is not clear, but it is using the bound (2.9) that we can find similar bounds to other more intuitive quantities. In Section 2.4 we make exactly this. Using Equation (2.9) we find a bound to the variation of the von Neumann entropy of a state of a region Y when we compare its evolution with and without a local quench on a region X distant from Y .

2.3 The von Neumann Entropy and Continuity Inequalities

In thermodynamics, the entropy function was derived in order to define mathematically which state could evolve adiabatically to another state. If state R has more entropy than state R' , then there is an adiabatic process which makes R' evolve until R [30].

In quantum information we have an analogy. Let ρ and ρ' be pure states of bipartite systems. If ρ has more entanglement than ρ' , then there is an LOCC (local operations and classical communication) such that through this LOCC it is possible to convert the state ρ' into ρ [31]. The *von Neumann entropy* is the unique entanglement measure between a bipartition of a system when it is in a pure state. It is given by the expression

$$S(\rho) = -\text{Tr}(\rho \log_2 \rho) \quad (2.10)$$

So, for estimating the variation of entanglement we shall need continuity inequalities for quantum entropy. We will also bound the variation of reduced states of the system, measured by the trace norm. For this, we shall use two well known inequalities.

Suppose that the Hilbert space of the many body system has dimension D . The following continuity inequality holds [32]:

$$|S(\rho) - S(\rho')| \leq \frac{1}{2} \|\rho - \rho'\|_1 \log_2 (D - 1) + h\left(\frac{1}{2} \|\rho - \rho'\|_1\right), \quad (2.11)$$

where $h(x) = -x \log_2 x - (1-x) \log_2 (1 - x)$ is the binary entropy function. Moreover, the quantum conditional entropy $S_{X|Y}(\rho_{XY}) = S(\rho_{XY}) - S(\rho_Y)$, where ρ_{XY} is a state of a bipartite system XY and ρ_Y is the corresponding reduced state of part Y , satisfies the continuity inequality [33]:

$$|S_{X|Y}(\rho_{XY}) - S_{X|Y}(\rho'_{XY})| \leq 4 \|\rho_{XY} - \rho'_{XY}\|_1 \log_2 D_X + 2h(\|\rho_{XY} - \rho'_{XY}\|_1), \quad (2.12)$$

valid whenever $\|\rho_{XY} - \rho'_{XY}\|_1 < 1$, where D_X is the Hilbert-space dimension of part X .

2.4 A Bound for the Variation of Von Neumann Entropy under Local Quenches

To understand the spreading of correlations and transport on many-body systems one may resort, both theoretically and experimentally [10, 20], to follow the dynamics of the system after a local quench. One can distinguish two kinds of local quenches: a sudden local change on the Hamiltonian H and on the initial state $|\psi\rangle$ of the many-body system. That is, in the first case, from time $t = 0$ and on, the Hamiltonian changes to $H + W$. For the second case, an initial state $|\psi\rangle$ is quickly changed to $U|\psi\rangle$. Both W and U must have support on a small portion of the

system. In either case, we can compare the evolution of the system with and without the applied quench.

First we show that, for small times, the reduced state of regions far from the region where the quench takes place is slightly perturbed. Note that inequality (2.13) shown below corresponds for $q = 1$ to a quenched Hamiltonian while for $q = 2$ to a quenched initial state.

Lemma 1. *Let $(\Gamma, \{\mathcal{H}\}_{i \in \Gamma}, \Phi)$ be a model satisfying the conditions described in Section 2.2 and let Λ be any finite subset of Γ . Let $X, Y \subset \Lambda$ be two subsets with $d(X, Y) > 0$. Let W be a self-adjoint operator on \mathcal{H}_Λ and let U_X be a unitary operator, both of them with support on X . Let $|\psi\rangle$ be a unit vector of \mathcal{H}_Λ and denote $|\psi^0(t)\rangle = e^{-iH_\Lambda t} |\psi\rangle$, $|\psi^1(t)\rangle = e^{-i(H_\Lambda + W)t} |\psi\rangle$, $|\psi^2(t)\rangle = e^{-iH_\Lambda t} U_X |\psi\rangle$. Denote the reduced states on region Y as follows $\rho_Y^q(t) = \text{Tr}_{\Lambda \setminus Y}(|\psi^q(t)\rangle \langle \psi^q(t)|)$, for $q = 0, 1, 2$. For any $\mu > 0$ and $t \in \mathbb{R}$ the following inequality holds true:*

$$\|\rho_Y^0(t) - \rho_Y^q(t)\|_1 \leq c_q e^{-\mu(d(X, Y) - v_\mu |t|)}, \quad (2.13)$$

for $q = 1, 2$, where $c_1 = \frac{2\|W\|\|F\|}{\mu v_\mu C_\mu} \min\{|\partial_\Phi X|, |\partial_\Phi Y|\}$ and $c_2 = \frac{2\|F\|}{C_\mu} \min\{|\partial_\Phi X|, |\partial_\Phi Y|\}$.

Proof. First we show the inequality for $q = 1$. Let U_Y be an operator acting on \mathcal{H}_Λ with support on Y and let \tilde{U}_Y be its restriction to \mathcal{H}_Y . We have then [34]:

$$|\text{Tr}\{[\rho_Y^0(t) - \rho_Y^1(t)]\tilde{U}_Y\}| = |\langle \psi^0(t) | U_Y | \psi^0(t) \rangle - \langle \psi^1(t) | U_Y | \psi^1(t) \rangle| \quad (2.14)$$

$$= |\langle \psi | e^{iH_\Lambda t} U_Y e^{-iH_\Lambda t} - e^{i(H_\Lambda + W)t} U_Y e^{-i(H_\Lambda + W)t} | \psi \rangle| \quad (2.15)$$

$$\leq \|e^{iH_\Lambda t} U_Y e^{-iH_\Lambda t} - e^{i(H_\Lambda + W)t} U_Y e^{-i(H_\Lambda + W)t}\| \quad (2.16)$$

$$= \|e^{-i(H_\Lambda + W)t} e^{iH_\Lambda t} U_Y e^{-iH_\Lambda t} e^{i(H_\Lambda + W)t} - U_Y\| \quad (2.17)$$

$$= \left\| \int_0^t dt' \frac{d}{dt'} e^{-i(H_\Lambda + W)t'} e^{iH_\Lambda t'} U_Y e^{-iH_\Lambda t'} e^{i(H_\Lambda + W)t'} \right\| \quad (2.18)$$

$$= \left\| \int_0^t dt' e^{-i(H_\Lambda + W)t'} [H_\Lambda + W - H_\Lambda, U_Y(t')] e^{-i(H_\Lambda + W)t'} \right\| \quad (2.19)$$

$$\leq \left| \int_0^t dt' \right| \| [W, U_Y(t')] \|, \quad (2.20)$$

where $U_Y(t) = e^{iH_\Lambda t} U_Y e^{-iH_\Lambda t}$. Recalling that W has support on X , we can apply inequality (2.9) to the integrand of the last expression and get:

$$|\text{Tr}\{[\rho_Y^0(t) - \rho_Y^1(t)]\tilde{U}_Y\}| \leq \frac{2\|W\|\|F\|}{C_\mu} \min\{|\partial_\Phi X|, |\partial_\Phi Y|\} e^{-\mu d(X, Y)} \int_0^{|t|} e^{\mu v_\mu t'} dt'.$$

Finally, from trace norm characterization (2.2) and observing that $\int_0^{|t|} e^{\mu v_\mu t'} dt' \leq (\mu v_\mu)^{-1} e^{\mu v_\mu |t|}$ we get inequality (2.13).

For $q = 2$, take U_Y , \tilde{U}_Y and $U_Y(t)$ as above, so [3]:

$$|\mathrm{Tr}\{[\rho_Y^0(t) - \rho_Y^2(t)]\tilde{U}_Y\}| = |\langle\psi^0(t)|U_Y|\psi^0(t)\rangle - \langle\psi^2(t)|U_Y|\psi^2(t)\rangle| \quad (2.21)$$

$$= |\langle\psi|(U_Y(t) - U_X^*U_Y(t)U_X)|\psi\rangle| \quad (2.22)$$

$$\leq \|U_Y(t) - U_X^*U_Y(t)U_X\| \quad (2.23)$$

$$= \|U_XU_Y(t) - U_Y(t)U_X\| \quad (2.24)$$

$$= \|[U_X, U_Y(t)]\|. \quad (2.25)$$

Again, using the Lieb-Robinson bound (2.9) and expression (2.2) for the trace norm, we get inequality (2.13) for $q = 2$. \square

If we use Lemma 1 above directly with the continuity inequality (2.11) for entropy we obtain bounds for the variation of entropy that grow linearly with $|Y|$, since the right hand side of Equation (2.11) grows logarithmically with $\dim(\mathcal{H}_Y)$. In order to avoid this we can stratify Y in sets of increasing distance to X and compute the entropy as a sum of conditional entropies between these sets. The advantage is twofold: (i) the conditional entropies are computed on regions of increasing distance to X and, hence, of exponentially decreasing variation; (ii) the continuity inequality (2.12) for conditional entropy depends on the dimension of just one of the parts. We must assume, however, that the volume of each set does not grow too fast with its distance to X in order to get the desired bound. We shall detail these conditions in the following.

For $l \in \mathbb{N}$, let

$$X_l = \{j \in \Gamma | d(j, X) = l\} \quad (2.26)$$

be the set of all points of Γ with distance l to X . For $i \in \Gamma$ and $l \in \mathbb{N}$, let

$$R_l(i) = \{j \in \Gamma | d(i, j) = l\} \quad (2.27)$$

be a sphere of radius l centered in i (see Figure 1.3). Denote by

$$\mathrm{Int}(X) = \{i \in X | R_1(i) \subseteq X\} \quad (2.28)$$

the interior of X and let $\partial X = X - \mathrm{Int}(X)$ be its boundary. Note that for systems with (non-zero) nearest-neighbor interactions it holds that $\partial X = \partial_\Phi X$. We must have then the following.

Lemma 2. For every finite $X \subseteq \Gamma$ and $l > 0$ it must hold that

$$X_l \subseteq \bigcup_{i \in \partial X} R_l(i). \quad (2.29)$$

Proof. Indeed, take $j \in X_l$ and $i \in X$ such that $d(j, X) = d(j, i) = l$. Clearly we have $j \in R_l(i)$. Take a path of length l connecting j to i . Since $l > 0$ this path necessarily contains a point k of $R_1(i)$. It must hold that $k \notin X$, otherwise one can construct a path of length $l - 1$ connecting j to a point of X , in contradiction with condition $d(j, X) = l$. In other words, $i \in \partial X$. \square

Now we are ready to state the following.

Theorem 1. Assume the same conditions and notation of Lemma 1. Furthermore, assume that

$$|R_l(i)| \leq b e^{\alpha l} \quad (2.30)$$

for every $i \in \Gamma$, $l \geq 0$ and some constants $b, \alpha \geq 0$. Suppose also that $D = \sup_{i \in \Gamma} \dim(\mathcal{H}_i) < \infty$. Let $t \in \mathbb{R}$ be such that $d(X, Y) > \frac{\mu}{\mu - \alpha} v_\mu |t|$. Then, the following inequalities hold true:

$$|S(\rho_Y^0(t)) - S(\rho_Y^q(t))| \leq \gamma_q e^{-\frac{\mu}{2}(d(X, Y) - v'_\mu |t|)}, \quad (2.31)$$

for $q = 1, 2$ and $\mu > 2\alpha$, where $\gamma_q = 4\sqrt{c_q}(1 - e^{-\frac{\mu}{2}})^{-1}(|\partial X|\sqrt{c_q}b \log_2 D + 1)$ and $v'_\mu = \frac{\mu}{\mu - \alpha}v_\mu$.

Proof. Define $Y_l = Y \cap X_{d(X, Y)+l}$ for $l \in \mathbb{N}$. If $N = \max\{l : Y_l \neq \emptyset\}$, the definitions of N and Y_l guarantee that $Y = \bigcup_{l=0}^N Y_l$. Moreover, if $\tilde{Y}_l = \bigcup_{m=l}^N Y_m$, we have $\tilde{Y}_0 = Y$, $\tilde{Y}_l = Y_l \cup \tilde{Y}_{l+1}$ and $Y_N = \tilde{Y}_N$. See Figure 2.1 for a pictorial description of all these sets.

All these definitions imply that for any density operator acting on \mathcal{H}_Y it must hold that:

$$S(\rho_Y) = \left(\sum_{l=0}^{N-1} S_{Y_l|\tilde{Y}_{l+1}}(\rho_{\tilde{Y}_l}) \right) + S(\rho_{Y_N}), \quad (2.32)$$

where $S_{Y_l|\tilde{Y}_{l+1}}(\rho_{\tilde{Y}_l})$ denotes the conditional entropy

$$S_{Y_l|\tilde{Y}_{l+1}}(\rho_{\tilde{Y}_l}) = S(\rho_{\tilde{Y}_l}) - S(\rho_{\tilde{Y}_{l+1}}). \quad (2.33)$$

The telescopic sum of Equation (2.32) is illustrated in the Figure 2.2. The coloured sets in parentheses represent each term of Equation (2.33) for each value of l . The last set, the one which is alone, represents the term $S(\rho_{Y_N})$ of Equation (2.32).

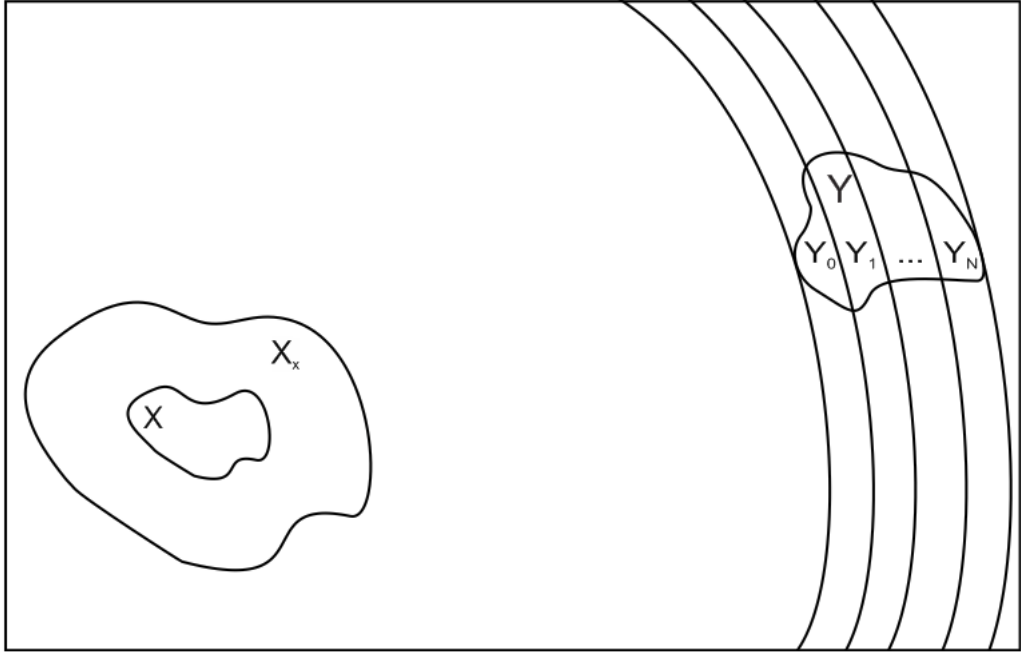


Figure 2.1: Pictorial depiction of sets X, Y, Y_l , and \tilde{X}_x defined in the proof of Theorem 1 and in Section 2.5.

$$\left(\text{Set } Y - \text{Set } Y_l \right) + \left(\text{Set } Y_l - \text{Set } Y_{l+1} \right) + \left(\text{Set } Y_{l+1} - \text{Set } Y_{l+2} \right) + \text{Set } Y_{l+2}$$

Figure 2.2: Pictorial illustration of Equations (2.32) and (2.33).

Letting $\Delta S_q(t) = S(\rho_Y^0(t)) - S(\rho_Y^q(t))$ for $q = 1, 2$, we have on the one hand:

$$\begin{aligned} |\Delta S_q(t)| &\leq \sum_{l=1}^{N-1} |S_{Y_l|\tilde{Y}_{l+1}}(\rho_{\tilde{Y}_l}^0(t)) - S_{Y_l|\tilde{Y}_{l+1}}(\rho_{\tilde{Y}_l}^q(t))| \\ &\quad + |S(\rho_{Y_N}^0(t)) - S(\rho_{Y_N}^q(t))|. \end{aligned} \tag{2.34}$$

On the other hand, from Lemma 1 we get, for $l = 0, \dots, N$:

$$\|\rho_{\tilde{Y}_l}^0(t) - \rho_{\tilde{Y}_l}^q(t)\| \leq c_q e^{-\mu(d(X,Y)+l-v_\mu t)}, \tag{2.35}$$

since $d(X, \tilde{Y}_l) = d(X, Y_l) = d(X, Y) + l$. Moreover, by using $\dim(\mathcal{H}_{Y_l}) \leq D^{|Y_l|}$, inequalities (2.35),

the continuity inequalities for entropy (2.11), and conditional entropy (2.12), the right hand side of Equation (2.34) can be bounded by:

$$\begin{aligned} & \sum_{l=0}^{N-1} \{4c_q e^{-\mu(d(X,Y)+l-v_\mu|t|)} \log_2(D^{|Y_l|}) + 2h(c_q e^{-\mu(d(X,Y)+l-v_\mu|t|)})\} \\ & + \frac{1}{2} c_q e^{-\mu(d(X,Y)+N-v_\mu|t|)} \log_2(D^{|Y_N|} - 1) + h\left(\frac{1}{2} c_q e^{-\mu(d(X,Y)+N-v_\mu|t|)}\right). \end{aligned} \quad (2.36)$$

In order to bound the binary entropy functions we use that $h(x) \leq 2\sqrt{x}$ for $x \in [0, 1]$, so we can write:

$$\begin{aligned} |\Delta S_q(t)| & \leq \sum_{l=0}^{N-1} \{4c_q e^{-\mu(d(X,Y)+l-v_\mu|t|)} \log_2(D^{|Y_l|}) + 4\sqrt{c_q} e^{-\mu(d(X,Y)+l-v_\mu|t|)/2}\} \\ & + \frac{1}{2} c_q e^{-\mu(d(X,Y)+N-v_\mu|t|)} \log_2(D^{|Y_N|} - 1) + \sqrt{2}\sqrt{c_q} e^{-\mu(d(X,Y)+N-v_\mu|t|)/2}. \end{aligned} \quad (2.37)$$

In this expression the last two terms are smaller than the term of index N of the summand. Therefore, we can bound the expression by a single sum ranging from 0 to N and get:

$$|\Delta S_q(t)| \leq \sum_{l=0}^N \{4c_q e^{-\mu(d(X,Y)+l-v_\mu|t|)} \log_2(D^{|Y_l|}) + 4\sqrt{c_q} e^{-\mu(d(X,Y)+l-v_\mu|t|)/2}\}. \quad (2.38)$$

$$= 4c_q \log_2(D) e^{-\mu(d(X,Y)-v_\mu|t|)} \sum_{l=0}^N |Y_l| e^{-\mu l} + 4\sqrt{c_q} e^{-\mu(d(X,Y)-v_\mu|t|)/2} \sum_{l=0}^N e^{-\mu l/2}, \quad (2.39)$$

where we get the equality by rearranging the terms. We can bound the second summand in Equation (2.39) immediately by $\sum_{l=0}^{\infty} e^{-\frac{\mu}{2}l} = (1 - e^{-\frac{\mu}{2}})^{-1}$. To bound the first summand we just have to observe that $|Y_l| \leq |\cup_{i \in \partial X} R_{d(X,Y)+l}(i)| \leq |\partial X| b e^{\alpha(d(X,Y)+l)}$, where the first inequality comes from the definition of Y_l and Lemma 2 while the second comes from hypothesis (2.30). Therefore,

$$\sum_{l=0}^{\infty} |Y_l| e^{-\mu l} \leq |\partial X| b e^{\alpha d(X,Y)} \sum_{l=0}^{\infty} e^{-(\mu-\alpha)l} = |\partial X| \frac{b e^{\alpha d(X,Y)}}{1 - e^{-(\mu-\alpha)}},$$

since $\mu > \alpha$, and we get

$$|\Delta S_q(t)| \leq 4c_q |\partial X| \log_2(D) b (1 - e^{-(\mu-\alpha)})^{-1} e^{-(\mu-\alpha)d(X,Y) + \mu v_\mu |t|} \quad (2.40)$$

$$+ 4(1 - e^{-\frac{\mu}{2}})^{-1} \sqrt{c_q} e^{-\frac{\mu}{2}(d(X,Y)-v_\mu|t|)}. \quad (2.41)$$

Finally, defining $v'_\mu = \frac{\mu}{\mu-\alpha} v_\mu$, using that $d(X, Y) > v'_\mu |t|$ and $\mu - \alpha > \frac{\mu}{2}$, we can conclude the desired bound:

$$|\Delta S_q(t)| \leq 4(1 - e^{-\frac{\mu}{2}})^{-1} (c_q |\partial X| b \log_2 D + \sqrt{c_q}) e^{-\frac{\mu}{2}(d(X,Y)-v'_\mu|t|)}. \quad (2.42)$$

□

Let us now consider some examples. They are all illustrated in Figure 2.3.

Example 1. If $\Gamma = \mathbb{Z}$ with $d(i, j) = |i - j|$ in Theorem 1, inequality (2.31) holds with $v_{\mu'} = v_{\mu}$ and $b = 2$. Indeed, one just has to realize that such metric space Γ satisfies (2.30) with $b = 2$ and $\alpha = 0$ since every sphere in this space has precisely two elements, irrespective the size of its radius.

Assuming further that r is the range of interaction [meaning that $\Phi(Z) = 0$ for every set Z with diameter larger than r] and X is a contiguous region, one has $|\partial X| = 2$ and $|\partial_{\Phi}X| \leq 2r$. Therefore, the bound is completely independent of the size of regions Y and X .

One says that Γ has *fractal dimension* n if there exists $n \geq 1$ and $a > 0$ such that

$$|R_l(i)| \leq al^{n-1} \quad (2.43)$$

for every $l > 0$ [4, 35]. Note that lattices \mathbb{Z}^n are particular cases of such space. In such models one has the following.

Example 2. In Theorem 1, if Γ has fractal dimension n , inequality (2.31) holds for every $\alpha > 0$ (and $\alpha < \frac{\mu}{2}$), with $b = a \frac{(n-1)!}{\alpha^{(n-1)}}$. Indeed, from Equation (2.43) we get that $|R_l(i)| \leq al^{n-1} \leq a \frac{(n-1)!}{\alpha^{(n-1)}} e^{\alpha l}$ for every $\alpha > 0$.

Finally, we note that a bound can be valid even for more “exotic” spaces. If Γ is a rooted tree graph with $n > 1$ branches, we have that $|R_l(i)| = n^l + 1$, so its fractal dimension is infinite. But we still have the following.

Example 3. In Theorem 1, if Γ is a rooted tree graph with n branches, inequality (2.31) holds for $\mu \geq 2 \ln n$, $\alpha = \ln n$, and $b = 2$. Since $|R_l(i)| \leq 2n^l = 2e^{l \ln n}$ we just have to set $\alpha = \ln n$ and $b = 2$.

Bellow, in the Figure 2.3 we show an illustration of some sets which we have described in the previous examples: the chain of example 1, a square lattice which has fractal dimension equal 3 and a rooted tree graph with 2 branches. Note that the lattices of Figure 1.2a.,b.,c. are also examples included in Example 2 and the lattice of Figure 1.2d. is included in Example 3.

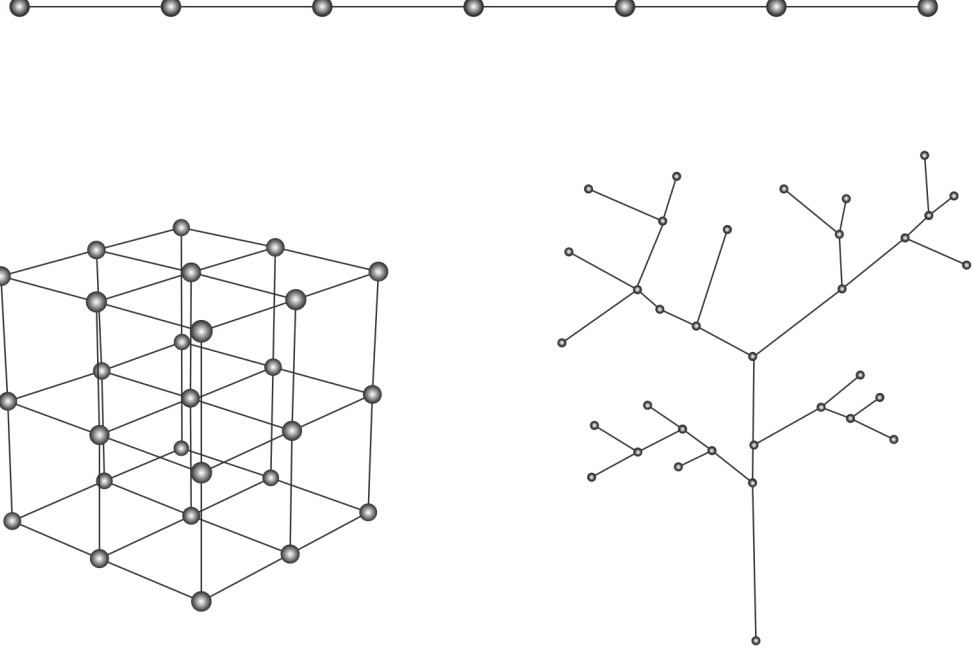


Figure 2.3: Illustration of lattices which are included in examples 1, 2 and 3, respectively.

2.5 Discussion

First of all, let us explain in what sense we claim that entanglement satisfies an “effective light-cone”. Let $\tilde{X}_x = \bigcup_{l=0}^x X_l$ be the enlargement of a subset $X \subset \Lambda$ up to distance x , as depicted in Figure 2.1. Again, as in Section 2.4, take $\rho_{\tilde{X}_x}^q(t)$ to be the reduced state in region \tilde{X}_x of the evolved states $|\psi^q(t)\rangle$, where $q = 0, 1$, or 2 . Recall that the system evolves without perturbations if $q = 0$ but is subjected to a local quench in region X , at $t = 0$, in the Hamiltonian for $q = 1$ or in the initial state if $q = 2$. Let $E_q(x, t) = S(\rho_{\tilde{X}_x}^q(t)) = S(\rho_{\Lambda - \tilde{X}_x}^q(t))$ be the entropy of entanglement of the evolved state $|\psi^q(t)\rangle$ under the bipartition defined by \tilde{X}_x , that is, $\Lambda = \tilde{X}_x \cup (\Lambda - \tilde{X}_x)$. For a large class of models our results show that this entanglement function satisfies an *effective* “light-cone”, whatever the size $|\Lambda|$ of the whole system. Namely, by using inequality (2.31) with $Y = \Lambda - \tilde{X}_x$, we see that whenever $d(X, \Lambda - \tilde{X}_x) = x \gtrsim v'_\mu t$ we shall have $|E^0(x, t) - E^q(x, t)| \approx 0$ for $q = 1$ and 2 . Therefore, significant variations of entanglement can take place only inside the “light-cone” $x \leq v'_\mu t$.

As a particular case of the above discussion, we point out some implications for t -DMRG simulations of local quenches on spin chains. In such algorithms one naturally computes the entanglement of the system for every bipartition (in two contiguous regions) and every instant of time. These values for entanglement are important to establish how large the sizes of the matrices involved in the simulation must be in order to achieve good approximations. In particular, a condition for the efficiency of the algorithms is that the simulated states must satisfy an area law for entanglement [6]. Now, assume that a quench in the Hamiltonian is applied on an extreme point of the chain and take x to be the distance between this site and the cutting point of a bipartition. As a particular case of the above discussion, we guarantee that $|E_0(x, t) - E_1(x, t)|$ satisfies the bound (2.31) with $x = d(X, Y)$ and has no dependence whatsoever with the size of the regions or the whole system. Now, if the initial state is an eigenstate of the unperturbed Hamiltonian and satisfies an area law, we have $E_0(x, t) = E_0(x, 0) \leq c_0$, where c_0 is some constant. Therefore, by our bound, the evolved state will still satisfy an area law for any finite time. Indeed, from Theorem 1 we have that $E_1(x, t) \leq c_0 + c_1 e^{\mu v|t|}$, for every $x \geq x_0$, where $c_1 = \gamma_1 e^{-\mu x_0}$, and some fixed $x_0 > v_\mu t$. Then, for some fixed value of t , we have an area law. Note that an area law, by itself, can already be drawn, for instance, from reference [24]. There, the authors find that $E_1(x, t) \leq c_0 + c'_1 |t|$ holds for every x , where c'_1 is a constant dependent only on the parameters of the Hamiltonian. Our bound, however, can impose a stronger restriction on the entanglement growth for fixed t and increasing values of x .

In reference [3] the authors show that a Lieb-Robinson bound indeed implies a limitation for the propagation of information throughout the many-body system in the information-theoretical sense. Assume two observers A and B have access to regions X and Y of the many-body system, respectively. They can establish a communication channel from A to B in the following way. Observer A can encode an alphabet with m letters in the state of the system by applying one out of m unitaries on the initial state $|\psi\rangle$, all of them with support on region X . Observer B can then perform measurements on region Y in order to discern which unitary was applied and, hence, which letter of the alphabet was intended to be sent. If p_i is the probability for the i th letter to be sent, the maximum amount of information that can pass through this channel is measured by the Holevo capacity, given by $C(t) = S(\sum_{i=1}^m p_i \rho_{Y,i}(t)) - \sum_{i=1}^m p_i (S(\rho_{Y,i}(t)))$, where $\rho_{Y,i}(t)$ is the reduced state on Y given by the evolution of $U_i |\psi\rangle$ at time t .

Through a bound for $|S(\rho_{Y,i}(t)) - S(\rho_{Y,j}(t))|$, for any $i \neq j$, the authors of [3] show that the Holevo capacity is small for small times ($t \ll d(X, Y)/v_\mu$). Their bound, however, is proportional to the volume of Y . Therefore, it is necessary to additionally assume this volume grows at most polynomially with $d(X, Y)$. By Example 2, for systems with n spatial dimensions, however, such additional assumption is no longer required. Even if observer B has access to an arbitrarily large portion of the system, no significant amount of information can be sent through the channel for small times.

We may add that the communication channel could be alternatively implemented by observer A encoding the letters of the alphabet on Hamiltonian perturbations W_i with support on X . Our results also guarantee the Holevo capacity would be small for small times, even for arbitrarily large regions Y .

Chapter 3

A Shielding Property for Thermal Equilibrium States on the Quantum Ising Model

The transverse Ising chain is a paradigmatic model of quantum many body systems. It is exactly soluble via Jordan-Wigner transformation [36] and exhibits a quantum phase transition from a paramagnetic phase to a ferromagnetic one [37]. It is frequently used as a benchmark for analytical [38] or numerical techniques [39]. It can be used to illustrate or test new concepts, such as the role of entanglement on phase transitions [14], decoherence of open quantum systems [40] and quantum thermodynamics definitions of work [41]. It is also more than a toy model, being used to describe some trapped cold rubidium atoms [42] and even solids [43].

The main result of this chapter is a property of the transverse Ising model which we have found and is presented in Theorem 2. Along the chapter we discuss implications to local quenches. This chapter is organized as the following.

In the first section we define the Ising models and in the second one we give further definitions. In Section 3.3 we discuss the dynamics of general quantum many body systems such that Hamiltonians satisfy some properties of commutation. The longitudinal and transverse Ising model are examples of systems included in this category. Actually, the transverse Ising model is an example under the condition that the magnetic field applied in one site at the middle of the chain has to be null.

In the Section 3.4, we write about local quenches without dynamics, that is, when one compare two systems with similar Hamiltonians, such that only some parameters in a local region differ from each other. In this same section we present our main result, the shielding property for thermal equilibrium states on the quantum Ising model. This result is valid for chains and lattices which can be divided in two subsets which have only one site in their interface. In Section 3.5 we present an alternative proof for the shielding property which is more intuitive.

In the following sections we discuss the validity of the shielding property for the lattices which have more sites in the interface between their subsets. In Section 3.6 we explain why the previous proofs do not work in this case and in Section 3.6 we discuss correlations, even with the validity of the shielding property. In Section 3.8 we present another proof for the shielding property, which is equivalent to the other two when the lattice has only one site in the interface, but which exhibit more structure when the lattice has more sites in the interface. In Sections 3.9, 3.10 and 3.10, we discuss consequences of this new proof.

3.1 The Ising Models

The *classical Ising model* was conceived in 1920 as a mathematical model of ferromagnetism in statistical mechanics. It was created by the physicist Wilhelm Lenz who has proposed the problem of solving this model to his student Ernst Ising. It is a model for lattice systems where each site i can be in one of two spin states $\sigma_i = \pm 1$. Note that σ_i is not a matrix in this definition, it is just a variable which can assume these two values.

Three important phases of this model are: ferromagnetic, antiferromagnetic and paramagnetic. In the ferromagnetic phase all the spins are aligned; in the antiferromagnetic the spins are anti-aligned; and in the paramagnetic phase there is no well defined order for this alignment. In the Figure 1.7 of chapter 1 we have a good illustration for these phases. Remember that there we were dealing with the XXZ model. The two cases have differences but, for our purposes in this text, we can say that both are similar.

The Hamiltonian of the classical Ising model on a general lattice (or graph) is given by

$$H = - \sum_{i,j} J_{ij} \sigma_i \sigma_j - \sum_i h_i \sigma_i, \quad (3.1)$$

where the coefficient J_{ij} represents the strength of interaction between sites i and j , while h_i represents an external magnetic field applied on site i . The edges of the lattice determine which parts of the system interact: $J_{ij} \neq 0$ if sites i and j are connected by an edge while $J_{ij} = 0$ otherwise.

The *quantum Ising model* is a generalization of the above model and the spin variables are treated as quantum features of the system. For this purpose, the states σ_i are replaced by some Pauli matrix σ_i^k , for $k = x, y, z$.

The *(quantum) longitudinal Ising model* has its Hamiltonian given by

$$H = - \sum_{i,j} J_{ij} \sigma_i^z \sigma_j^z - \sum_i h_i \sigma_i^z. \quad (3.2)$$

The longitudinal Ising model has a direct correspondence with the classical Ising model since its Hamiltonian is a diagonal matrix in the standard basis of the Hilbert space. Therefore it is used to call by quantum Ising model only the transverse one, which we describe as following.

The *quantum or transverse Ising model* has its Hamiltonian given by:

$$H = - \sum_{i,j} J_{ij} \sigma_i^z \sigma_j^z - \sum_i h_i \sigma_i^x. \quad (3.3)$$

Note that the only difference between Equations (3.3) and (3.2) is the last term, where in the first equation it is in the x -direction while the other is in the z -direction. Physically it means that in Hamiltonian (3.2) the external magnetic field is applied in the same direction of the interaction between the spins and in Hamiltonian (3.3) it is applied in a perpendicular direction. This changing makes all the difference and we will see that the longitudinal and transverse Ising models have different properties.

The Hamiltonian of a more general transverse Ising model, where the external magnetic field also has a component in the y -direction, can be written as:

$$H = - \sum_{\langle i,j \rangle} J_{ij} \sigma_i^z \sigma_j^z - \sum_i h_i \sigma_i^x - \sum_i g_i \sigma_i^y. \quad (3.4)$$

On the one hand, this Hamiltonian is different from the Hamiltonian of Equation (3.3), because

of the terms involving σ_i^y . On the other hand, note that

$$\begin{aligned} h_j \sigma_i^x + g_i \sigma_i^y &= \sqrt{h_i^2 + g_i^2} \times \left(\frac{h_i}{\sqrt{h_i^2 + g_i^2}} \sigma_i^x + \frac{g_i}{\sqrt{h_i^2 + g_i^2}} \sigma_i^y \right) \\ &= \sqrt{h_i^2 + g_i^2} \sigma_i^{a_i x + b_i y} = \sqrt{h_i^2 + g_i^2} \sigma_i^{x_i}, \end{aligned}$$

where $x_i = a_i x + b_i y$ is some direction perpendicular to z , with $a_i = h_i / \sqrt{h_i^2 + g_i^2}$ and $b_i = g_i / \sqrt{h_i^2 + g_i^2}$. Thus the Hamiltonian (3.4) can be written as

$$H = - \sum_{\langle i,j \rangle} J_{ij} \sigma_i^z \sigma_j^z - \sum_i \sqrt{h_i^2 + g_i^2} \sigma_i^{x_i} \quad (3.5)$$

Define y_i such that $\sigma_i^z \sigma_i^{x_i} = \sigma_i^{y_i}$. We have that the operators $\sigma_i^z, \sigma_i^{x_i}, \sigma_i^{y_i}$ and $\mathbb{1}_i$ satisfy the same algebra as $\sigma^z, \sigma^x, \sigma^y$ and $\mathbb{1}$. Furthermore these new operators associated to the space of different sites still commute between each other, that is, $[\sigma_i^a, \sigma_j^b] = 0$ if $i \neq j$, for $a = x_i, y_i, z$ and $b = x_j, y_j, z$. In this sense, Equation (3.4) is equivalent to Equation (3.3).

3.2 Further Definitions: Subsets and Gibbs State

Here we provide some definitions for the development of the text. Many times in this chapter we will use some general sets of our lattices, but which have some properties. To avoid repeating similar definitions, we will define them now and use the same letter for the similar situations. We also define the thermal equilibrium states, since our main result is made for a system in this context.

3.2.1 Subsets of the Lattice

Let the finite lattice Λ as was defined in Section 1.1. Let the sets X and Y be two subsets of Λ such that $X \cup Y = \Lambda$. Denote by $S = X \cap Y$, $A = X \setminus Y$ and $B = Y \setminus X$. Furthermore, if $i \in A$ and $j \in B$, we suppose that i and j are not connected by an edge. We call S the *interface* between A and B , or between X and Y . We illustrate these sets in the Figure 3.1.a. and b.

Note that the sets X and Y are different from those defined in Chapter 2.

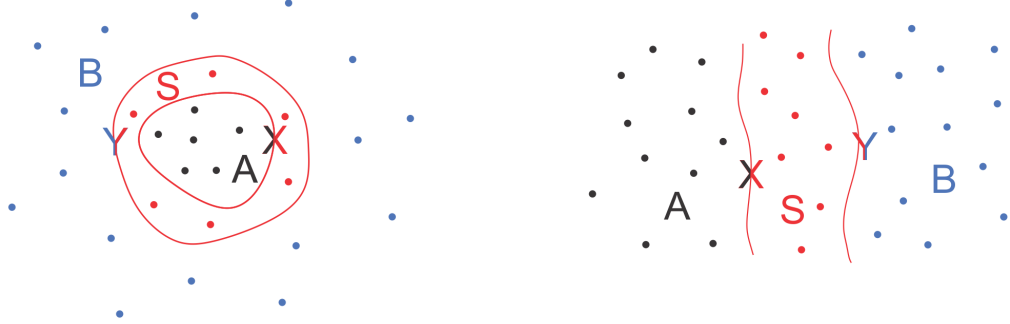


Figure 3.1: Two illustrations for the sets X , Y , A , B and S . The sites of A and B do not interact directly between each other and the set S is called interface.

3.2.2 Gibbs State

The Gibbs state of a quantum many body system with Hamiltonian H is given by

$$\rho = \frac{e^{-\beta H}}{\text{Tr}(e^{-\beta H})} \quad (3.6)$$

where $\beta = 1/k_B T$, k_B is the Boltzmann constant and T is the temperature of the system. This is the state of thermal equilibrium of the system. That is, if the system is in contact with a thermal reservoir at temperature T and it is in equilibrium, then the state of the system is given by Equation (3.6).

Furthermore, when $\beta \rightarrow \infty$, or equivalently, when $T \rightarrow 0$, we have that the state ρ tends to the ground state of the system. Thus, the ground state is the equilibrium thermal state of the system at null temperature. For further details, see App. B.

3.3 Dynamics After a Local Quench on Systems with Locally Commuting Hamiltonians

Last chapter we studied a light-cone behaviour of a many body system after a local quench. Here we will see that systems with local commuting Hamiltonians are particular cases where the

light-cone have null velocity.

Let H be *any* many-body Hamiltonian that can be written as $H = H_X + H_Y$, where $\text{supp}(H_X) = X$ and $\text{supp}(H_Y) = Y$, and suppose that

$$[H_X, H_Y] = 0. \quad (3.7)$$

Remember that the equation above implies that $e^{-it(H_X+H_Y)} = e^{-itH_X}e^{-itH_Y}$. If \mathcal{O} is any observable with $\text{supp}(\mathcal{O}) \subseteq A = Y \setminus S$, then H_X and \mathcal{O} commute. Therefore, the expected value of \mathcal{O} at time t is given by:

$$\begin{aligned} \langle \mathcal{O}(t) \rangle_\rho &= \text{Tr}(\rho(t)\mathcal{O}) \\ &= \text{Tr}(e^{-itH_X}e^{-itH_Y}\rho e^{itH_Y}e^{itH_X}\mathcal{O}) \\ &= \text{Tr}(e^{-itH_Y}\rho e^{itH_Y}\mathcal{O}), \end{aligned} \quad (3.8)$$

where ρ is any initial state for the system. From the second line to the third line we used the fact that e^{itH_X} commutes with \mathcal{O} and that the trace is invariant under cyclic permutations.

From Equation (3.8) we can see that the expected value of \mathcal{O} has dependence only on H_Y . Since \mathcal{O} is an arbitrary observable of region A , it holds that the reduced state of the system in region A has dependence only on the parameters of region Y (assuming the initial state ρ does not hold any dependence on the Hamiltonian).

Note that the Hamiltonian considered above is static. Now, suppose that the Hamiltonian has a time dependence and it is written as

$$H(t) = H_X(t) + H_Y(t). \quad (3.9)$$

Suppose that

$$[H_X(t_1), H_Y(t_2)] = 0 \quad (3.10)$$

for all $t_1, t_2 \geq 0$. These commutation relations imply that

$$\left[\int_0^t H_X(t')dt', \int_0^t H_Y(t')dt' \right] = 0, \quad (3.11)$$

for all $t \geq 0$. Then, following the same steps of Equation (3.8), the expected value of an observable

\mathcal{O} (with $\text{supp}(\mathcal{O}) \subseteq A$) is given by

$$\begin{aligned}\langle \mathcal{O}(t) \rangle_\rho &= \text{Tr}(\rho(t)\mathcal{O}) \\ &= \text{Tr} \left(e^{-i \int_0^t H_X(t') dt'} e^{-i \int_0^t H_Y(t') dt'} \rho e^{i \int_0^t H_Y(t') dt'} e^{-i \int_0^t H_X(t') dt'} \mathcal{O} \right) \\ &= \text{Tr} \left(e^{-i \int_0^t H_Y(t') dt'} \rho e^{-i \int_0^t H_Y(t') dt'} \mathcal{O} \right).\end{aligned}\tag{3.12}$$

We arrive at the same conclusion: the reduced state of set A has no dependence on $H_X(t)$, for all $t \geq 0$. Then, respecting commutation with the Hamiltonian of set Y , one is free to make quenches on the Hamiltonian of set X and do not change the reduced state of A .

Now, remember that in Chapter 2 we have defined sets X and Y (see Figure 2.1) and we had that $X \cup Y \neq \Lambda$ and that $X \cap Y = \emptyset$, different from the sets X and Y defined in Section 3.2.1. To drop confusions, now we will refer to the sets X and Y of Chapter 2 by \bar{X} and \bar{Y} , respectively.

In Chapter 2 we have considered a sudden local quench. The Hamiltonian H is suddenly changed to $H + W$, where $\text{supp}(W) = \bar{X}$. If $[H, W] = 0$, to any observable with support outside set \bar{X} , by Equation (3.12), the expected value of this observable has no dependence on W . Since $\bar{X} \cap \bar{Y} = \emptyset$, we have that the observables of \bar{Y} have no dependence on W . We can conclude that the evolved state $\rho_{\bar{Y}}(t)$ is the same as if there was no quench. Remember that Equation (2.31) provides a bound for the quantity $|S(\rho_{\bar{Y}}^0(t)) - S(\rho_{\bar{Y}}^q(t))|$, which is the difference between the entropy of the evolution of the state of set \bar{Y} for the cases with and without the quench. In our particular case here we would have a critical value, that is, $|S(\rho_{\bar{Y}}^0(t)) - S(\rho_{\bar{Y}}^q(t))| = 0$.

The longitudinal Ising model (Equation (3.2)) is an example of a system such that condition (3.7) is always satisfied, no matter which choice of sets X and Y we take. Furthermore, we could have J_{ij} and h_i as functions of time for $i, j \in X$. Condition (3.10) would be satisfied for any function of these parameters. By Equation (3.12) the observables of the set A would have no dependence on these changes.

On the other hand, the transverse Ising model (Equation (3.3) or (3.4)) does not satisfy condition (3.7) in general. However suppose that the external magnetic field in all the sites of the interface are null for all $t \geq 0$. Then, observables in set A would have no dependence on the parameters of H_X . By Equation (3.12) again, one is free to change the strength of the interactions and of the external magnetic field of set X , in the sense that, if someone is able only to measure observables of set A , she or he will never know about these changes.

As a visual illustration of this effect, we have simulated, via t -DMRG [23, 27], the evolution of a transverse Ising model on a chain with 60 sites with initial parameters $J_i = 1$ for all the sites, $h_{15} = 0$ and $h_i = \frac{1}{2}$ for $i \neq 15$. The system is initially prepared in the ground state, when we perform a local quench in the first site, changing its magnetic field to $h_1 = -10$. We show in Figure 3.2 the magnetization of each site of the chain as a function of time. At the left part of the plot we see the perturbation propagating and being reflected on site 15, where we have made the external magnetic field null. On the right part we can see that the magnetization of all the sites after site 15 remain unaltered.

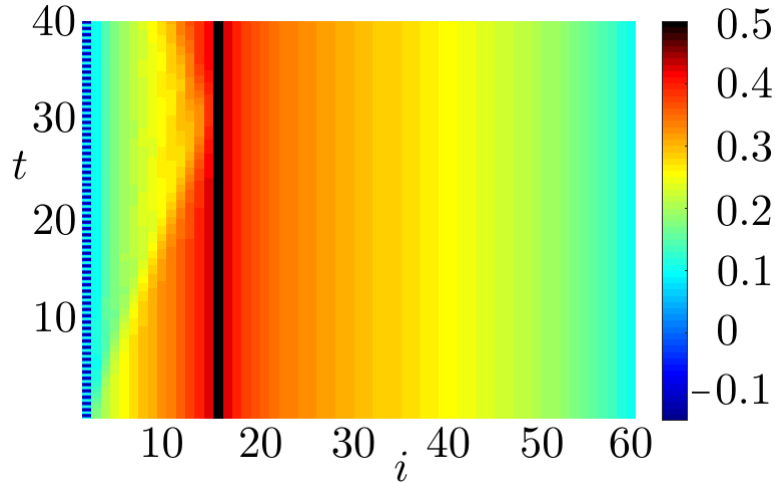


Figure 3.2: Temporal evolution of the magnetization of each site of a transverse quantum Ising chain. The external magnetic field of site 15 was fixed null and the evolution was calculated via tDMRG.

3.4 The Equilibrium States of Locally Perturbed Systems

Until now we have worked on the effect of local quenches on the dynamical properties of lattice systems. A related problem is to consider, in the same lattice, two similar Hamiltonians which differ only in a “small” region and compare the equilibrium states outside this region.

For example, in references [44, 45] it is shown that the norm of the difference between the perturbed and unperturbed reduced states of the ground states exponentially decays with the distance between the region where the perturbation takes place and the region where we take the

reduced state. In reference [46] it is shown that, above a critical temperature, the Gibbs states are also stable against distant Hamiltonian perturbations.

Now, if we apply these results of references [44, 45, 46] on the Ising models we will not find anything really different comparing with other lattice models, since these bounds are not tight in general. But the transverse Ising model does have a special behaviour under some conditions. In the following we will enunciate and prove this theorem. In the rest of this chapter we will discuss the features and consequences of this special property.

3.4.1 The Shielding Property for Thermal Equilibrium States on the Quantum Ising Model

We consider the Gibbs states (Equation (3.6)) at arbitrary temperature of the transverse Ising model defined on finite open chains. Namely, we take the spins to be embedded on a straight line, where they interact only with their first neighbours, so we can use integer numbers i to index each site:

$$H = - \sum_{i=1}^{N-1} J_i \sigma_i^z \sigma_{i+1}^z - \sum_{i=1}^N h_i \sigma_i^x. \quad (3.13)$$

Note that this is just a particular case of Equation (3.3). The previous one is for general lattices and the last one for chains.

We assume the couplings and fields to be arbitrary, with the exception that the field must be null in some particular site L . We show that the reduced state of one side, say the sites to the right of site L (those with $i \geq L$), have no dependence on the parameters of the Hamiltonian of the other side, that is, the sites with $i < L$. We will refer to this feature as the *shielding property*.

Theorem 2. *Let a chain of N sites be described by the transverse Ising model. Suppose that for some fixed site L we have $h_L = 0$. If the state ρ of the chain is the Gibbs state, then the reduced state of sites L, \dots, N has no dependence on $h_1, \dots, h_{L-1}, J_1, \dots, J_{L-1}$, and is given by*

$$\rho_{L, \dots, N} = \frac{e^{-\beta H''}}{\text{Tr}(e^{-\beta H''})}, \quad (3.14)$$

where H'' is given by

$$H'' = - \sum_{i=L}^{N-1} (J_i \sigma_i^z \sigma_{i+1}^z + h_{i+1} \sigma_{i+1}^x), \quad (3.15)$$

defined on the space of sites L, \dots, N .

Note that this is a surprising effect, given that the exchange coupling J_{L-1} , which intermediates an interaction between each halve of the chain, can be arbitrarily large. Let us show the proof before discussing implications, generalizations and related issues with this result.

Proof. We first rewrite the Ising Hamiltonian in the following way. If we have that $h_L = 0$ for some $L = 2, \dots, N - 1$, we can set $H = H^I + H^{II}$, where

$$H^I = - \sum_{i=1}^{L-1} (J_i \sigma_i^z \sigma_{i+1}^z + h_i \sigma_i^x) \quad (3.16)$$

and

$$H^{II} = - \sum_{i=L}^{N-1} (J_i \sigma_i^z \sigma_{i+1}^z + h_{i+1} \sigma_{i+1}^x). \quad (3.17)$$

Note that H^I has support on the space of sites $1, \dots, L$, while H^{II} has support on the space of L, \dots, N . However even though they have intersecting supports they commute. In any case, we can write:

$$H^I = H' \mathbb{1}_{L+1} \dots \mathbb{1}_N \quad (3.18)$$

and

$$H^{II} = \mathbb{1}_1 \dots \mathbb{1}_{L-1} H'', \quad (3.19)$$

where H' is defined on the space of sites $1, \dots, L$ while H'' on the space of L, \dots, N , and we are omitting the tensor product among operators.

With all of it in mind, we can write then

$$e^{-\beta H} = e^{-\beta H^I} \cdot e^{-\beta H^{II}} \quad (3.20)$$

$$= (e^{-\beta H'} \mathbb{1}_{L+1} \dots \mathbb{1}_N) \cdot (\mathbb{1}_1 \dots \mathbb{1}_{L-1} e^{-\beta H''}). \quad (3.21)$$

Therefore, the reduced density operator of the Gibbs state on sites L, \dots, N , satisfies:

$$\rho_{L, \dots, N} \propto \text{Tr}_{1, \dots, L-1} (e^{-\beta H}) \quad (3.22)$$

$$= \{\text{Tr}_{1, \dots, L-1} (e^{-\beta H'}) \mathbb{1}_{L+1} \dots \mathbb{1}_N\} \cdot e^{-\beta H''}. \quad (3.23)$$

We will show that the partial trace of $e^{-\beta H'}$, appearing in Equation (3.23), is a multiple of the identity $\mathbb{1}_L$, so the theorem follows after normalization. Writing the exponential $e^{-\beta H'}$ as its series expansion, the partial trace becomes

$$\text{Tr}_{1, \dots, L-1} (e^{-\beta H'}) = \sum_{n=0}^{\infty} \frac{\beta^n}{n!} \{\text{Tr}_{1, \dots, L-1} (H'^n)\}. \quad (3.24)$$

To reach the desired result it suffices to show that $\text{Tr}_{1,\dots,L-1}(H'^n) = c_n \mathbb{1}_L$, for all $n = 0, 1, 2, \dots$, where c_n is some constant. The case $n = 0$ is trivial, so let us take care of positive values of n . First, we have that

$$H'^n = \left(- \sum_{i=1}^{L-1} (J_i \mathbb{1}_1 \dots \mathbb{1}_{i-1} \sigma_i^z \sigma_{i+1}^z \mathbb{1}_{i+2} \dots \mathbb{1}_L + h_i \mathbb{1}_1 \dots \mathbb{1}_{i-1} \sigma_i^x \mathbb{1}_{i+1} \dots \mathbb{1}_L) \right)^n. \quad (3.25)$$

Note that $H' = \tilde{H}_{(1)} \mathbb{1}_L + \bar{H}_{(1)} \sigma_L^z$, where $\tilde{H}_{(1)}$ and $\bar{H}_{(1)}$ are defined on the space of the sites $1, \dots, L-1$. So any power of H' will have this form, that is:

$$H'^n = \tilde{H}_{(n)} \mathbb{1}_L + \bar{H}_{(n)} \sigma_L^z. \quad (3.26)$$

More explicitly, we have that

$$H'^n = \left(\sum_{\eta_1, \dots, \eta_{L-1}} a_{(n, \eta_1, \dots, \eta_{L-1}, \mathbb{1}_L)} \eta_1 \eta_2 \dots \eta_{L-1} \right) \mathbb{1}_L + \left(\sum_{\eta_1, \dots, \eta_{L-1}} a_{(n, \eta_1, \dots, \eta_{L-1}, \sigma^z)} \eta_1 \eta_2 \dots \eta_{L-1} \right) \sigma_L^z \quad (3.27)$$

where the sum ranges over variables $\eta_1, \dots, \eta_{L-1}$ and each of these η_i assume the values $\sigma_i^z, \sigma_i^x, \sigma_i^y$ and $\mathbb{1}_i$. Writing in a more concise way:

$$H'^n = \sum_{\eta_1, \dots, \eta_L} a_{(n, \eta_1, \dots, \eta_L)} \eta_1 \eta_2 \dots \eta_L, \quad (3.28)$$

where the sum is made on the variables η_1, \dots, η_L . For $i = 1, \dots, L-1$, the variable η_i assumes the values $\sigma_i^z, \sigma_i^x, \sigma_i^y$ or $\mathbb{1}_i$, and the variable η_L assumes only the values σ_L^z or $\mathbb{1}_L$.

We will prove that each term of \bar{H}_n has null trace. For concreteness and ease of notation, we will detail the argument for the term $\bar{H}_{(3)}$, where the field is null at site $L = 3$ and the chain has $J_1 = J_2 = 1$. The proof for any term of H'^n , for all $n = 1, 2, \dots$, all values of L (between 2 and $N-1$), will follow naturally the same steps.

With these assumptions, Equation (3.26) becomes

$$\begin{aligned} H'^3 &= -(\sigma_1^z \sigma_2^z + h_1 \sigma_1^x + \sigma_2^z \sigma_3^z + h_2 \sigma_2^x)^3 \\ &= -\{(4 + h_1^2 + h_2^2) \sigma_1^z \sigma_2^z + (4 + h_1^2 + h_2^2) h_1 \sigma_1^x \mathbb{1}_2 + (2 + h_1^2 + h_2^2) h_2 \mathbb{1}_1 \sigma_2^x - 2h_1 h_2 \sigma_1^y \sigma_2^y\} \mathbb{1}_3 \\ &\quad - \{(2 + h_1^2 + h_2^2) \sigma_1^z \mathbb{1}_2 + (2 + 2h_1^2) \mathbb{1}_1 \sigma_2^z - 2ih_1 h_2 \sigma_1^x \sigma_2^y + 2h_2 \sigma_1^z \sigma_2^x\} \sigma_3^z. \end{aligned} \quad (3.29)$$

Here, $\bar{H}_{(3)}$ is the operator in the curly brackets of the last two lines of Equation (3.29). We can see that its trace is null due to the fact that every one of its terms has at least one Pauli matrix in its factors. We will show why this must be the case.

Take for instance the last term of Equation (3.29), $\sigma_1^z \sigma_2^x \sigma_3^z$. It was obtained by the multiplication of the terms $\sigma_1^z \sigma_2^z \mathbb{1}_3$, $\mathbb{1}_1 \sigma_2^x \mathbb{1}_3$ and $\mathbb{1}_1 \sigma_2^z \sigma_3^z$, which we will call $\kappa_{[1]}$, $\kappa_{[2]}$ and $\kappa_{[3]}$. That is:

$$\begin{aligned} \kappa_{[1]} \cdot \kappa_{[2]} \cdot \kappa_{[3]} &= (\sigma_1^z \sigma_2^z \mathbb{1}_3) \cdot (\mathbb{1}_1 \sigma_2^x \mathbb{1}_3) \cdot (\mathbb{1}_1 \sigma_2^z \sigma_3^z) \\ &\propto (\sigma_1^z \sigma_2^y \mathbb{1}_3) \cdot (\mathbb{1}_1 \sigma_2^z \sigma_3^z) \\ &\propto (\sigma_1^z \sigma_2^x \sigma_3^z) = \eta_1 \eta_2 \eta_3. \end{aligned} \quad (3.30)$$

Note that the products of η 's are tensorial products, while the products of κ 's are matrix products. We can represent schematically as in Figures 3.3 and 3.4 the product in Equation (3.30) as a “board game”.

In Figure 3.3 we show how the game is constructed. For sites 1 and 2 we associate a square while for site 3, where $h_3 = 0$, we associate a line. We put $L = 3$ white pieces on this game, occupying the vertices of the squares and the lines. We will label these vertices as σ_i^x , σ_i^y , σ_i^z and $\mathbb{1}_i$, for $i = 1, 2, 3$.

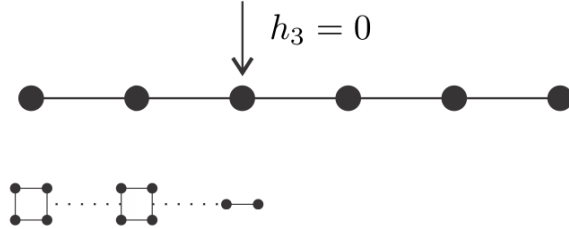


Figure 3.3: Board game associated to a chain when $h_3 = 0$.

In figure 3.4 we show example steps of the game, where each row is one step. We put one white piece for each site i , for $i = 1, 2, 3$, and these pieces can move on the square or line associated to this site. In the first row we put these pieces positioned on the labelled spaces in a way that the term $\kappa_{[1]} = \sigma_1^z \sigma_2^z \mathbb{1}_3$ is represented. In the next step (second row) we change the positions of these pieces to represent $\kappa_{[1]} \cdot \kappa_{[2]}$ which is proportional to $\sigma_1^z \sigma_2^y \mathbb{1}_3$. And again (third row) we change their positions to represent $\kappa_{[1]} \cdot \kappa_{[2]} \cdot \kappa_{[3]}$ which is proportional to $\sigma_1^z \sigma_2^x \sigma_3^z$.

We will say that a piece is on the left when it is in some position labelled by σ_i^z or σ_i^y . At the beginning we start with two pieces on the left, an even number. Multiplying $\kappa_{[1]}$ by $\kappa_{[2]}$ we move

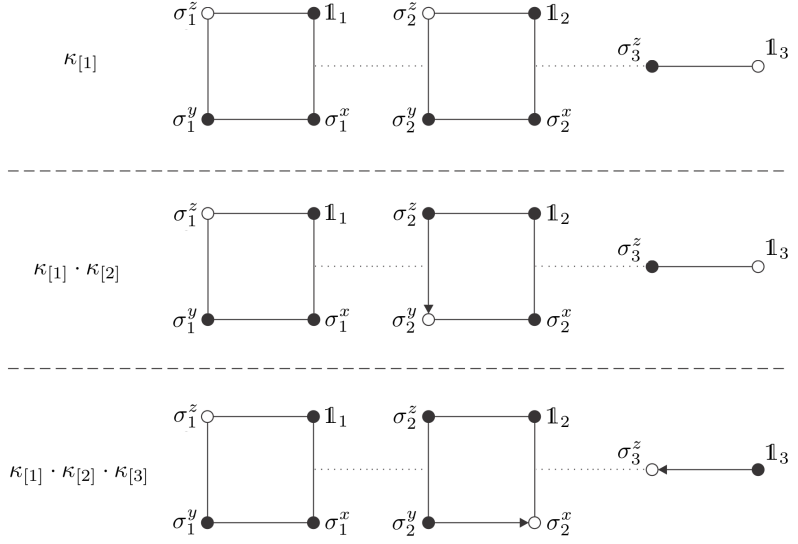


Figure 3.4: Scheme to understand the product $\kappa_{[1]}\kappa_{[2]}\kappa_{[3]}$ as a “board game”. The rows represent different steps ($n = 3$) of a board game with $L = 3$ white pieces. The pieces can move from one vertex to another only when they are connected by continuous lines.

one piece vertically without changing the number of pieces on the left side. Multiplying $\kappa_{[1]} \cdot \kappa_{[2]}$ by $\kappa_{[3]}$ we change the side of two pieces, so the number of pieces on the left is still even. We have an even number of pieces on the left and because of this at least one of the pieces corresponding to sites 1 or 2 has to be different of identity. This guarantees that the partial trace is null.

We can easily generalize the argument for the general case. Figure 3.4 would be similar, but with L pieces and n rows. The important fact is that: it does not matter the positions of the pieces corresponding to $\kappa_{[1]} \cdot \dots \cdot \kappa_{[l-1]}$, if $\kappa_{[l]} = \sigma_i^x$, it will just move the i -th piece vertically, and if $\kappa_{[l]} = \sigma_i^z\sigma_{i+1}^z$ it will just change the side of pieces i and $i + 1$. Furthermore, these are the only possible “moves”. As $\kappa_{[1]}$ always has an even number of pieces on the left and the allowed moves just change the side of an even number of pieces, we have that the product $\kappa_{[1]} \dots \kappa_{[L]}$ (proportional to $\eta_1 \dots \eta_L$) just has an even number of pieces on the left. Then, if $\eta_L = \sigma_L^z$, at least one η_i , for $i = 1, \dots, L - 1$, is a Pauli matrix, and then

$$\text{Tr}_{1,\dots,L-1}(\eta_1 \dots \eta_{L-1} \sigma_L^z) = \text{Tr}(\eta_1 \dots \eta_{L-1}) \sigma_L^z = 0 \quad (3.31)$$

which implies that $\text{Tr}(\bar{H}_{(n)}) = 0$. Therefore, by Equation (3.26) we have that $\text{Tr}_{1,\dots,L-1}(H'^n) = \text{Tr}(\tilde{H}_{(n)})\mathbb{1}_L$, which implies that $\text{Tr}_{1,\dots,L-1}(e^{-\beta H'}) = c\mathbb{1}_L$.

□

3.4.2 The Shielding Property on General Lattices with One Site in the Interface

We can make the proof of Theorem 2 to more general lattices and slightly more general Hamiltonians and we can state the following.

Theorem 3. *Let Λ be a lattice as described in Section 3.2.1 with $S = \{L\}$ for some site L . Assume that the Hamiltonian of the system is:*

$$H = - \sum_{i,j} J_{ij} \sigma_i^z \sigma_j^z - \sum_i h_i \sigma_i^x - \sum_i g_i \sigma_i^y, \quad (3.32)$$

where $h_L = g_L = 0$. For any temperature, the reduced state on the set Y of the Gibbs state of the whole lattice has no dependence on h_i , g_i and $J_{i,j}$, for all $i, j \in X$. Furthermore, the reduced state is given by

$$\rho_Y = \frac{e^{-\beta H''}}{\text{Tr}(e^{-\beta H''})}, \quad (3.33)$$

where $H'' = - \sum_{i,j \in B} (J_{ij} \sigma_i^z \sigma_j^z + h_j \sigma_i^x + g_i \sigma_i^y)$.

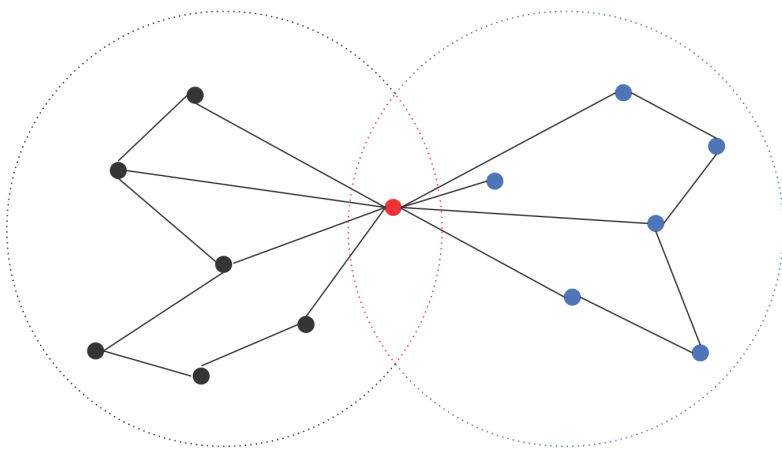


Figure 3.5: An example of a more general lattice.

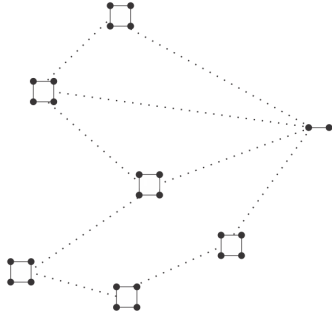


Figure 3.6: Scheme for the proof of the Theorem 3. It is analogous to Figure 3.4.

Proof: The proof is along the same lines of Theorem 2. When the lattice is not a chain, the argument of the board game is analogous to the argument for chains and it is pictured in Figure 3.6. The fact that we have an even number of pieces on the left does not depend on the relative geometry of the squares, so this fact is true for this alternative board game and the previous proof follows naturally.

Now, the Hamiltonian of this theorem is different from the Hamiltonian of the first theorem, because of the terms involving σ_i^y . But as we have already discussed in Section 3.1 by Equation (3.5) we can see that the Hamiltonian (3.32) (or (3.4)) can be put in the same form of the Hamiltonian (3.3). Thus we conclude the Hamiltonian (3.32) in a more general lattice satisfies the shielding property. \square

This shows that if a system is described by the transverse quantum Ising model on a lattice which separates two regions by only one site then the shielding property is satisfied. Note that in each side of the lattice we can even have long range interactions between sites. Moreover, the transverse field may vary from site to site, as long as it is always transverse to the interaction direction.

Moreover, it is only necessary that one side of the chain is described by the transverse Ising model and that the Hamiltonians on each side commute. Say that the left side is described by the transverse Ising model and the right side also has, for instance, external magnetic field in the z-direction. By the same arguments of the proofs of Theorems 2 and 3, it is possible to show that the reduced state of the right side has no dependence on the parameters of the left side. Of course

the left side can have dependence on the parameters of the right side.

3.4.3 The Shielding Property for an Open Chain of Three Spins

In this section we provide two examples which illustrate why the result of Theorem 2 is counter-intuitive. Suppose we have a chain with three sites (namely 1, 2 and 3) with ferromagnetic interaction between adjacent sites in the z -direction. Suppose an arbitrarily large magnetic field is applied on site 1 and it becomes polarized. One could expect that sites 2 and 3 will also have polarized magnetizations. This is true when the magnetic field is applied in the z -direction, the same direction of the interactions. However this is not the case for the quantum Ising model, since there the external magnetic field is transverse. When the magnetic field is applied in some orthogonal direction (say x -direction) our intuitive notion fails. Note moreover that this is just a particular consequence of the proof of Theorem 2. In the following we show the equations and results which characterize two examples, but the reader interested in the explicitly calculations can find them in App. C.

Longitudinal Ising Model with Three Spins

For the longitudinal Ising model with three spins we consider the following Hamiltonian.

$$H = -h\sigma_1^z - \sigma_1^z\sigma_2^z - \sigma_2^z\sigma_3^z. \quad (3.34)$$

For simplicity we are considering that the interactions between sites 1 and 2 and between 2 and 3 are equal to 1, but our conclusions would be similar for other choices of parameters. We can show that the reduced state of site 3 is given by

$$\rho_3 = \frac{1}{2}\mathbb{1} + \frac{1}{2}\tanh^2(\beta)\tanh(\beta h)\sigma_3^z, \quad (3.35)$$

and thus the expected value of its magnetization in the z -direction is given by

$$\langle\sigma_3\rangle = \tanh^2(\beta)\tanh(\beta h). \quad (3.36)$$

We can see that it has an explicitly dependence on the magnetic field applied on site 1, even with null external magnetic field in the interface (site 2).

Analogously we can consider a chain with N sites such that only in site 1 is applied a non-zero external magnetic field (Hamiltonian given by $H = -h_1\sigma_1^z - \sigma_1^z\sigma_2^z - \dots - \sigma_{N-1}^z\sigma_N^z$). We can find that the reduced state at site i , for $i = 1, \dots, N$, is given by

$$\rho_i = \frac{1}{2}\mathbb{1} + \frac{1}{2}\tanh^{i-1}(\beta)\tanh(h_1\beta)\sigma_i^z, \quad (3.37)$$

and then the magnetization in the z -direction of this same site is given by

$$\langle\sigma_i\rangle = \tanh^{i-1}(\beta)\tanh(h_1\beta). \quad (3.38)$$

Thus, the reduced state on every site of the lattice has dependence on the external magnetic field h_1 on site 1. We can see that this behaviour is completely different from that related in Theorem 2.

Transversal Ising Model with Three Spins

Now, consider the transverse Ising model with three sites, given by the following Hamiltonian

$$H = -h\sigma_1^x - J_1\sigma_1^z\sigma_2^z - J_2\sigma_2^z\sigma_3^z. \quad (3.39)$$

We can show that the reduced state of sites 2 and 3 is given by

$$\rho_{2,3} = \frac{1}{4}\left(\mathbb{1} + \frac{\sinh(\beta J_2)}{\cosh(\beta J_2)}\sigma_2^z\sigma_3^z\right), \quad (3.40)$$

which does not have dependence on the strength of the magnetic field h nor on the exchange coupling J_1 , confirming the predictions of Theorem 2.

3.5 Duality for the Tranverse Ising Model

The result of Theorem 2 can also be explained by the duality of the quantum Ising chain [47], perhaps in a more intuitive way. The duality allows us to write the Hamiltonian in terms of a Hamiltonian for a dual chain where the parameters h 's and J 's swap their roles. To be more precise, define the operators:

$$\mu_{i+1/2}^z = \sigma_i^z\sigma_{i+1}^z, \quad \mu_{j+1/2}^x = \prod_{k=j+1}^N \sigma_k^x \quad (3.41)$$

for $i = 1, \dots, N - 1$ and $j = 0, \dots, N - 1$. Set $\mu_{N+1/2}^z = \sigma_N^z$, $\mu_{1/2}^z = \sigma_1^z$ and $\mu_{N+1/2}^x = \mathbb{1}$. With these definitions, Hamiltonian (3.13) can be written as:

$$H = - \sum_{j=1}^{N-1} J_j \mu_{j+1/2}^z - \sum_{j=1}^N h_j \mu_{j-1/2}^x \mu_{j+1/2}^x. \quad (3.42)$$

Since the operators $\mu_{i+1/2}^x$ and $\mu_{i+1/2}^z$ satisfy the algebra of Pauli operators, the Hamiltonian H written as in Equation (3.42) can be seen as the Hamiltonian of a dual spin chain (actually, it is not true for $i = N$, but for large N this is not relevant). Since h_j appears multiplying $\mu_{i-1/2}^x \mu_{i+1/2}^x$, it can be interpreted as the strength of the interaction between the dual sites, and as J_j appears multiplying $\mu_{j+1/2}^z$ only, it can be interpreted as the external magnetic field.

Therefore, as we assume $h_L = 0$, for some $L = 2, \dots, N - 1$, the dual chain has two decoupled halves (see figure 3.7). We can then safely conclude that the reduced states of each side of the dual chain do not have dependence on the parameters of the Hamiltonian of the other side, since the whole state is a product of the Gibbs states of each half.

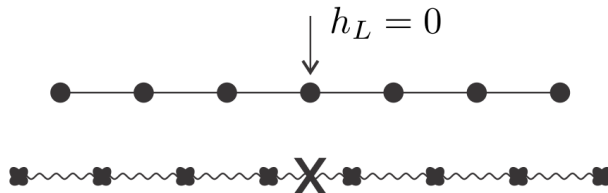


Figure 3.7: Representations of the original and of the dual chains. The sites of the dual chain correspond to the links of the original chain and vice-versa. Making the external magnetic field null in one site of the original chain is equivalent to cutting off the interaction in the dual chain.

To arrive on our desired conclusions for the original chain we can explore the fact that all the local observables of one side of the original chain is a combination of observables of only that side of the dual chain. This is possible to show by finding the inverse of Equations (3.41) as follows:

$$\begin{aligned} \sigma_i^z &= \prod_{k=0}^{i-1} \mu_{k+1/2}^z, & \sigma_i^x &= \mu_{i-1/2}^x \mu_{i+1/2}^x \quad \text{for } i = 1, \dots, N - 1 \\ && &= \mu_{N+1/2}^x \quad \text{for } i = N. \end{aligned} \quad (3.43)$$

and

$$\begin{aligned}\sigma_i^y &= i\sigma_i^z\sigma_i^x = i\mu_{i-1/2}^x\mu_{i+1/2}^x \prod_{k=0}^{i-1} \mu_{k+1/2}^z \quad \text{for } i = 1, \dots, N-1 \\ &= i\mu_{N+1/2}^x \prod_{k=0}^{N-1} \mu_{k+1/2}^z \quad \text{for } i = N.\end{aligned}\tag{3.44}$$

Since the Gibbs state of the dual chain is a product state, a local observable of one side of the original chain can be written only as a function of the parameters of the Hamiltonian on the same side. We conclude that the reduced state $\rho_{1, \dots, L-1}$ of the original chain does not depend on the parameters $h_L, \dots, h_N, J_L, \dots, J_N$. This argument, however, does not clearly show the desired property for the reduced state containing site L , although Theorem 2 ensures it must also hold in that case.

3.6 Inconclusive Proofs for Lattices with More Sites in the Interface

The shielding property is a strong property in the sense that it holds for any choice of parameters in the sets A and B , respecting the condition that the external magnetic field is null in the site L , which is the interface between A and B . But if we have more sites in the interface we cannot attest if the property holds using the arguments of the previous proofs anymore. In this section we will explain why the previous proofs are inconclusive in these cases. First we discuss the proof using the game board and later the proof using the duality of the Ising model.

Game Board and More Sites in the Interface

Let us consider, for simplicity, that the interface contains two sites. In Figure 3.8 we illustrate one example of a chain with two sites in the interface. Suppose that the external magnetic field applied in these two sites is null. We will follow steps analogous to the proof of Section 3.4.1.

We will enumerate the sites of set A with labels $1, \dots, L-1$, the two sites of the interface will be labelled by L and L' and the sites of set B are labelled with $L+1, \dots, N$. The Hamiltonian of

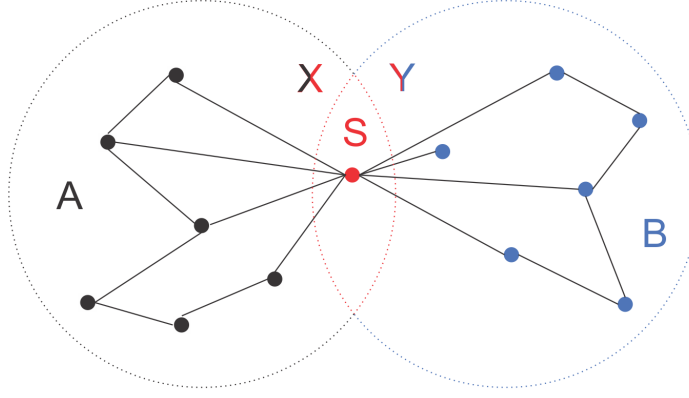


Figure 3.8: Example of a lattice with two sites in the interface.

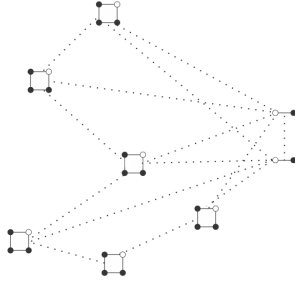


Figure 3.9: Scheme for the proof analogous as in Figure 3.4.

this system is given by Equation (3.3) with $h_L = h_{L'} = 0$. We can set $H = H^I + H^{II}$, with

$$H^I = - \sum_{\substack{i,j=1 \\ i < j}}^{L-1} J_{ij} \sigma_i^z \sigma_j^z - \sum_{i=1}^{L-1} (J_{iL} \sigma_i^z \sigma_L^z + J_{iL'} \sigma_i^z \sigma_{L'}^z) - \sum_{i=1}^{L-1} h_i \sigma_i^x \quad (3.45)$$

and

$$H^{II} = - \sum_{\substack{i,j=L+1 \\ i < j}}^N J_{ij} \sigma_i^z \sigma_j^z - \sum_{i=L+1}^N (J_{Li} \sigma_L^z \sigma_i^z + J_{L'i} \sigma_{L'}^z \sigma_i^z) - \sum_{i=L+1}^N h_i \sigma_i^x \quad (3.46)$$

Such as in Section 3.4.1 we have that H^I has support on the space of sites $1, \dots, L$, while H^{II} has support on the space of L, \dots, N , and they commute with each other. That is:

$$[H^I, H^{II}] = 0, \quad H^I = H' \mathbb{1}_{L+1} \dots \mathbb{1}_N \quad \text{and} \quad H^{II} = \mathbb{1}_1 \dots \mathbb{1}_{L-1} H''. \quad (3.47)$$

The partial trace of the Gibbs state is proportional to

$$\mathrm{Tr}_{1, \dots, L-1} (e^{-\beta H'}) = \{\mathrm{Tr}_{1, \dots, L-1} (e^{-\beta H'}) \mathbb{1}_{L+1} \dots \mathbb{1}_N\} \cdot e^{-\beta H''} \quad (3.48)$$

It is now that the situation becomes different from that of section 3.4.1, since here we cannot guarantee that $\text{Tr}_{1,\dots,L-1}(e^{-\beta H'}) = \mathbb{1}_L \mathbb{1}_{L'}$ anymore. If we proceed in the same way as before we would find a game board for this new lattice as pictured in Figure 3.9. There we illustrate an undesired situation for the purpose of the proof. The argument that we could have only an even number of white pieces in the left positions is also valid here, but not useful. We could have a situation where all the pieces of the set A are on the positions which represent the identity operator and the two pieces of the interface sites occupying the positions which represent the operators σ_L^z and $\sigma_{L'}^z$. Thus, we can only guarantee that

$$\text{Tr}_{1,\dots,L-1}(e^{-\beta H'}) = c_1 \mathbb{1}_L \mathbb{1}_{L'} + c_2 \sigma_L^z \sigma_{L'}^z \quad (3.49)$$

where c_1 and c_2 are constants which can have dependence on the parameters of set X . In the case of section 3.4.1 the constant disappears after the normalization. Now, we cannot guarantee that these constants will disappear, therefore the proof is inconclusive. Actually, for some cases these constants will have dependence on the parameters of the set X and we will provide some examples in the next section.

Duality and More Sites in the Interface

To explain why the proof using the duality for the Ising model is inconclusive for lattices with more sites in the interface let us consider the lattice of Figure 3.10.a. Let the interface be composed of sites 2 and 3 and the Hamiltonian of the system be given by

$$H = -\sigma_1^z \sigma_2^z - \sigma_2^z \sigma_3^z - \sigma_2^z \sigma_4^z - \sigma_3^z \sigma_4^z - h_1 \sigma_1^x - h_2 \sigma_2^x - h_3 \sigma_3^x - h_4 \sigma_4^x \quad (3.50)$$

A similar duality of that in Section 3.5 would require a lattice as in Figure 3.10.b. The operators associated to these dual sites would require equivalent properties of the Pauli matrices. Call them μ_I^k , μ_{II}^k , μ_{III}^k and μ_{IV}^k , for $k = z, x, y$. One of these properties is that they have to be a square root of identity operator, that is $(\mu_K^k)^2 = \mathbb{1}$, for $k = z, x, y$ and $K = I, II, III, IV$. The dual Hamiltonian would have the form

$$H = -\mu_I^z - \mu_{II}^z - \mu_{III}^z - \mu_{IV}^z - h_1 \mu_I^x \mu_{III}^x - h_2 \mu_I^x \mu_{II}^x - h_3 \mu_{III}^x \mu_{IV}^x - h_4 \mu_{II}^x \mu_{IV}^x \quad (3.51)$$

Comparing Equations (3.50) and (3.51) and using the property that the dual operators are square roots of identity operator, we have that

$$\mu_I^x \mu_{II}^x = \sigma_2^x, \quad \mu_I^x \mu_{III}^x = \sigma_1^x, \quad \mu_{II}^x \mu_{IV}^x = \sigma_4^x, \quad \text{and} \quad \mu_{III}^x \mu_{IV}^x = \sigma_3^x. \quad (3.52)$$

With the first two equalities we have that $\mu_{II}^x \mu_{III}^x = \sigma_1^x \sigma_2^x$ and with the last two we have that $\mu_{II}^x \mu_{III}^x = \sigma_3^x \sigma_4^x$. Thus we would have that $\sigma_1^x \sigma_2^x = \sigma_3^x \sigma_4^x$, which is an inconsistency.

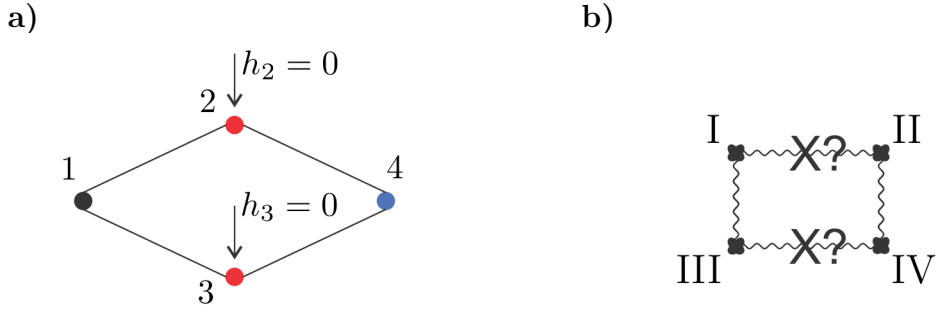


Figure 3.10: a) Example of a system with two sites on the interface which does not satisfy the shielding property. The reduced state on site 4 has dependence on the external magnetic field h_1 applied on site 1. b) An example of dual lattice where links swap their roles with sites, when the original lattice has more than one site in the interface. In this section we show that it does not work as in Section 3.5.

On the other hand, we could try to make a linear dual chain using similar definitions for the dual operators as those done in Equation (3.41). So, define

$$\mu_{i+1/2}^z = \sigma_i^z \sigma_{i+1}^z, \quad \mu_{j-1/2}^x = \prod_{k=j}^4 \sigma_k^x = \sigma_j^x \dots \sigma_4^x \quad (3.53)$$

for $i = 1, 2, 3$, $j = 1, 2, 3, 4$, and define $\mu_{4+1/2}^z = \mathbb{1}$. We can rewrite the Hamiltonian (3.50) as

$$H = -\mu_{1+1/2}^z - \mu_{2+1/2}^z \mu_{4+1/2}^z - \mu_{3+1/2}^z - \mu_{2+1/2}^z \mu_{3+1/2}^z \\ - h_1 \mu_{0+1/2}^x \mu_{1+1/2}^x - h_2 \mu_{1+1/2}^x \mu_{2+1/2}^x - h_3 \mu_{2+1/2}^x \mu_{3+1/2}^x - h_4 \mu_{3+1/2}^x \mu_{4+1/2}^x. \quad (3.54)$$

But this form is not similar to the previous one. First, the transverse Ising model have interactions only in perpendicular directions of external magnetic fields, while in Equation (3.54) we have interactions in the same direction of the external magnetic fields: the terms $-\mu_{1+1/2}^z$ and $-\mu_{3+1/2}^z$ represent external magnetic fields in the z -direction while the terms $-\mu_{2+1/2}^z \mu_{4+1/2}^z$ and

$-\mu_{2+1/2}^z \mu_{3+1/2}^z$ represent interactions also in the z -direction. Furthermore, we are working with Ising models with interactions only between first neighbours and the term $-\mu_{2+1/2}^z \mu_{4+1/2}^z$ of Equation (3.54) is an interaction of long range.

Therefore, we cannot use Equation (3.54) to reach the same conclusions that we had in Section 3.5. Actually, for the system of Figure 3.10.a., we can show that the magnetization of site 4 has dependence on the external magnetic field h_1 applied in site 1, even with $h_2 = h_3 = 0$, for positive temperatures, that is, $\beta < \infty$. See App. D for the detailed calculations.

3.7 Correlations and the Shielding Property

The shielding property states that the reduced state of set Y has no dependence on the parameters of set A . However, it does not guarantee that these sets do not have correlations. Take for example the chain of three sites considered in Section 3.4.3. By Equation (3.40) we can see that the correlation $\langle \sigma_1^z \sigma_3^z \rangle - \langle \sigma_1^z \rangle \langle \sigma_3^z \rangle$ between sites 1 and 3 is given by

$$\langle \sigma_1^z \sigma_3^z \rangle - \langle \sigma_1^z \rangle \langle \sigma_3^z \rangle = \tanh(\beta J_2) \tanh\left(\beta \sqrt{J_1^2 + h^2}\right) \frac{J_1}{\sqrt{J_1^2 + h^2}} \quad (3.55)$$

which is different from zero.

Another interesting example to be considered is the following. Let a chain of 5 sites where the external magnetic field is null on sites 2 and 4. The Hamiltonian of this system is given by

$$H = -h_1 \sigma_1^x - J_1 \sigma_1^z \sigma_2^z - J_2 \sigma_2^z \sigma_3^z - h_3 \sigma_3^x - J_3 \sigma_3^z \sigma_4^z - J_4 \sigma_4^z \sigma_5^z - h_5 \sigma_5^x. \quad (3.56)$$

By the shielding property, Theorem 2, we have that neither $\langle \sigma_1^z \rangle$ nor $\langle \sigma_5^z \rangle$ have dependence on h_3 . But, we can show that the correlation $\langle \sigma_1^z \sigma_5^z \rangle - \langle \sigma_1^z \rangle \langle \sigma_5^z \rangle$ has dependence on h_3 . This can be understood looking at this chain in a bit different way, as shown in Figure 3.11. There we see this chain as a two dimensional lattice, where sets 2 and 4 are the interface, site 3 is set A and sites 1 and 5 compose set B . Now, we have a lattice where the interface contains more than one site, where we already know that the shielding property does not hold, in general. We can understand the quantity $\sigma_1^z \sigma_5^z$ as an observable of one side of the lattice, which can have dependence on the parameters of the other side of the lattice, since the interface has two sites.

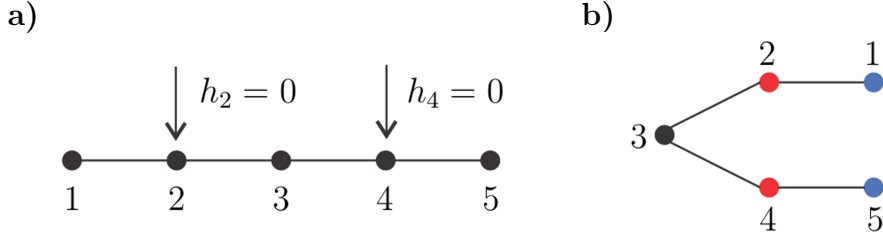


Figure 3.11: **a)** A chain with 5 sites described by the transverse Ising model with external magnetic field null in sites 2 and 4. The observables on site 1 and on site 5 separately have no dependence on the parameter h_3 , but the correlations still exist. **b)** To explain the fact that the correlations still exist we can see the chain as a two dimensional lattice where the interface considered now has two sites.

3.8 The Parity Operator and the Shielding Property

Here, we show an alternative proof for the shielding property which is equivalent to the other two proofs in the case of one site in the interface, but which exhibits more structure when the interface contains more sites. Furthermore, this proof allows us to understand why the examples of the previous sections satisfy the shielding property on the ground state and do not satisfy for the Gibbs states with positive temperatures.

For simplicity, let us consider a lattice which is “almost” a chain as we can see in the Figure 3.12. The interface is given by the red sites and are labelled by L and L' . The set A is on the left of the interface and its sites are in black, labelled from 1 to $L - 1$; the set B is on the right of the interface and its sites are in blue, labelled from $L + 1$ to N .

The Hamiltonian of this system is given by Equation (3.3), with $h_L = h_{L'} = 0$. We will decompose this Hamiltonian in three terms:

$$H = H^I + H^S + H^{II}, \quad \text{where } H^S = -J_{LL'}\sigma_L^z\sigma_{L'}^z, \quad (3.57)$$

$$H^I = -\sum_{i=1}^{L-1} (J_i\sigma_i^z\sigma_{i+1}^z + h_i\sigma_i^x) - J_{L-1}\sigma_{L-1}^z\sigma_L^z - J'_{L-1}\sigma_{L-1}^z\sigma_{L'}^z, \quad (3.58)$$

and

$$H^{II} = -\sum_{i=L+1}^{N-1} (J_i\sigma_i^z\sigma_{i+1}^z + h_{i+1}\sigma_{i+1}^x) - J_L\sigma_L^z\sigma_{L+1}^z - J'_L\sigma_{L'}^z\sigma_{L+1}^z. \quad (3.59)$$

Note that these three operators commute with $\mathbb{1}_1 \dots \mathbb{1}_{L-1} \sigma_L^z \mathbb{1}_{L'} \mathbb{1}_{L+1} \dots \mathbb{1}_N$ and $\mathbb{1}_1 \dots \mathbb{1}_L \sigma_L^z \mathbb{1}_{L+1} \dots \mathbb{1}_N$. Then we can write H^I , H^{II} and H^S in a basis of eigenvectors of the operators

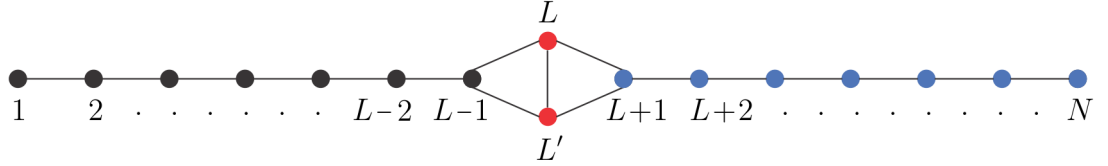


Figure 3.12: A lattice which is almost a chain. The interface contains two sites (in red) which we label by L and L' . The sites of set A (in black) are on the left of the interface and we label them by $1, 2, \dots, L - 1$. The sites of set B (in blue) are on the right of the interface and we label them by $L + 1, \dots, N$.

$\mathbb{1}_1 \dots \mathbb{1}_{L-1} \sigma_L^z \mathbb{1}_{L'} \mathbb{1}_{L+1} \dots \mathbb{1}_N$ and $\mathbb{1}_1 \dots \mathbb{1}_L \sigma_{L'}^z \mathbb{1}_{L+1} \dots \mathbb{1}_N$. They assume the following form

$$H^S = -J_{LL'} \mathbb{1}_{1, \dots, L-1} \sigma_L^z \sigma_{L'}^z \mathbb{1}_{L+1, \dots, N} = - \sum_{s, s' = -1, 1} ss' J_{LL'} \frac{\mathbb{1}_L + s\sigma_L^z}{2} \otimes \frac{\mathbb{1}_{L'} + s'\sigma_{L'}^z}{2}, \quad (3.60)$$

$$H^I = H' \otimes \mathbb{1}_{L+1, \dots, N} = \sum_{s, s' = -1, 1} H'^{(s, s')} \otimes \frac{\mathbb{1}_L + s\sigma_L^z}{2} \otimes \frac{\mathbb{1}_{L'} + s'\sigma_{L'}^z}{2} \otimes \mathbb{1}_{L+1, \dots, N}, \quad (3.61)$$

where

$$\begin{aligned} H'^{(s, s')} = & \left(- \sum_{i=1}^{L-2} J_i \mathbb{1}_{1, \dots, i-1} \sigma_i^z \sigma_{i+1}^z \mathbb{1}_{i+2, \dots, L-1} - \sum_{i=1}^{L-1} h_i \mathbb{1}_{1, \dots, i-1} \sigma_i^x \mathbb{1}_{i+1, \dots, L-1} \right) \\ & - s J_{L-1} \mathbb{1}_{1, \dots, L-2} \sigma_{L-1}^z - s' J'_{L-1} \mathbb{1}_{1, \dots, L-2} \sigma_{L-1}^z, \end{aligned} \quad (3.62)$$

and

$$H^{II} = \mathbb{1}_{1, \dots, L-1} \otimes H'' = \sum_{s, s' = -1, 1} \mathbb{1}_{1, \dots, L-1} \otimes \frac{\mathbb{1}_L + s\sigma_L^z}{2} \otimes \frac{\mathbb{1}_{L'} + s'\sigma_{L'}^z}{2} \otimes H''^{(s, s')}, \quad (3.63)$$

where

$$\begin{aligned} H''^{(s, s')} = & \left(- \sum_{i=L+1}^N J_i \mathbb{1}_{L+1, \dots, i-1} \sigma_i^z \sigma_{i+1}^z \mathbb{1}_{i+2, \dots, N} - \sum_{i=L+1}^N h_i \mathbb{1}_{L+1, \dots, i-1} \sigma_i^x \mathbb{1}_{i+1, \dots, N} \right) \\ & - s J_{L+1} \sigma_{L+1}^z \mathbb{1}_{L+2, \dots, N} - s' J'_{L+1} \sigma_{L+1}^z \mathbb{1}_{L+2, \dots, N}. \end{aligned} \quad (3.64)$$

We want to calculate the reduced state of the Gibbs state in each side of the “chain”. To do this, first note that

$$[H^I, H^{II}] = 0, \quad [H^I, H^S] = 0 \quad \text{and} \quad [H^S, H^{II}] = 0, \quad (3.65)$$

then the Gibbs state is proportional to

$$e^{-\beta H} = e^{-\beta H^I} e^{-\beta H^S} e^{-\beta H^{II}} \quad (3.66)$$

$$= \left(e^{-\beta H'} \mathbb{1}_{L+1, \dots, N} \right) \left(\mathbb{1}_{1, \dots, L-1} e^{-\beta \sigma_L^z \sigma_{L'}^z} \mathbb{1}_{L+1, \dots, N} \right) \left(\mathbb{1}_{1, \dots, L-1} e^{-\beta H''} \right) \quad (3.67)$$

Now, let Pr be some projector operator and B some operator. We have that

$$e^{-\beta Pr \otimes B} = \sum_n \frac{-\beta^n}{n!} (Pr \otimes B)^n = Pr \otimes \sum_n \frac{-\beta^n}{n!} (B)^n = Pr \otimes e^{-\beta B}. \quad (3.68)$$

Since $\frac{\mathbb{1}_L + s\sigma_L^z}{2} \otimes \frac{\mathbb{1}_{L'} + s'\sigma_{L'}^z}{2}$ is a projector operator, for $s, s' = 1, -1$, we can write

$$e^{-\beta H''} = \sum_{s, s' = -1, 1} \frac{\mathbb{1}_L + s\sigma_L^z}{2} \otimes \frac{\mathbb{1}_{L'} + s'\sigma_{L'}^z}{2} \otimes e^{-\beta H''(s, s')}. \quad (3.69)$$

We also have

$$e^{-\beta H'} = \sum_{s, s' = -1, 1} e^{-\beta H'(s, s')} \otimes \frac{\mathbb{1}_L + s\sigma_L^z}{2} \otimes \frac{\mathbb{1}_{L'} + s'\sigma_{L'}^z}{2}, \quad (3.70)$$

and

$$e^{-\beta \sigma_L^z \sigma_{L'}^z} = \sum_{s, s' = -1, 1} e^{-\beta ss' J_{LL'}} \frac{\mathbb{1}_L + s\sigma_L^z}{2} \otimes \frac{\mathbb{1}_{L'} + s'\sigma_{L'}^z}{2}. \quad (3.71)$$

Thus, the Gibbs state is proportional to

$$e^{-\beta H} = \sum_{s, s' = -1, 1} e^{-\beta ss' J_{LL'}} e^{-\beta H'(s, s')} \otimes \frac{\mathbb{1}_L + s\sigma_L^z}{2} \otimes \frac{\mathbb{1}_{L'} + s'\sigma_{L'}^z}{2} \otimes e^{-\beta H''(s, s')} \quad (3.72)$$

Now, let us consider a parity operator on the sites $1, \dots, L-1$, defined by

$$P = \prod_{i=1}^{L-1} \sigma_i^x. \quad (3.73)$$

Then it satisfies

$$PH'^{(s, s')}P = H'^{(-s, -s')}, \quad (3.74)$$

for $s, s' = 1, -1$, which can be verified by direct calculations. Using the cyclic property of the trace and that $P^2 = \mathbb{1}_{1, \dots, L-1}$, we have

$$\text{Tr} (H'^{(s, s')}) = \text{Tr} (PH'^{(s, s')}P) = \text{Tr} (H'^{(-s, -s')}), \quad (3.75)$$

which means that

$$\text{Tr} (H'^{(1, 1)}) = \text{Tr} (H'^{(-1, -1)}) \quad \text{and} \quad \text{Tr} (H'^{(1, -1)}) = \text{Tr} (H'^{(-1, 1)}) \quad (3.76)$$

Using this property we can compute the partial trace of the Equation (3.72), obtaining:

$$\mathrm{Tr}_{1,\dots,L-1}\left(e^{-\beta H}\right) = \sum_{s,s'=-1,1} e^{-ss'J_{LL'}} \mathrm{Tr}\left(e^{-\beta H'(s,s')}\right) \frac{\mathbb{1}_L + s\sigma_L^z}{2} \otimes \frac{\mathbb{1}_{L'} + s'\sigma_{L'}^z}{2} \otimes e^{-\beta H''(s,s')} . \quad (3.77)$$

Therefore:

$$\begin{aligned} \frac{\mathrm{Tr}_{1,\dots,L-1}(e^{-\beta H})}{\mathrm{Tr}(e^{-\beta H})} &= e^{-J_{LL'}} \frac{\mathrm{Tr}\left(e^{-\beta H'^{(1,1)}}\right)}{\mathrm{Tr}(e^{-\beta H})} \left(\frac{\mathbb{1}_L + \sigma_L^z}{2} \otimes \frac{\mathbb{1}_{L'} + \sigma_{L'}^z}{2} \otimes e^{-\beta H''^{(1,1)}} \right. \\ &\quad \left. + \frac{\mathbb{1}_L - \sigma_L^z}{2} \otimes \frac{\mathbb{1}_{L'} - \sigma_{L'}^z}{2} \otimes e^{-\beta H''^{(-1,-1)}} \right) \\ &+ e^{J_{LL'}} \frac{\mathrm{Tr}\left(e^{-\beta H'^{(1,-1)}}\right)}{\mathrm{Tr}(e^{-\beta H})} \left(\frac{\mathbb{1}_L + \sigma_L^z}{2} \otimes \frac{\mathbb{1}_{L'} - \sigma_{L'}^z}{2} \otimes e^{-\beta H''^{(1,-1)}} \right. \\ &\quad \left. + \frac{\mathbb{1}_L - \sigma_L^z}{2} \otimes \frac{\mathbb{1}_{L'} + \sigma_{L'}^z}{2} \otimes e^{-\beta H''^{(1,-1)}} \right). \end{aligned} \quad (3.78)$$

This equation shows that, in general, the shielding property does not hold when the interface contains two sites. Indeed, in Equation (3.78) the terms $\frac{\mathbb{1}_L + s\sigma_L^z}{2} \otimes \frac{\mathbb{1}_{L'} + s'\sigma_{L'}^z}{2}$ represent sectors in the Hilbert space where the spins of the sites of the interface are well defined in the z -direction. That is, the sign of s and s' define the spins directions of the sites in the interface. For example, the term $\frac{\mathbb{1}_L + \sigma_L^z}{2} \otimes \frac{\mathbb{1}_{L'} - \sigma_{L'}^z}{2}$ is the projector on the sector where the spin in site L is positive in the z -direction and the spin in site L' is negative in this same direction. Note also that the terms $\mathrm{Tr}(e^{-\beta H'(s,s')})$ multiply the terms which appear $\frac{\mathbb{1}_L + s\sigma_L^z}{2} \otimes \frac{\mathbb{1}_{L'} + s'\sigma_{L'}^z}{2}$ and $\frac{\mathbb{1}_L - s\sigma_L^z}{2} \otimes \frac{\mathbb{1}_{L'} - s'\sigma_{L'}^z}{2}$. Now, suppose that

$$\mathrm{Tr}\left(e^{-\beta H'^{(1,-1)}}\right) = 0. \quad (3.79)$$

This hypothesis with our observations above means that the interface spins can only be both positive or both negative, that is, they are aligned. Taking the global trace on Equation (3.78) we get that

$$e^{-J_{LL'}} \frac{\mathrm{Tr}(e^{-\beta H'^{(1,1)}})}{\mathrm{Tr}(e^{-\beta H})} = \frac{1}{\mathrm{Tr}\left(e^{-\beta H''^{(1,1)}} + e^{-\beta H''^{(-1,-1)}}\right)}, \quad (3.80)$$

so we would have

$$\begin{aligned} \frac{\mathrm{Tr}_{1,\dots,L-1}(e^{-\beta H})}{\mathrm{Tr}(e^{-\beta H})} &= \frac{1}{\mathrm{Tr}\left(e^{-\beta H''^{(1,1)}} + e^{-\beta H''^{(-1,-1)}}\right)} \left(\frac{\mathbb{1}_L + \sigma_L^z}{2} \otimes \frac{\mathbb{1}_{L'} + \sigma_{L'}^z}{2} \otimes e^{-\beta H''^{(1,1)}} \right. \\ &\quad \left. + \frac{\mathbb{1}_L - \sigma_L^z}{2} \otimes \frac{\mathbb{1}_{L'} - \sigma_{L'}^z}{2} \otimes e^{-\beta H''^{(-1,-1)}} \right), \end{aligned} \quad (3.81)$$

which has no explicitly dependence on H^I . Thus we could conclude that the reduced state of the right set has no explicitly dependence on the parameters of the left set. However, the hypothesis of Equation (3.79) is too strong for the Gibbs state with positive temperatures, in general. On the other hand, for the ground state, we can find parameters which maintain the spins aligned. In the case of the ground state, instead of Equation (3.79), we assume that

$$\lim_{\beta \rightarrow \infty} \frac{\text{Tr}(e^{-\beta H'^{(1,-1)}})}{\text{Tr}(e^{-\beta H})} = 0. \quad (3.82)$$

We point out that we could also have a similar discussion replacing $H'^{(1,-1)}$ by $H'^{(1,1)}$ in Equations (3.79) and (3.82). In this case, we would find that the spins of the interface are anti-aligned.

In conclusion, we have that if the system is in a state such that the two spins of the interface are with a well defined relative alignment between each other (that is, either aligned in the same direction or in opposite directions), then we can have the shielding property.

Finally, this proof and conclusions can be generalized for any lattice and any number m of sites in the interface. Remember that the interface is defined in Section 3.2 and we have the condition that the external magnetic field is null on all sites of it. Let us maintain the labelling that $i \in A$, for $i = 1, \dots, L-1$ and $i \in B$ for $i = L+1, \dots, N$ and label the sites of the interface S by L_1, \dots, L_m . The equivalent to Equation (3.62) would be

$$H'^{(s_1, \dots, s_m)} = - \sum_{\substack{i,j=1 \\ i < j}}^{L-1} J_{ij} \sigma_i^z \sigma_j^z - \sum_{i=1}^{L-1} h_i \sigma_i^x - \sum_{k=1}^m \sum_{i=1}^{L-1} s_k J_{iL_k} \sigma_L^z \quad (3.83)$$

where here we have hidden the identity operators from the notation for simplicity. Using the parity operator as in Equation (3.75), we would have that

$$\text{Tr} (H'^{(s_1, \dots, s_m)}) = \text{Tr} (H'^{(-s_1, \dots, -s_m)}) \quad (3.84)$$

Let s_1^*, \dots, s_m^* be fixed values for the variables s_1, \dots, s_m , where $s_i = \pm 1$, for $i = 1, \dots, m$. Suppose that

$$\text{Tr} (e^{-\beta H'^{(s_1^*, \dots, s_m^*)}}) \neq 0, \quad \text{and that} \quad \text{Tr} (e^{-\beta H'^{(s_1, \dots, s_m)}}) = 0. \quad (3.85)$$

for all $(s_1, \dots, s_m) \neq (s_1^*, \dots, s_m^*)$ and $(s_1, \dots, s_m) \neq (-s_1^*, \dots, -s_m^*)$. Thus, similarly to Equa-

tion (3.81), we have

$$\frac{\text{Tr}_{1,\dots,L-1}(e^{-\beta H})}{\text{Tr}(e^{-\beta H})} = \frac{1}{\text{Tr}\left(e^{-\beta H''(s_1^*,\dots,s_m^*)} + e^{-\beta H''(-s_1^*,\dots,-s_m^*)}\right)} \left[\left(\bigotimes_{i=1}^m \frac{\mathbb{1}_L + s_i^* \sigma_i^z}{2} \right) \otimes e^{-\beta H''(s_1^*,\dots,s_m^*)} \right. \\ \left. + \left(\bigotimes_{i=1}^m \frac{\mathbb{1}_L - s_i^* \sigma_i^z}{2} \right) \otimes e^{-\beta H''(-s_1^*,\dots,-s_m^*)} \right], \quad (3.86)$$

and it means that if the system is in the Gibbs state, then the reduced state of set Y does not have explicitly dependence on the parameters of set A . Furthermore, if we have that

$$\lim_{\beta \rightarrow \infty} \frac{\text{Tr}(e^{-\beta H'(s_1^*,\dots,s_m^*)})}{\text{Tr}(e^{-\beta H})} \neq 0, \quad \text{and that} \quad \lim_{\beta \rightarrow \infty} \frac{\text{Tr}(e^{-\beta H'(s_1,\dots,s_m)})}{\text{Tr}(e^{-\beta H})} = 0. \quad (3.87)$$

for all $s_1, \dots, s_m \neq s_1^*, \dots, s_m^*$ and $s_1, \dots, s_m \neq -s_1^*, \dots, -s_m^*$, then we can conclude that if the system is in the ground state, then the reduced state of set Y does not have dependence on the parameters of set A .

We say that a family of m spins have *well defined alignment between each other* in the z -direction if the state of the whole system lies in one of the sectors defined by $\bigotimes_{i=1}^m \frac{\mathbb{1}_L + s_i^* \sigma_i^z}{2}$ or by $\bigotimes_{i=1}^m \frac{\mathbb{1}_L - s_i^* \sigma_i^z}{2}$, for s_1^*, \dots, s_m^* fixed.

Again, we conclude that if the spins of the interface have a well defined alignment between each other then the reduced state of the set Y does not have explicit dependence on the parameters of set A .

An example of system which exemplifies this connection between the shielding property and a well defined alignment of the spins of the interface is that of Figure 3.10.a. The reduced state of the interface spins is given by

$$\rho_{2,3} = \frac{1}{4} \mathbb{1} + \frac{1}{4} f(\beta, h_1, h_4) \sigma_2^z \sigma_3^z. \quad (3.88)$$

The function f is a function of the inverse of the temperature of the system β , and of the external magnetic fields h_1 and h_4 . We have that $0 \leq f(\beta, h_1, h_4) < 1$ for finite values of β and for all h_1, h_4 , which means that the spins of the interface do not have a well defined alignment between each other. It agrees with the fact that this system does not satisfy the shielding property for positive temperatures. When $\beta \rightarrow \infty$ we have that $f(\beta, h_1, h_4) \rightarrow 1$ for all h_1, h_4 , which means that the

spins of the interface have a well defined alignment between each other. Thus, it guarantees that this system satisfies the shielding property for the ground state, which agrees with our explicit calculations in Appendix D.

3.9 Implicit Dependence

In Theorem 2 of Section 3.4.1 we show that the reduced state of one side of a chain described by the transverse Ising model *has no dependence* on the parameters of the other side of the chain, if the external magnetic field is null in the interface. Comparing it with the last section, we see that we need the further restriction: the reduce state of one side of some lattice described by the transverse Ising model *has no explicit dependence* on the parameters of the other side of the lattice, if the external magnetic field is null in the interface *and* the spins of the interface have a well defined alignment between each other.

Firstly, we point out that the condition which requires the spins of the interface to have a well defined alignment between each other is trivial when we have only one site in the interface, because a unique site is always aligned with itself.

Now, note that in the second statement we have the word “explicit” when we talk about the dependence on the parameters. In the case of more than one site in the interface, once the numbers s_1, \dots, s_m which define the alignment of the sites of the interface are fixed, the reduced state of set Y has no dependence on the parameters of set A . But, the alignment of the sites of the interface could have dependence on the parameters of set A , causing a more subtle dependence of the reduced state of set Y on these parameters.

Consider the space of parameters, where we describe the parameters $h_i, J_{i,j}$, for i, j sites of the lattice. We define that some system *satisfy the shielding property for a window of parameters* if there is a hypercube in the space of parameters such that when they are allowed to vary only on this hypercube, then the system satisfy the shielding property.

Let us consider the following system, which exemplifies this validity of the shielding property. Consider the lattice of Figure 3.13. Suppose that the Hamiltonian of this system is given by the Ising model, with the external magnetic field being null in all sites and the strength of interactions labelled in this figure. In this same figure we can see the labelling of each site. We will consider

the interface given by the two sites in the intersection of the pentagons, coloured red. The sites in black are in set A and the sites in blue are in the set B . The interaction labelled with a is the free parameter which we will change in set A to observe the modifications in set Y .

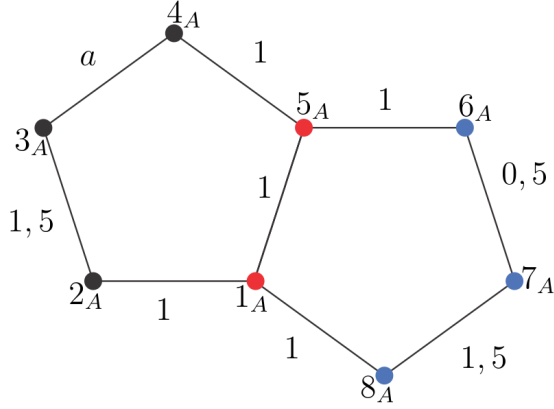


Figure 3.13: Example of lattice system which the reduced state of set Y has dependence on the parameters of set A .

Now, suppose that we wish to measure the observable $\sigma_{6_A}^z \sigma_{7_A}^z$. We can show that if $a > 0, 5$ we will always measure $\sigma_{6_A}^z \sigma_{7_A}^z = 1$, if $a < 0, 5$ we will always measure $\sigma_{6_A}^z \sigma_{7_A}^z = -1$ and if $a = 0, 5$ the answer of this measurement is random (see Appendix E for detailed calculations). So, if someone has access only to the set Y , she/he can infer if a is larger or smaller than $0, 5$, but this person could not infer the actual value of a . This shows the dependence of the reduced state of Y on the parameters of A .

We can show the same conclusions we have got for the above system for a system arbitrarily large. In Figure 3.14 we show a system which is an extension of the previous one. In this figure, we have drawn a system with six “pentagons”, but we can choose one with an arbitrarily large number of “pentagons” and our conclusions would be the same. To calculate the ground state of these systems we use the same arguments which we have used in the previous example (more details can be found in Appendix E). In these cases we can also find couple of sites i and j such that the observable $\sigma_i^z \sigma_j^z$ is equal 1 if $a > 0, 5$ and equal -1 if $a < 0, 5$.

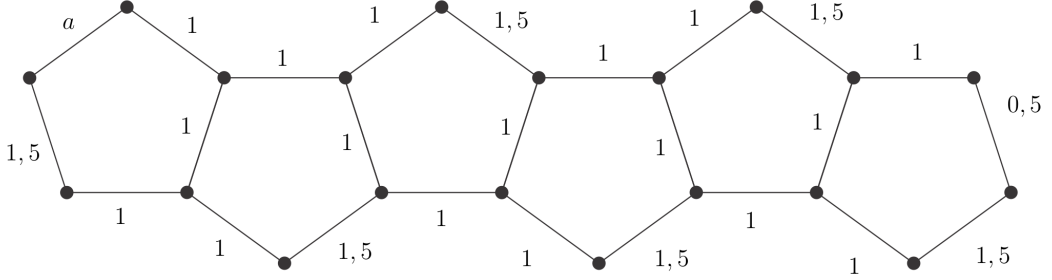


Figure 3.14: Example of lattice system arbitrarily large which the reduced state of set Y has dependence on the parameters of set A . It is the extension of the system of Figure 3.13. In this particular figure we have drawn six “pentagons”, but we can choose a similar system with any number of pentagons.

3.10 Frustration Free Satisfy the Shielding Property

In this section we will enunciate a Theorem which follows from the calculations of Section 3.8. Before, let us make two definitions.

Here we state the first one. We say that a lattice is *connected* if we cannot separate it into two sub-lattices such that none site of one sub-lattice has interaction with the sites of the other sub-lattice.

The second definition is the following. Take a lattice system with arbitrary Hamiltonian $H = \sum_X H_X$. We say that the system is *frustration free* if the ground state ρ_g also minimizes the energy associated with each term of the Hamiltonian separately: $\text{Tr}(\rho_g H_X) = \min_{\text{Tr}\rho=1} \{\text{Tr}(\rho H_X)\}$. That is, any global ground state ρ is a ground state for each H_X .

With this, we can state:

Theorem 4. *Let a lattice system be described on the finite lattice Λ by the transverse Ising model. Suppose that we have two subsets X and Y , with $X \cap Y = S$, a connected lattice, and the magnetic field applied on the sites of S is null. Furthermore the sites of $A = \Lambda \setminus Y$ do not interact directly with the sites of $B = \Lambda \setminus X$. If the system is frustration free for a hypercube of parameters, then the system satisfy the shielding property for this window of parameters.*

This corollary holds since the condition of frustration free guarantee that the spins of the

interface S have a well defined alignment between each other. Indeed consider the lattice given in Figure 3.15. Take the Hamiltonian of the Ising model, but make all the external magnetic fields null. The sites have interaction if they are connected by an edge and the strengths of the interactions are labelled in the figure. It is fixed -1 for some interactions and equal a variable M for the others. If $M < 0$, it is easy to see that all the spins are aligned when the system is in the ground state and the system is frustration free. Note that the observable $\sigma_3^z \sigma_4^z$ is always equal to 1.

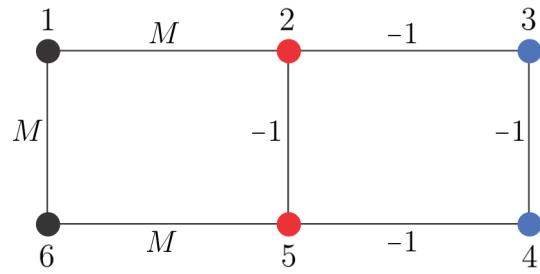


Figure 3.15: Example of system which is frustration free when $M < 0$ and satisfies the shielding property. The shielding property is dropped only for $M = 2$, when the system is frustrated.

But suppose that we take $M \gg 0$. We expect that the sites 1, 2, 5 and 6 turn to be anti-aligned between each other, that is, site 2 opposite to site 1, site 1 opposite to site 6 and so on. Thus, it could also change the state of sites 3 and 4 and consequently the value of $\sigma_3^z \sigma_4^z$. This is exactly what happens if we take $M > 2$. In this case the value of $\sigma_3^z \sigma_4^z$ will be not well defined anymore and the ground state is not unique anymore.

Conclusions

In this thesis we have worked with lattice systems and their behaviour when submitted to local quenches. We have seen the concept of an effective light-cone which arises for systems with short range interactions, which means that a local quench takes a finite amount of time to perturb considerably a distant region from this quench. There are many ways of measuring this perturbation, and the one we have worked with is the von Neumann entropy of this distant region. This entropy measures the entanglement of a pure state of a bipartite system. We have shown a bound for the variation of the von Neumann entropy, comparing the perturbed and the unperturbed system. This bound decreases exponentially with the distance between the region where we have made the quench and the region which we are calculating the entropy. Furthermore, it is valid for any size of the region for which we calculate the entropy.

As we have discussed in details in Section 2.5, our bound for the von Neumann entropy implies that entanglement in these systems satisfies an “effective light-cone”. Furthermore, our bound shows that the system satisfy an area law, which guarantee the efficiency of methods like t -DMRG. Finally, suppose that this many body system is used by two agents to establish a communication between them and that each agent has access only to a region of this system. If these two regions are distant from each other, the information which one agent can receive from the other is not significant after a small amount of time.

We have also discussed that when the terms of the Hamiltonian of two regions of the system commute, then one cannot send any information to the other side no matter how much time passes, which is a particular case of the above discussion. An example of systems with this property is the transverse Ising model.

The transverse Ising model, in some sense, satisfy strange property. As we have shown, the transverse Ising chain satisfy the shielding property. It means that if we divide the chain into

two halves with one site in their intersection (or interface) and if the external magnetic field is null in this site, then the reduced state of one side of the chain does not have dependence on the parameters of the other side. This property is also valid for lattices of any dimension and any configuration, if the interface between the two halves is only one site. An example of lattice which satisfy this requirement is the Bethe lattice (Figure 1.2.d.).

A more intuitive way of understanding the shielding property is via the duality of the Ising chain, where we can write the Hamiltonian in an alternative way. In this new form, we can understand that the parameters which represent interactions and magnetic fields swap their roles. A null magnetic field in the original chain would mean a null interaction in the dual chain, which explain why the two halves would be “decoupled”.

When the interface contains more than one site we can guarantee that the shielding property holds only when the spins of the interface have a well defined alignment between each other. In this case, the reduced state of one side has only an implicit dependence on the parameters of the other site. If we have access only to one side of the lattice, we could infer if the parameters are smaller or greater than some constants, but not their exactly value. A corollary which follows from this analysis is that if a system is free of frustration, then it satisfy the shielding property.

On the other side, we cannot infer if a frustrated systems satisfy or do not satisfy the shielding property. As we could see in the example of Section 3.10, the system considered there is frustrated and *do* satisfy the shielding property for $0 < M < 1$ and it is frustrated and *do not* satisfy the shielding property for $M > 1$. One further research direction is to try to find hypothesis such that every frustrated system with these hypothesis do (or do not) satisfy the shielding property.

Appendix A

Detailing the Hypothesis for the Proof of Lieb-Robinson Bound

In this appendix we present the calculations of our statements on examples where conditions (2.4), (2.5) and (2.6) are satisfied. A function F which satisfies conditions (2.4) and (2.5) for any $\mu \geq 0$ can be given by

$$F(x) = \frac{1}{(1+x)^{d+\epsilon}} \quad (\text{A.1})$$

for some $\epsilon > 0$.

The first statement is that F satisfies Equation (2.4), given by

$$\|F\| := \sup_{i \in \Gamma} \sum_{j \in \Gamma} F(d(i, j)) < \infty. \quad (\text{A.2})$$

To see this note that the summand above is the same on all possible choices of i . Thus the supremum is reached on any value of i . Choose the value $i = 0$, and then we have $d(i, j) = |j|$.

Then, we can write

$$\|F\| = \sum_{j \in \mathbb{Z}^d} \frac{1}{(1+|j|)^{d+\epsilon}}. \quad (\text{A.3})$$

It is well known that this series converges for all $\epsilon > 0$, proving our first statement.

The second statement is that Equation (2.5) is true. It is given by

$$C := \sup_{i,j \in \mathbb{Z}^d} \sum_{k \in \mathbb{Z}^d} \left(\frac{1+d(i,j)}{(1+d(i,k))(1+d(k,j))} \right)^{d+\epsilon} < \infty \quad (\text{A.4})$$

We can see the validity of the above condition verifying that C is upper bounded by

$$C \leq 2^{d+\epsilon+1} \sum_{n \in \mathbb{Z}^d} \frac{1}{(1+|n|)^{d+\epsilon}}. \quad (\text{A.5})$$

To prove this we shall change variables, choosing $n = i - k$ and $a = i - j$. Note that

$$d(i, j) = |i - j| = |a| , \quad d(i, k) = |i - k| = |n| , \quad (\text{A.6})$$

and

$$d(k, j) = |k - j| = |(i - j) - (i - k)| = |a - n| = d(a, n). \quad (\text{A.7})$$

With the above equation we can see that the supremum over x and y does not have dependence on these variables separately, but only on their difference a . So we can write

$$C \leq \sup_{a \in \mathbb{Z}^d} \sum_{n \in \mathbb{Z}^d} \left(\frac{1+|a|}{(1+|n|)(1+d(a,n))} \right)^{d+\epsilon}. \quad (\text{A.8})$$

Now we will separate the above sum in two terms. Those where $|n| \leq |a|/2$ and those where $|n| > |a|/2$. Note that for the first case we have that $d(a, n) \geq |a|/2$ and then

$$\frac{1}{1+d(a,n)} \leq \frac{1}{1+|a|/2}. \quad (\text{A.9})$$

In the second case we have that

$$\frac{1}{1+|n|} \leq \frac{1}{1+|a|/2}. \quad (\text{A.10})$$

Thus we can write

$$\begin{aligned} C &\leq \sup_{a \in \mathbb{Z}^d} \sum_{\substack{n \in \mathbb{Z}^d \\ |n| \leq |a|/2}} \left(\frac{1+|a|}{1+|a|/2} \right)^{d+\epsilon} \frac{1}{(1+|n|)^{d+\epsilon}} \\ &\quad + \sup_{a \in \mathbb{Z}^d} \sum_{\substack{n \in \mathbb{Z}^d \\ |n| > |a|/2}} \left(\frac{1+|a|}{1+|a|/2} \right)^{d+\epsilon} \frac{1}{(1+d(a,n))^{d+\epsilon}} \end{aligned} \quad (\text{A.11})$$

Making the sums not only on their respective subsets, but on the whole space, and rearranging some terms, we have that

$$C \leq \sup_{a \in \mathbb{Z}^d} \left(\frac{2+2|a|}{2+|a|} \right)^{d+\epsilon} \left(\sum_{n \in \mathbb{Z}^d} \frac{1}{(1+|n|)^{d+\epsilon}} + \sum_{n \in \mathbb{Z}^d} \frac{1}{(1+d(a,n))^{d+\epsilon}} \right) \quad (\text{A.12})$$

Note the second term in the parenthesis is actually independent of a , therefore:

$$C \leq \sup_{a \in \mathbb{Z}^d} \left(\frac{2 + 2|a|}{2 + |a|} \right)^{d+\epsilon} \cdot 2 \sum_{n \in \mathbb{Z}^d} \frac{1}{(1 + |n|)^{d+\epsilon}} \quad (\text{A.13})$$

The supremum of $\left(\frac{2+2|a|}{2+|a|} \right)$ is 2. So we can conclude that statement (A.5) holds, which implies that condition (2.5) is true for this example of function.

We have also stated that Equation (2.6) is satisfied by systems in the lattice $\Gamma = \mathbb{Z}^d$, when the interactions are only between first neighbours or when they decay exponentially, for example. For these two examples, the interactions are only between pairs of sites, thus fixed i and j , the only set X such that $i, j \in X$ and we could have $\Phi(X) \neq 0$ is the set $X = \{i, j\}$. Thus, we can write Equation (2.6) as

$$\|\Phi\|_\mu := \sup_{i,j \in \Gamma} \frac{\|\Phi(\{i, j\})\|}{e^{-\mu(d(i, j))} F(d(i, j))} \quad (\text{A.14})$$

For the case of first neighbour interactions we have an additional condition which we suppose that there is some number $M < \infty$ such that $\|\Phi(X)\| \leq M$, for all $X \subset \Gamma$. Furthermore, if $d(i, j) \neq 1$, then $\Phi(\{i, j\}) = 0$, and the above equation becomes

$$\|\Phi\|_\mu := \sup_{i,j \in \Gamma} \frac{\|\Phi(\{i, j\})\|}{e^{-\mu} F(1)} \leq \frac{M}{e^{-\mu} F(1)} < \infty. \quad (\text{A.15})$$

and since $M < \infty$ we have that Condition (2.6) is satisfied for all $\mu \geq 0$.

Now, for the case of exponential decay, we have that there are constants $c, a > 0$ such that $\|\Phi(\{i, j\})\| \leq ce^{-ad(i, j)}$, for all $i, j \in \Gamma$. Using the function F given in Equation (A.1), the Equation (A.14) becomes

$$\|\Phi\|_\mu \leq \sup_{i,j \in \Gamma} \frac{ce^{-ad(i, j)}}{e^{-\mu(d(i, j))} F(d(i, j))} \quad (\text{A.16})$$

and using Equation (A.1), we have that

$$\|\Phi\|_\mu \leq \sup_{i,j \in \Gamma} \frac{ce^{-(a-\mu)d(i, j)}}{(1 + d(i, j))^{d+\epsilon}}. \quad (\text{A.17})$$

For this type of interaction, condition (2.6) is satisfied for all μ such that $0 \leq \mu \leq a$.

Appendix B

Thermal Equilibrium States

Let S be a system which is in thermal equilibrium with a thermal reservoir at temperature T (see Figure B.1). From Statistical Mechanics, we have that the probability p_j of finding this system in a configuration with energy E_j is given by

$$p_j = \frac{n_j e^{-\beta E_j}}{\sum_k n_k e^{-\beta E_k}} \quad (\text{B.1})$$

where k_B is the Boltzmann constant, $\beta = 1/k_B T$ and n_k is the number of possible configurations with energy E_k . Suppose also that $E_{k_1} < E_{k_2}$ for $k_1 < k_2$. The *partition function* $Z = \sum_k e^{-\beta n_k E_k}$ is the sum over all the allowed energies of the system.

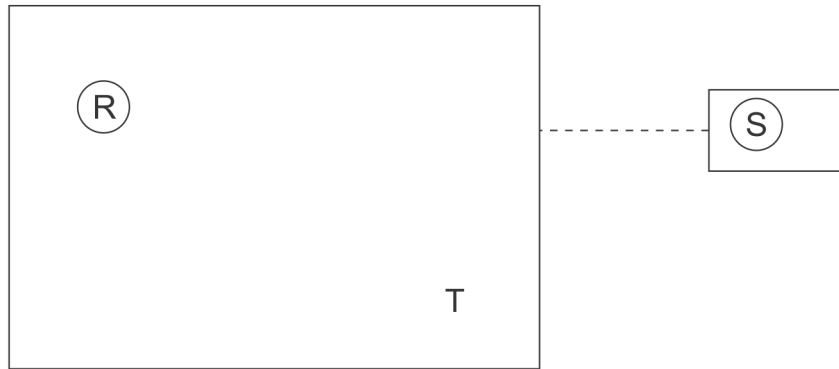


Figure B.1: A system S in contact with a thermal reservoir R at temperature T . (Figure extracted from reference [48]).

When the system S is a quantum system in the state ρ , the probability of finding it with energy E_j is given by

$$p_j = \text{Tr}(\rho P_j), \quad (\text{B.2})$$

where P_j is the projector on the Hilbert subspace of the states with energy E_j .

The Gibbs state, as we have defined in Equation (3.6), is given by

$$\rho = \frac{e^{-\beta H}}{\text{Tr}(e^{-\beta H})}. \quad (\text{B.3})$$

Using the spectral decomposition of $H = \sum_j E_j P_j$ and putting Equation (B.3) into Equation (B.2) we recover the probabilities (B.1). Then, we can say that the Gibbs state is a state of thermal equilibrium.

When the temperature of the system is null, that is, when β tends to infinity, we have that the Gibbs state is the normalized projection on the ground state sector. We can see this by the following calculation.

$$\begin{aligned} \lim_{\beta \rightarrow \infty} \frac{e^{-\beta H}}{\text{Tr}(e^{-\beta H})} &= \lim_{\beta \rightarrow \infty} \frac{\sum_j (P_j e^{-\beta H})}{\sum_i \text{Tr}(P_i e^{-\beta H})} \\ &= \lim_{\beta \rightarrow \infty} \frac{\sum_j e^{-\beta E_j} P_j}{\sum_i n_i e^{-\beta E_i}} \cdot \frac{e^{\beta E_0}}{e^{\beta E_0}} \\ &= \lim_{\beta \rightarrow \infty} \frac{P_0 + \sum_{j \neq 0} e^{-\beta(E_j - E_0)} P_j}{n_0 + \sum_{i \neq 0} n_i e^{-\beta(E_i - E_0)}}. \end{aligned} \quad (\text{B.4})$$

Since $E_0 < E_j$, $\lim_{\beta \rightarrow \infty} e^{-\beta(E_j - E_0)} = 0$ and the limit of the above equation becomes

$$\lim_{\beta \rightarrow \infty} \frac{e^{-\beta H}}{\text{Tr}(e^{-\beta H})} = \frac{P_0}{n_0}, \quad (\text{B.5})$$

which is the ground sector.

Appendix C

Calculations for the Ising Model in a Chain with Three Sites

Here we exhibit the calculations of the two examples given in Section 3.4.3. Both are chains with three sites described by the Ising model, where the first of them is the longitudinal Ising model and the second the transverse Ising model.

Longitudinal Ising Model with Three Spins

Consider the three 1/2-spins with the following Hamiltonian:

$$H = -h\sigma_1^z - \sigma_1^z\sigma_2^z - \sigma_2^z\sigma_3^z. \quad (\text{C.1})$$

Since terms in the r.h.s commute with each other it holds that:

$$e^{-\beta H} = e^{\beta\sigma_1^z\sigma_2^z}e^{\beta\sigma_2^z\sigma_3^z}e^{\beta h\sigma_1^z}. \quad (\text{C.2})$$

The series expansion of the first term of the equation above is given by

$$e^{\beta\sigma_1^z\sigma_2^z} = \sum_{n=0}^{\infty} \frac{(\beta)^n}{n!} (\sigma_1^z\sigma_2^z)^n = \left(\sum_{n \text{ even}} \frac{(\beta)^n}{n!} \right) \mathbb{1} + \left(\sum_{n \text{ odd}} \frac{(\beta)^n}{n!} \right) \sigma_1^z\sigma_2^z, \quad (\text{C.3})$$

and then we can write

$$e^{\beta\sigma_1^z\sigma_2^z} = \cosh(\beta)\mathbb{1} + \sinh(\beta)\sigma_1^z\sigma_2^z. \quad (\text{C.4})$$

Analogously, the second term of equation (C.2) is given by

$$e^{\beta\sigma_2^z\sigma_3^z} = \cosh(\beta)\mathbb{1} + \sinh(\beta)\sigma_2^z\sigma_3^z, \quad (\text{C.5})$$

and the third term by

$$e^{\beta h \sigma_1^z} = \cosh(\beta h) \mathbb{1} + \sinh(\beta h) \sigma_1^z. \quad (\text{C.6})$$

Using the equations above we can see that the Gibbs state is proportional to

$$e^{-\beta H} = (\cosh(\beta) \mathbb{1} + \sinh(\beta) \sigma_1^z \sigma_2^z)(\cosh(\beta) \mathbb{1} + \sinh(\beta) \sigma_2^z \sigma_3^z)(\cosh(\beta h) \mathbb{1} + \sinh(\beta h) \sigma_1^z). \quad (\text{C.7})$$

Defining $a = \cosh(\beta)$, $b = \sinh(\beta)$, $c(h) = \cosh(\beta h)$ and $d(h) = \sinh(\beta h)$, the equation above becomes

$$\begin{aligned} e^{-\beta H} &= a^2 c(h) \mathbb{1} + a^2 d(h) \sigma_1^z + a b d(h) \sigma_2^z + a b c(h) \sigma_1^z \sigma_2^z \\ &\quad + a b c(h) \sigma_2^z \sigma_3^z + b^2 c(h) \sigma_1^z \sigma_3^z + a b d(h) \sigma_1^z \sigma_2^z \sigma_3^z + b^2 d(h) \sigma_3^z. \end{aligned} \quad (\text{C.8})$$

We can see that $\text{Tr} e^{-\beta H} = 8a^2 c(h)$. Making the normalization and the partial trace on the equation above, the reduced state of site three becomes

$$\rho_3 = \text{Tr}_{1,2} \frac{e^{-\beta H}}{8a^2 c(h)} = \frac{1}{2} \mathbb{1} + \frac{1}{2} \frac{b^2 d(h)}{a^2 c(h)} \sigma_3^z \quad (\text{C.9})$$

$$= \frac{1}{2} \mathbb{1} + \frac{1}{2} \tanh^2(\beta) \tanh(\beta h) \sigma_3^z \quad (\text{C.10})$$

Thus we can see that the expected value of observable σ_3^z is given by

$$\langle \sigma_3^z \rangle = \text{Tr}(\rho_3 \sigma_3^z) = \text{Tr} \left(\frac{1}{2} \sigma_3^z + \frac{1}{2} \tanh^2(\beta) \tanh(\beta h) \mathbb{1} \right), \quad (\text{C.11})$$

and then

$$\langle \sigma_3 \rangle = \tanh^2(\beta) \tanh(\beta h), \quad (\text{C.12})$$

which is the Equation (3.36) from the main text. With this equation we can see that the magnetization of site 3 has an explicitly dependence on the magnetic field applied on site 1, even with null external magnetic field in the interface (site 2).

Transversal Ising Model with Three Spins

Consider the Hamiltonian:

$$H = -h \sigma_1^x - J_1 \sigma_1^z \sigma_2^z - J_2 \sigma_2^z \sigma_3^z. \quad (\text{C.13})$$

If we define

$$H^I = -h\sigma_1^x - J_1\sigma_1^z\sigma_2^z \quad \text{and} \quad H^{II} = -J_2\sigma_2^z\sigma_3^z, \quad (\text{C.14})$$

we can write the Gibbs state of the system as

$$\frac{e^{-\beta H}}{\text{Tr}(e^{-\beta H})} = \frac{e^{-\beta H^I} e^{-\beta H^{II}}}{\text{Tr}(e^{-\beta H})}, \quad (\text{C.15})$$

since H^I and H^{II} commute.

Using the series expansion of the exponential to write the first term, we have

$$e^{-\beta H^I} = \sum_{n=0}^{\infty} \frac{(-\beta)^n}{n!} (H^I)^n. \quad (\text{C.16})$$

Remembering that σ_1^z and σ_1^x anti-commute, we can evaluate the powers of H^I in the following way.

$$(H^I)^2 = (J_1^2 + h^2) \mathbb{1}. \quad (\text{C.17})$$

Then, for every even n , we have that

$$(H^I)^n = [(H^I)^2]^{n/2} = (\sqrt{J_1^2 + h^2})^n \mathbb{1}. \quad (\text{C.18})$$

So, for every odd n , we have that

$$(H^I)^n = (H^I)^{(n-1)} \cdot H^I = (\sqrt{J_1^2 + h^2})^{n-1} H^I,$$

which can be written as

$$(H^I)^n = (\sqrt{J_1^2 + h^2})^n \frac{H^I}{\sqrt{J_1^2 + h^2}}. \quad (\text{C.19})$$

Putting Equations (C.18) and (C.19) into Equation (C.16), we have that

$$\begin{aligned} e^{-\beta H^I} &= \left(\sum_{n \text{ even}} \frac{(-\beta \sqrt{J_1^2 + h^2})^n}{n!} \right) \mathbb{1} + \left(\sum_{n \text{ odd}} \frac{(-\beta \sqrt{J_1^2 + h^2})^n}{n!} \right) \frac{H^I}{\sqrt{J_1^2 + h^2}} \\ &= \cosh(\beta \sqrt{J_1^2 + h^2}) \mathbb{1} - \sinh(\beta \sqrt{J_1^2 + h^2}) \frac{H^I}{\sqrt{J_1^2 + h^2}}. \end{aligned} \quad (\text{C.20})$$

Analogously, the other term of Equation (C.15) becomes

$$e^{-\beta H^{II}} = \cosh(\beta J_2) \mathbb{1} - \sinh(\beta J_2) \frac{H^{II}}{J}. \quad (\text{C.21})$$

Putting Equations (C.20) and (C.21) into Equation (C.15) we have that the Gibbs state of the system is given by

$$\begin{aligned} \frac{e^{-\beta H}}{\text{Tr}(e^{-\beta H})} &= \frac{1}{8} \left(\mathbb{1} + \tanh(\beta J_2) \sigma_2^z \sigma_3^z + \tanh \left(\beta \sqrt{J_1^2 + h^2} \right) \frac{(h\sigma_1^x + J_1 \sigma_1^z \sigma_2^z)}{\sqrt{J_1^2 + h^2}} \right. \\ &\quad \left. + \tanh(\beta J_2) \tanh \left(\beta \sqrt{J_1^2 + h^2} \right) \frac{J_1 \sigma_1^z \sigma_3^z + h \sigma_1^x \sigma_2^z \sigma_3^z}{\sqrt{J_1^2 + h^2}} \right). \end{aligned} \quad (\text{C.22})$$

If we take the partial trace on the first site we get the reduced state $\rho_{2,3}$ of sites 2 and 3. By the equation above, it is equal to

$$\rho_{2,3} = \frac{\text{Tr}_1(e^{-\beta H})}{\text{Tr}(e^{-\beta H})} = \frac{1}{4} \left(\mathbb{1} + \frac{\sinh(\beta J_2)}{\cosh(\beta J_2)} \sigma_2^z \sigma_3^z \right).$$

It is Equation (3.40) from the main text, which confirms the predictions of Theorem 2.

Appendix D

Calculations for the Ising Model in a Lattice with Four Sites

In this appendix we exhibit the calculations of the example shown in Figure 3.10.a. We define its Hamiltonian given by

$$H = -\sigma_1^z \sigma_2^z - \sigma_2^z \sigma_3^z - h_1 \sigma_1^x - \sigma_2^z \sigma_4^z - \sigma_3^z \sigma_4^z - h_4 \sigma_4^x$$

and we wish to compute the magnetization $\langle \sigma_4^x \rangle$. More than that, we will compute the reduced state of site 4. To do this we first perform the partial trace over site 1, followed by the partial trace of sites 2 and 3, giving the desired reduced state.

We can write the Hamiltonian as

$$H = (H' \otimes \mathbb{1}_4) \cdot (\mathbb{1}_1 \otimes H'') \quad (\text{D.1})$$

where $H' = -\sigma_1^z \sigma_2^z - \sigma_2^z \sigma_3^z - h_1 \sigma_1^x$, defined on the space of sites 1, 2 and 3, and $H'' = -\sigma_2^z \sigma_4^z - \sigma_3^z \sigma_4^z - h_4 \sigma_4^x$, defined on the space of sites 2, 3 and 4. Then we have that

$$e^{-\beta H} = (e^{-\beta H'} \otimes \mathbb{1}_4) \cdot (\mathbb{1}_1 \otimes e^{-\beta H''}), \quad (\text{D.2})$$

so we get that

$$\text{Tr}_1(e^{-\beta H}) = \{\text{Tr}_1(e^{-\beta H'}) \otimes \mathbb{1}_4\} \cdot e^{-\beta H''}. \quad (\text{D.3})$$

To calculate $\text{Tr}_1(e^{-\beta H'})$, let us compute $\text{Tr}_1(H'^n)$ and use the series expansion of $e^{-\beta H'}$ (3.24) to find its partial trace. We have that

$$H'^2 = (2 + h_1^2) \mathbb{1} + 2\sigma_2^z \sigma_3^z = a_1 \mathbb{1} + 2\sigma_2^z \sigma_3^z \quad (\text{D.4})$$

where $a_1 = 2 + h_1^2$. Then, it is easy to find even powers of H' , that is

$$H'^{2n} = \sum_{k=0}^n \binom{n}{k} a_1^{n-k} 2^k (\sigma_2^z \sigma_3^z)^k = \left(\sum_{\substack{k=0 \\ even}}^n \binom{n}{k} a_1^{n-k} 2^k \right) \mathbb{1} + \left(\sum_{\substack{k=0 \\ odd}}^n \binom{n}{k} a_1^{n-k} 2^k \right) \sigma_2^z \sigma_3^z. \quad (\text{D.5})$$

Summarizing, we can write

$$H'^{2n} = b_n \mathbb{1} + c_n \sigma_2^z \sigma_3^z. \quad (\text{D.6})$$

With this equation it is also possible to calculate odd powers of H' , that is

$$H'^{2n+1} = (b_n \mathbb{1} + c_n \sigma_2^z \sigma_3^z).(\sigma_1^z \sigma_2^z + \sigma_2^z \sigma_3^z + h_1 \sigma_1^x).$$

The above equation shows us that $\text{Tr}(H'^{2n+1}) = 0$, for all $n = 0, 1, 2, \dots$. Then we have that

$$\text{Tr}_1(e^{-\beta H'}) = \text{Tr}_1 \left(\sum_{m=0}^{\infty} \frac{\beta^m}{m!} H'^m \right) = \sum_{m=0}^{\infty} \frac{\beta^m}{m!} \text{Tr}_1(H'^m) = \sum_{\substack{m=0 \\ even}}^{\infty} \frac{\beta^m}{m!} \text{Tr}_1(H'^m). \quad (\text{D.7})$$

Taking $m = 2n$ and using Equation (D.6), we have that

$$\text{Tr}_1(e^{-\beta H'}) = \sum_{n=0}^{\infty} \frac{\beta^{2n}}{(2n)!} \text{Tr}_1 H'^{2n} = \sum_{n=0}^{\infty} \frac{\beta^{2n}}{(2n)!} (2b_n \mathbb{1} + 2c_n \sigma_2^z \sigma_3^z), \quad (\text{D.8})$$

and, after some arrangements, we get

$$\text{Tr}_1(e^{-\beta H'}) = \left(\sum_{n=0}^{\infty} \frac{\beta^{2n} 2b_n}{(2n)!} \right) \mathbb{1} + \left(\sum_{n=0}^{\infty} \frac{\beta^{2n} 2c_n}{(2n)!} \right) \sigma_2^z \sigma_3^z. \quad (\text{D.9})$$

We can write the above equation as

$$\text{Tr}_1(e^{-\beta H'}) = A \mathbb{1} + B \sigma_2^z \sigma_3^z, \quad (\text{D.10})$$

where

$$A = \sum_{n=0}^{\infty} \sum_{\substack{k=0 \\ even}}^n \frac{2\beta^{2n}}{(2n)!} \frac{n!}{(n-k)!k!} a_1^{n-k} 2^k \quad (\text{D.11})$$

and

$$B = \sum_{n=0}^{\infty} \sum_{\substack{k=0 \\ odd}}^n \frac{2\beta^{2n}}{(2n)!} \frac{n!}{(n-k)!k!} a_1^{n-k} 2^k. \quad (\text{D.12})$$

Now, let us calculate $e^{-\beta H''}$. The powers of H'' will follow the same arguments of the powers of H' , so we have that

$$H''^{2n} = \alpha_n \mathbb{1} + \epsilon_n \sigma_2^z \sigma_3^z \quad (\text{D.13})$$

and

$$H''^{2n+1} = (\alpha_n \mathbb{1} + \gamma_n \sigma_2^z \sigma_3^z)(\sigma_2^z \sigma_4^z + \sigma_3^z \sigma_3^z + h_4 \sigma_4^x), \quad (\text{D.14})$$

where α_n and ϵ_n can be found analogously to what was done for b_n and c_n . Using the Taylor series of $e^{-\beta H''}$, we have that

$$e^{-\beta H''} = C \mathbb{1} + D \sigma_2^z \sigma_3^z + E \sigma_2^z \sigma_4^z + F \sigma_3^z \sigma_4^z + G \sigma_4^x + H \sigma_2^z \sigma_3^z \sigma_4^x, \quad (\text{D.15})$$

where

$$C = \sum_{n=0}^{\infty} \sum_{\substack{k=0 \\ even}}^n \frac{2\beta^{2n}}{(2n)!} \frac{n!}{(n-k)!k!} a_4^{n-k} 2^k, \quad (\text{D.16})$$

$$D = \sum_{n=0}^{\infty} \sum_{\substack{k=0 \\ odd}}^n \frac{2\beta^{2n}}{(2n)!} \frac{n!}{(n-k)!k!} a_4^{n-k} 2^k, \quad (\text{D.17})$$

$$G = h_4 \sum_{n=0}^{\infty} \sum_{\substack{k=0 \\ even}}^n \frac{2\beta^{2n+1}}{(2n+1)!} \frac{n!}{(n-k)!k!} a_4^{n-k} 2^k \quad (\text{D.18})$$

and

$$H = h_4 \sum_{n=0}^{\infty} \sum_{\substack{k=0 \\ odd}}^n \frac{2\beta^{2n+1}}{(2n+1)!} \frac{n!}{(n-k)!k!} a_4^{n-k} 2^k, \quad (\text{D.19})$$

where we have set $a_4 = 2 + h_4^2$. We do not show the expressions of E and F here, since they are not used.

Putting Equations (D.10) and (D.15) in Equation (D.3), performing the partial trace on spaces of sites 2 and 3, and normalizing the trace of resulting operator, we have that the reduced state of site 4 is given by

$$\rho_4 = \frac{1}{2} \mathbb{1} + \frac{1}{2} \frac{AG + BH}{AC + BD} \sigma_4^x. \quad (\text{D.20})$$

Finally, we get that

$$\langle \sigma_4^x \rangle = \frac{AG + BH}{AC + BD}. \quad (\text{D.21})$$

We can show that the magnetization (D.21) is independent of h_1 when the value of β goes to infinity. More specifically, it is equal to $\frac{1}{\sqrt{4+h_4^2}}$ when $\beta \rightarrow \infty$.

In conclusion, it is shown that the shielding property does not work, in general, when the interface has more than one site when the temperature is positive. For null temperature, however, the shielding property still holds in this example.

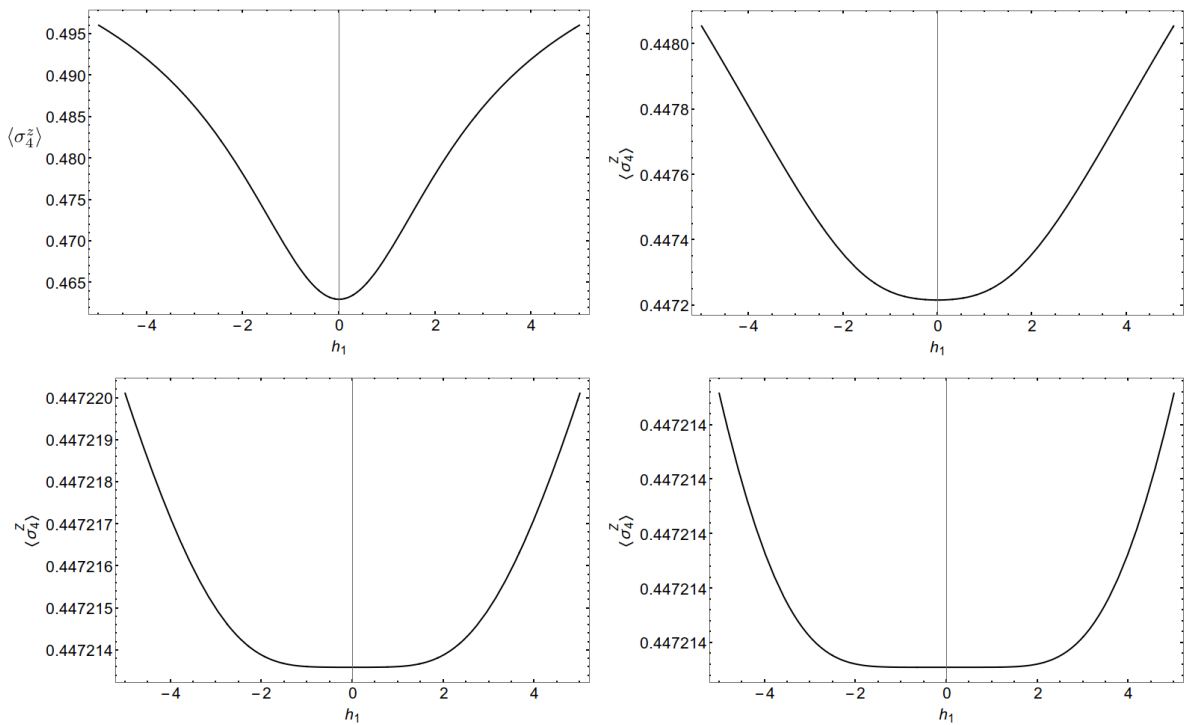


Figure D.1: Plots of the value of the magnetization $\langle \sigma_4^x \rangle$ of site 4 as a function of the external magnetic field h_1 applied in site 1. Each plot was done for different values of β , which are $\beta = 1, 4, 7$ and 10 . Note that the scale of each plot is also different.

Appendix E

Calculation for the Ising Lattice with Implicit Dependence

In this appendix we will show the calculations of the ground state of the system of Figure 3.13 as a function of the parameter a . The method shown here can also be adapted to the calculations of the ground state of the system of Figure 3.14, which is a finite system of arbitrary size.

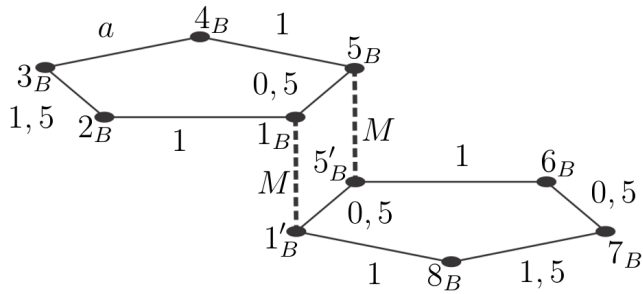


Figure E.1: A second system built to help the calculations of the energies of the ground state of the system illustrated in Figure 3.13. We take $M \ll -1$, which obliges the sites which have interactions of strength M to be with spins aligned in the same direction. It guarantee that the states of system of item a. is in correspondence with the probable states of system of item b.

Now, in the system of Figure 3.13, since the external magnetic field is null in all the sites and

the interactions are only in the z -direction, we have that the ground state is given by states where the magnetization in each site are only in the z -direction. Thus, it suffices to calculate the energy of each configuration of the spins in the z -direction. The configurations with the smallest energy are the ground states.

To calculate the ground state of this system we are going to calculate first the ground state of the system of Figure E.1. In this system we can see that we have two couples of sites connected by an interaction of strength M . We choose M to be negative but sufficiently large in modulus, which guarantees that the two sites connected by this interaction are always found with their spins aligned in the same direction. With this hypothesis we can make a correspondence between the systems of Figures 3.13 and E.1. Let the following correspondence between the sites of these systems be

$$\begin{aligned} 2_A &\rightarrow 2_B & 3_A &\rightarrow 3_B & 4_A &\rightarrow 4_B & 6_A &\rightarrow 6_B & 7_A &\rightarrow 7_B & 8_A &\rightarrow 8_B \\ 1_A &\rightarrow \{1_B \cup 1'_B\} & 5_A &\rightarrow \{5_B \cup 5'_B\} \end{aligned} \quad (\text{E.1})$$

Each site outside the interface of the first system has correspondence with another site of the second system and the sites of the interface have correspondence with a set of two sites. Since the spins of sites 1_B and $1'_B$ (5_B and $5'_B$) are equal, then the spin of this couple of sites has the same degree of freedom as the spin of site 1_A (5_A).

If the system of Figure E.1. is in a state where all spins have a well defined alignment between each other and has energy $E + 2M$, then the correspondent state of the system of Figure 3.13. has energy E .

To calculate the energy of the states of the system of Figure E.1, we shall compute the energy of a system which is a simple pentagon, shown in Figure E.2. It is also described by the Ising model with null external magnetic field in all the sites and the interactions strength are given in the figure.

In Figure E.3 we can find the energy of each configuration of the spins of the system of Figure E.2. Note that the energy for a system described by the Ising model with null external magnetic field in all sites is defined by the relative alignment of the spins between each other, and not by their spatial alignment. If we take a certain configuration with energy E , the configuration where we invert all the spins to their opposite direction, comparing with the previous configuration

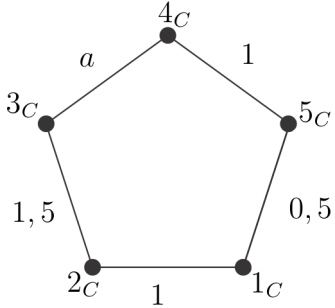


Figure E.2: A system described by the Ising model, where the external magnetic field is null in all the sites and the strength of the interactions are labelled in this figure.

it also has energy E . Because of this, in Figure E.3 we had only drawn half of the possible configurations.

In Figure E.3, we highlight the configurations of the smallest energy. One of them happens for $a \geq 0, 5$ and has energy $-3 - a$ and the other happens for $a \leq 0, 5$ with energy $-4 + a$. We call the configuration with energy $-3 - a$ which is drawn in the Figure E.3 by \mathcal{C}_1 and the configuration with energy $-3 - a$ but with opposite alignment (which is not drawn) by \mathcal{C}'_1 . The configuration with energy $-4 + a$ drawn in Figure E.3 we call by \mathcal{C}_2 and the one with energy $-4 + a$ but with opposite alignment (which is not drawn) by \mathcal{C}'_2 .

Now, let us turn our attention to the system of Figure E.1. The left subset, that of sites 1_B , 2_B , 3_B , 4_B , and 5_B , is in correspondence with the system of Figure E.2, making

$$1_B \rightarrow 1_C \quad 2_B \rightarrow 2_C \quad 3_B \rightarrow 3_C \quad 4_B \rightarrow 4_C \quad 5_B \rightarrow 5_C \quad (\text{E.2})$$

Thus, the configurations of the smallest energy for this subset are \mathcal{C}_1 and \mathcal{C}'_1 for $a \geq 0, 5$ and \mathcal{C}_2 and \mathcal{C}'_2 for $a \leq 0, 5$.

Making $a = 0, 5$, the right subset, that of sites $1'_B$, $5'_B$, 6_B , 7_B and 8_B , is in the following correspondence with the system of Figure E.2.

$$1'_B \rightarrow 1_C \quad 5'_B \rightarrow 5_C \quad 6_B \rightarrow 4_C \quad 7_B \rightarrow 3_C \quad 8_B \rightarrow 2_C. \quad (\text{E.3})$$

The configurations of minimum energy for this subset are \mathcal{C}_1 , \mathcal{C}'_1 , \mathcal{C}_2 and \mathcal{C}'_2 .

Now, let us analyse the whole system. Suppose that the state of the right and left subsets are both with the configuration \mathcal{C}_i (or \mathcal{C}'_i), given the above correspondences, then we will say that the state of whole system is with the configuration $\mathcal{C}_i\mathcal{C}_i$ (or $\mathcal{C}'_i\mathcal{C}'_i$).

Once the subset of the left is with some configurations where the sites 1_B and 5_B have positive spins, for example, it obligates, via the interactions of strength M , the right subset to have a

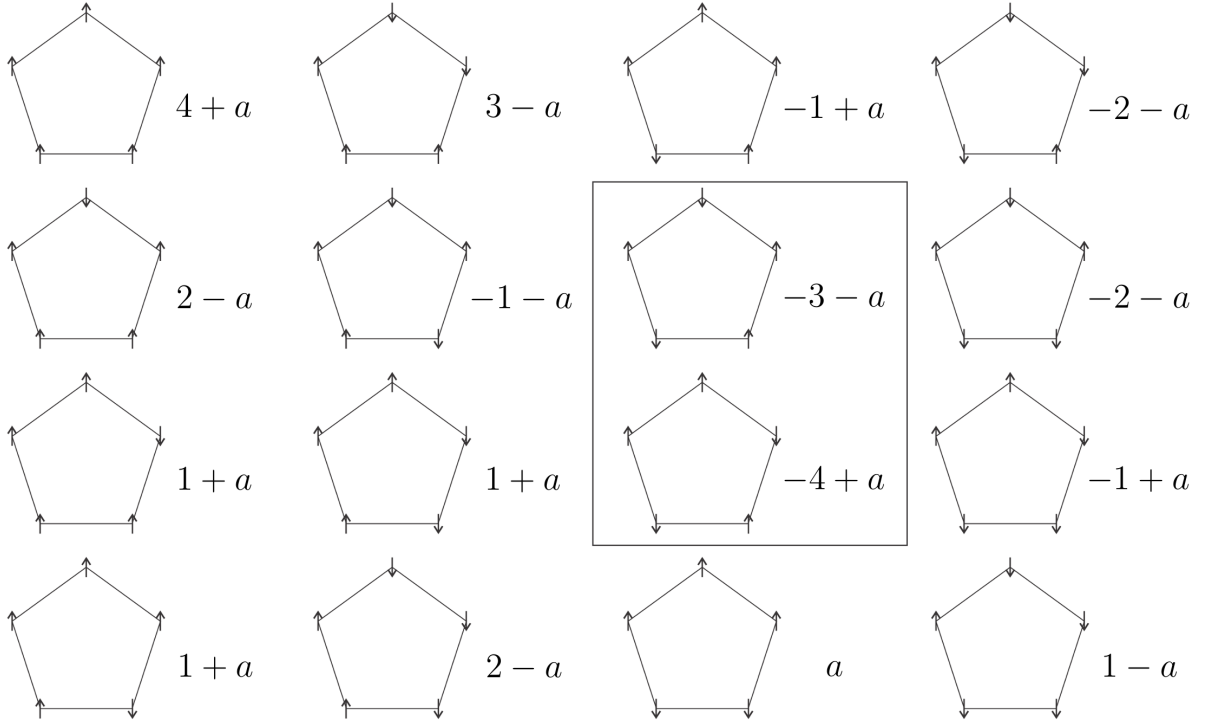


Figure E.3: Energy values for the system of Figure E.2 for the possible alignment of the spins. Note that since the external magnetic field is null in all the sites the energy of a certain spins alignment is the same for the state with opposite alignment. Because of this we have just illustrated half of the spins alignment possibilities. We highlight the two configurations of smallest energy, one for $a \geq 0, 5$ with energy $-3 - a$ and the other for $a \leq 0, 5$ with energy $-4 + a$.

configuration where $1'_B$ and $5'_B$ are also positive. Thus, if the system is in the ground state and the left subset is with the configuration \mathcal{C}_i or \mathcal{C}'_i , then the subset of the right is with the configurations \mathcal{C}_i or \mathcal{C}'_i , respectively, for $i = 1, 2$.

We can conclude that the ground state of the system of Figure E.1 is the combination of configurations $\mathcal{C}_1\mathcal{C}_1$ and $\mathcal{C}'_1\mathcal{C}'_1$ for $a \geq 0, 5$ the combination of the configurations $\mathcal{C}_2\mathcal{C}_2$ and $\mathcal{C}'_2\mathcal{C}'_2$ for $a \leq 0, 5$. The conclusion is exactly the same for the system of Figure 3.13 as we have already explained in the beginning of the example.

Now, take the observable $\sigma_{6_A}^z \sigma_{7_A}^z$. If $a > 0, 5$ we have that the system is in the configuration $\mathcal{C}_1\mathcal{C}_1$ and $\mathcal{C}'_1\mathcal{C}'_1$, where these two spins are always in agreement. We would always measure $\sigma_{6_A}^z \sigma_{7_A}^z = 1$. Similarly, if $a < 0, 5$ we would always measure $\sigma_{6_A}^z \sigma_{7_A}^z = -1$ and if $a = 0, 5$ the answer of this

measurement would be random. This is the conclusion which we have stated in the main text.

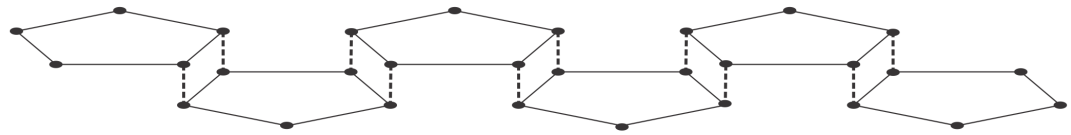


Figure E.4: A second system built to help the calculations of the energies of the ground state of the system illustrated in Figure 3.14. It is used in the same way as the system of Figure E.1 is used to make the calculations for the system of Figure 3.13.

In the main text, we have also mentioned a system (Figure 3.14) which is an extension of the system of Figure 3.13. In that figure, we have drawn a system with six pentagons, but it could have an arbitrarily large number of pentagons.

Bibliography

- [1] E. Lieb and D. Robinson, The Finite Group Velocity of Quantum Spin Systems, *Commun. Math. Phys.* **28**, 251-257 (1972).
- [2] B. Nachtergael, H. Raz, B. Schlein, and R. Sims, Lieb-Robinson Bounds for Harmonic and Anharmonic Lattice Systems, *Commun. Math. Phys.* **286**, 1073-1098 (2009).
- [3] S. Bravyi, M. B. Hastings, and F. Verstraete, Lieb-Robinson bounds and the generation of correlations and topological quantum order, *Phys. Rev. Lett.* **97**, 050401 (2006).
- [4] M. Hastings and T. Koma, Spectral Gap and Exponential Decay of Correlations, *Commun. Math. Phys.* **265**, 781 (2006).
- [5] M. Reed and B. Simon, II: Fourier Analysis, Self-Adjointness, Vol. 2. Elsevier (1975).
- [6] J. Eisert, M. Cramer, and M. B. Plenio, Area laws for the entanglement entropy: A review, *Rev. Mod. Phys.* **82**, 277 (2010); M. B. Hastings, An Area Law for One Dimensional Quantum Systems, *JSTAT*, P08024 (2007).
- [7] R. C. Drumond and N. S. Móller, Bounding entanglement spreading after a local quench , *Phys. Rev. A* **95**, 062301 (2017).
- [8] N. S. Móller, A. L. de Paula Jr, and R. C. Drumond, A Shielding Property for Thermal Equilibrium States on the Quantum Ising Model, *Phys. Rev. E* **97**, 032101 (2018).
- [9] I. Bloch, Ultracold quantum gases in optical lattices, *Nature Physics* **1**, 23-30 (2005).
- [10] M. Cheneau, P. Barmettler, D. Poletti, M. Endres, P. Schauß, T. Fukuhara, C. Gross, I. Bloch, C. Kollath, and S. Kuhr, Lightcone-like spreading of correlations in a quantum many-body system, *Nature* **481**, 484-487 (2012).

- [11] J. J. Sakurai and J. Napolitano, Modern quantum mechanics, Pearson Higher Ed (2014).
- [12] A. L. de Paula Jr, H. Bragança, R. G. Pereira, R. C. Drumond, and M. C. O. Aguiar, Spinon and bound state excitation light cones in Heisenberg XXZ Chains, Phys. Rev. B **95**, 045125 (2017).
- [13] M. Nielsen and I. Chuang, Quantum Computation and Quantum Information, Cambridge University Press, Cambridge, UK (2000).
- [14] F. G. S. L. Brandão, Entanglement and quantum order parameters, New J. Phys. **7**, 254 (2005).
- [15] S. R. White, Density Matrix Formulation for Quantum Renormalization Groups, Phys. Rev. Lett. **69**, 2863 (1992); A. L. Malvezzi, An introduction to numerical methods in lowdimensional quantum systems, Braz. J. Phys. **33**, 55 (2003).
- [16] U. Schollwoeck, The density-matrix renormalization group in the age of matrix product states, Ann. Phys. **326**, 96 (2011).
- [17] I. P. McCulloch, From density-matrix renormalization group to matrix product states, J. Stat. Mech. P10014 (2007).
- [18] J. Eisert, M. Friesdorf, and C. Gogolin, Quantum many-body systems out of equilibrium, Nat. Phys. **11**, 124-130 (2015).
- [19] A. Polkovnikov, K. Sengupta, A. Silva, and M. Vengalattore, Nonequilibrium dynamics of closed interacting quantum systems, Rev. Mod. Phys. **83**, 863 (2011).
- [20] V. Eisler, and I. Peschel, Evolution of entanglement after a local quench, J. Stat. Mech. P06005 (2007).
- [21] M. Friesdorf, A. H. Werner, W. Brown, V. B. Scholz, and J. Eisert, Many-Body Localization Implies that Eigenvectors are Matrix-Product States, Phys. Rev. Lett. **114**, 170505 (2015); R. Sims and G. Stolz, Many-body localization: Concepts and simple models, Markov Process and Related Fields **21**, 791-822 (2015).

- [22] P. Calabrese and J. Cardy, Entanglement entropy and conformal field theory, *J. Phys. A* **42**, 504005 (2009).
- [23] G. De Chiara, M. Rizzi, D. Rossini, and S. Montangero, Density matrix renormalization group for dummies, *J. Comput. Theor. Nanosci.* **5**, 1277-1288 (2008).
- [24] J. Eisert and T. J. Osborne, General Entanglement Scaling Laws from Time Evolution, *Phys. Rev. Lett.* **97**, 150404 (2006); C. K. Burrell and T. J. Osborne, Bounds on the Speed of Information Propagation in Disordered Quantum Spin Chains, *Phys. Rev. Lett.* **99**, 167201 (2007).
- [25] D. W. Robinson, Return to equilibrium, *Commun. Math. Phys.* **31**, 171-189 (1973); M. Rigol, A. Muramatsu, and M. Olshanii, Hard-core bosons on optical superlattices: Dynamics and relaxation in the superfluid and insulating regimes, *Phys. Rev. A* **74**, 053616 (2006); M. A. Cazalilla, Effect of Suddenly Turning on Interactions in the Luttinger Model, *Phys. Rev. Lett.* **97**, 156403 (2006); T. Farrelly, F. G. S. L. Brandão, and M. Cramer, Thermalization and Return to Equilibrium on Finite Quantum Lattice Systems, *Phys. Rev. Lett.* **118**, 140601 (2017).
- [26] P. Jurcevic, B. P. Lanyon, P. Hauke, C. Hempel, P. Zoller, R. Blatt, and C. F. Roos, Quasiparticle engineering and entanglement propagation in a quantum many-body system, *Nature* **511**, 202-205 (2014).
- [27] A. L. de Paula Jr, Dinâmica de não equilíbrio em cadeias de spin, PhD Thesis, Departamento de Física, Universidade Federal de Minas Gerais, in preparation.
- [28] J. Watrous, Theory of Quantum Information, Cambridge University Press (2018).
- [29] B. Nachtergaele, Y. Ogata, and R. Sims, Propagation of Correlations in Quantum Lattice Systems, *J. Stat. Phys.* **124** 1-13 (2006).
- [30] H. B. Callen, Thermodynamics and an Introduction to Thermostatistics, John Wiley Sons, New York (1985).
- [31] C.H. Bennett, H.J. Bernstein, S. Popescu, and B. Schumacher, Concentrating partial entanglement by local operations, *Phys. Rev. A* **53**, 2046-2052 (1996).

- [32] K. M. R. Audenaert, A sharp continuity estimate for the von Neumann entropy, *J. Phys. A* **40**, 8127-8136 (2007).
- [33] R. Alicki and M. Fannes, Continuity of quantum conditional information, *J. Phys. A* **37**, L55 (2004).
- [34] M. Kasner, Entanglement-enhanced spreading of correlations, *New J. Phys.* **17**, 123024 (2015).
- [35] T. Koma and H. Tasaki, Classical XY model in 1.99 dimensions, *Phys. Rev. Lett.* **74** 3916-3919 (1995), Erratum in *Phys. Rev. Lett.* **75** 984 (1995).
- [36] E. H. Lieb, T. D. Schultz, and D. C. Mattis, Two Soluble Models of an Antiferromagnetic Chain, *Ann. Phys.* **16**, 407-466 (1961).
- [37] B. K. Chakrabarti, A. Dutta, and P. Sen, Quantum Ising Phases and Transitions in Transverse Ising models, Springer-Verlag, Berlin (1996).
- [38] T. Giamarchi, Quantum Physics in One Dimension, Oxford University Press, Oxford (2004).
- [39] F. Verstraete, D. Porras, and J. I. Cirac, DMRG and periodic boundary conditions: a quantum information perspective, *Phys. Rev. Lett.* **93**, 227205 (2004); R. Orus, A Practical Introduction to Tensor Networks: Matrix Product States and Projected Entangled Pair States, *Annals of Physics* **349**, 117-158 (2014).
- [40] P. Haikka, J. Goold, S. McEndoo, F. Plastina, and S. Maniscalco, Non-Markovianity, Loschmidt echo, and criticality: A unified picture, *Phys. Rev. A* **85**, 060101(R) (2012).
- [41] F. Cosco, M. Borrelli, P. Silvi, S. Maniscalco, and G. De Chiara, Nonequilibrium quantum thermodynamics in Coulomb crystals, *Phys. Rev. A* **95**, 063615 (2017); L. Fusco, S. Pigeon, T. J. G. Apollaro, A. Xuereb, L. Mazzola, M. Campisi, A. Ferraro, M. Paternostro, and G. De Chiara, Assessing the Nonequilibrium Thermodynamics in a Quenched Quantum Many-Body System via Single Projective Measurements, *Phys. Rev. X* **4**, 031029 (2014).
- [42] J. Simon, W. S. Bakr, R. Ma, M. E. Tai, P. M. Preiss, and M. Greiner, Quantum simulation of antiferromagnetic spin chains in an optical lattice, *Nature* **472**, 307-312 (2011).

- [43] R. Coldea, D.A. Tennant, E.M. Wheeler, E. Wawrzynska, D. Prabhakaran, M. Telling, K. Habicht, P. Smeibidl, and K. Kiefer, Quantum Criticality in an Ising Chain: Experimental Evidence for Emergent E_8 Symmetry, *Science* **327**, 177-180 (2010).
- [44] W. De Roeck and M. Schutz, Local perturbations perturb-exponentially-locally, *J. Math. Phys.* **56**, 061901 (2015).
- [45] S. Bachmann, S. Michalakis, B. Nachtergaelle, and R. Sims, Automorphic Equivalence within Gapped Phases of Quantum Lattice Systems, *Commun. Math. Phys.* **309**, 835-871 (2012).
- [46] M. Kliesch, C. Gogolin, M. J. Kastoryano, A. Riera, and J. Eisert, Locality of temperature, *Phys. Rev. X* **4**, 031019 (2014).
- [47] P. Fendley, Modern Statistical Mechanics, <http://galileo.phys.virginia.edu/pf7a/book.html>, in preparation.
- [48] S. R. A. Salinas, Introdução a Física Estatística, São Paulo: Editora da Universidade de São Paulo (2008).